eROSITA Calibration and First Results

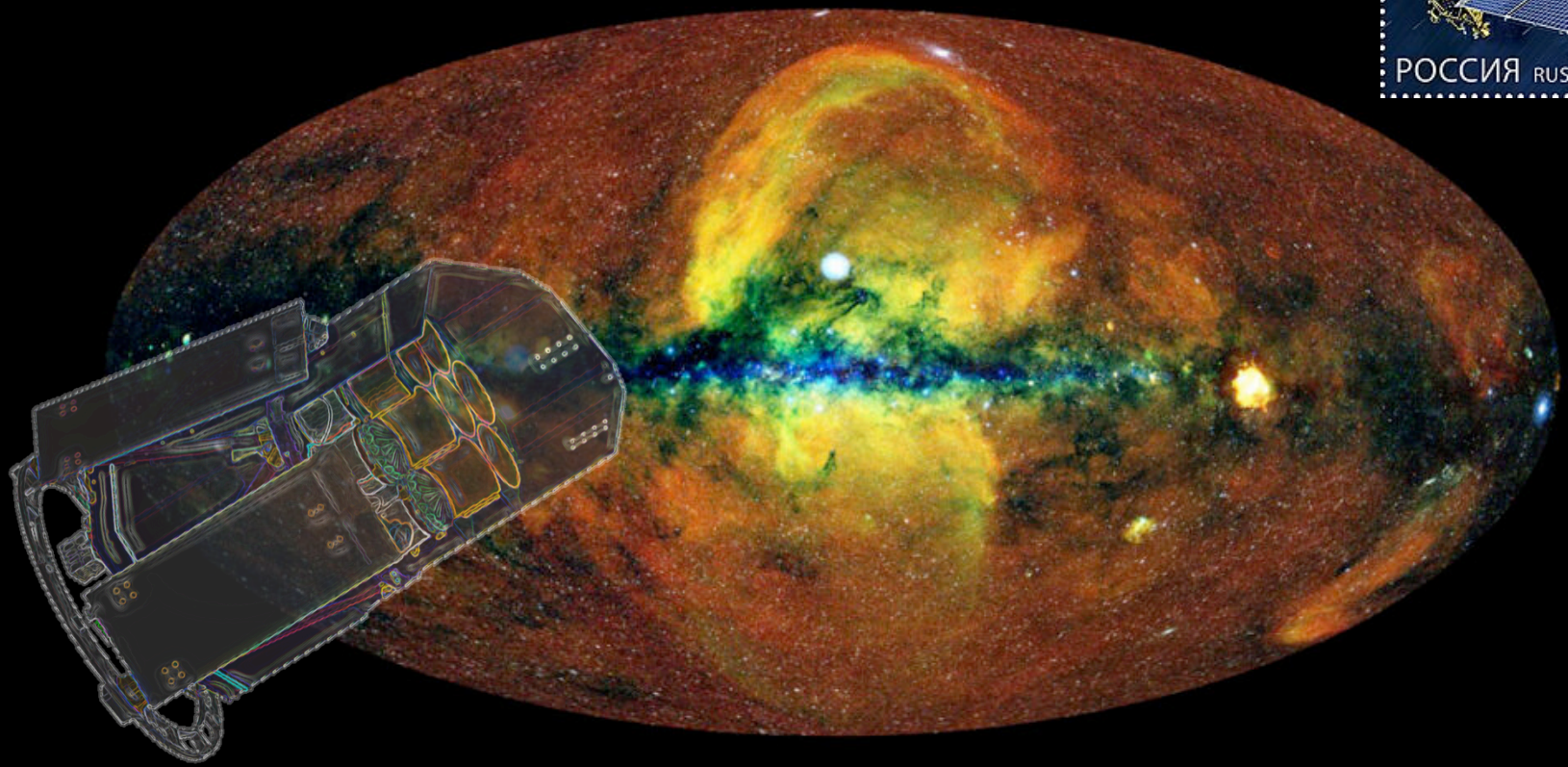

IACHEC, 2021 April 23

Konrad Dennerl, MPE

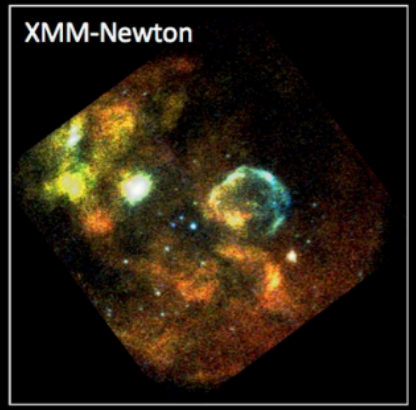

EPIC-PN FL
Dennerl et al. 2001

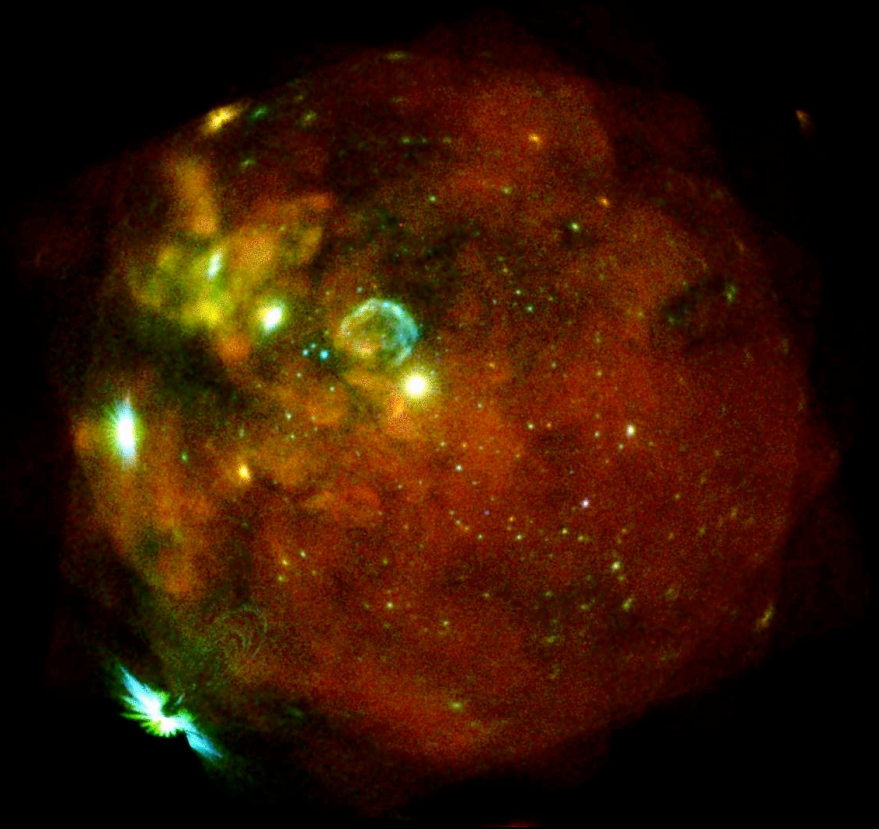

Credit: F. Haberl, M. Freyberg, C. Maitra

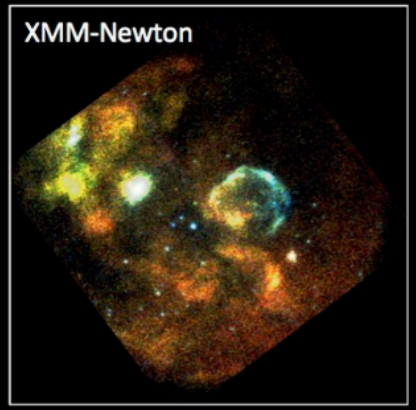

EPIC-PN FL
Dennerl et al. 2001

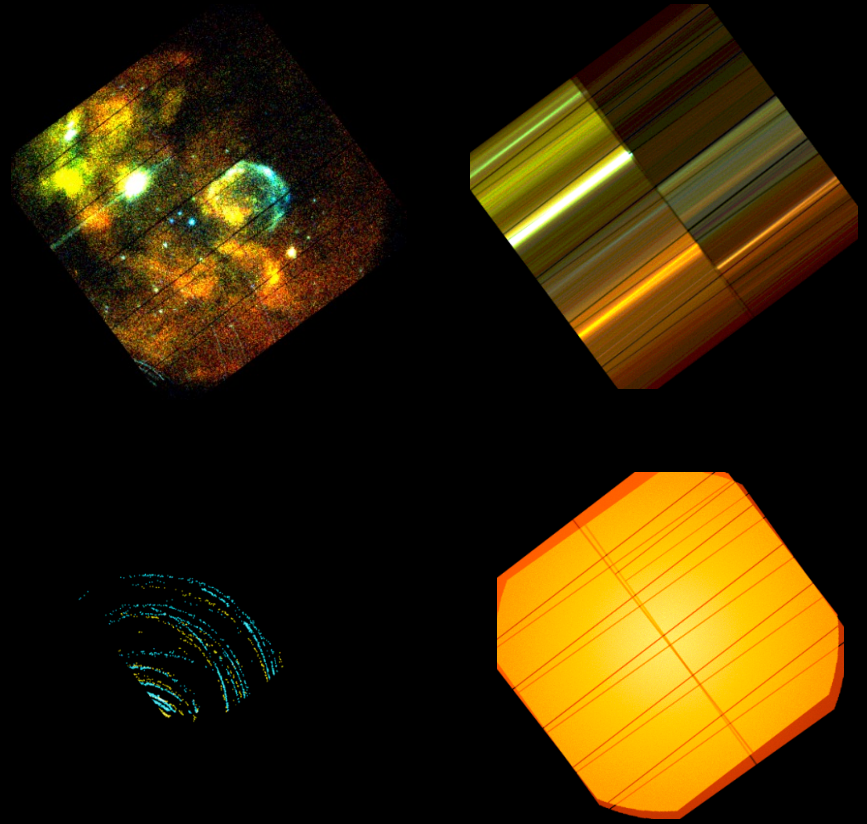

Dennerl et al. 2001

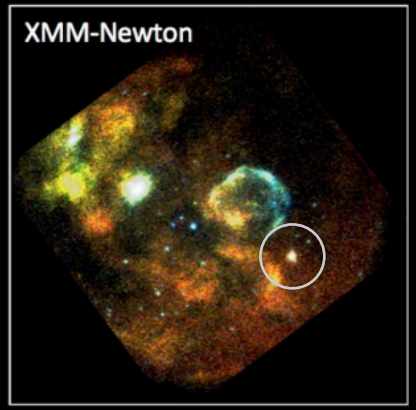

EPIC-PN FL
Dennerl et al. 2001

SN 1987A

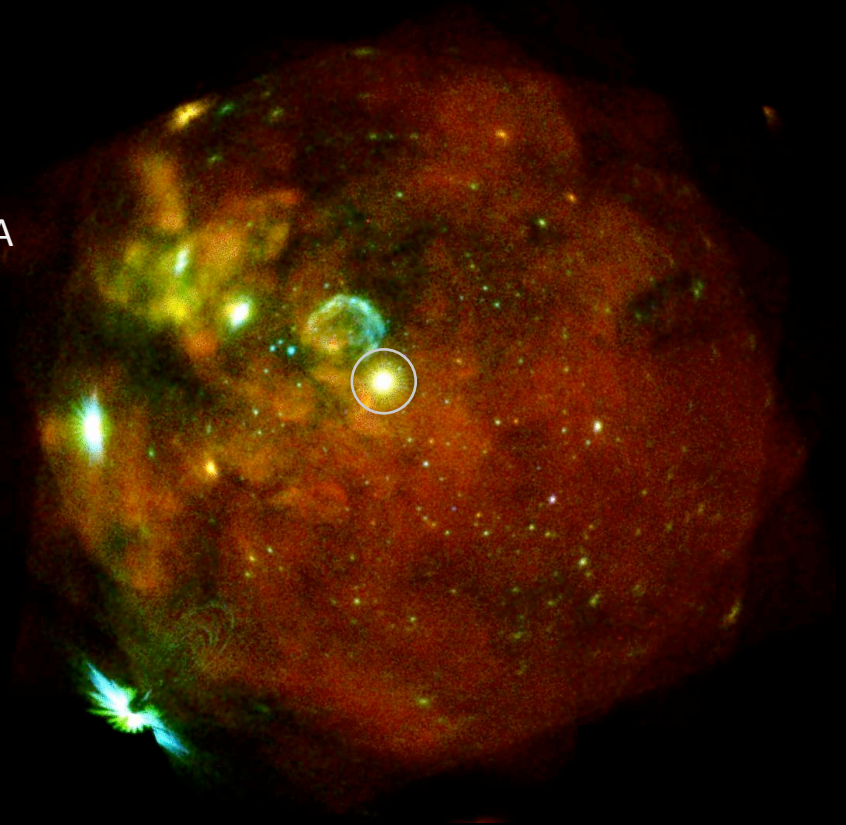

Credit: F. Haberl, M. Freyberg, C. Maitra

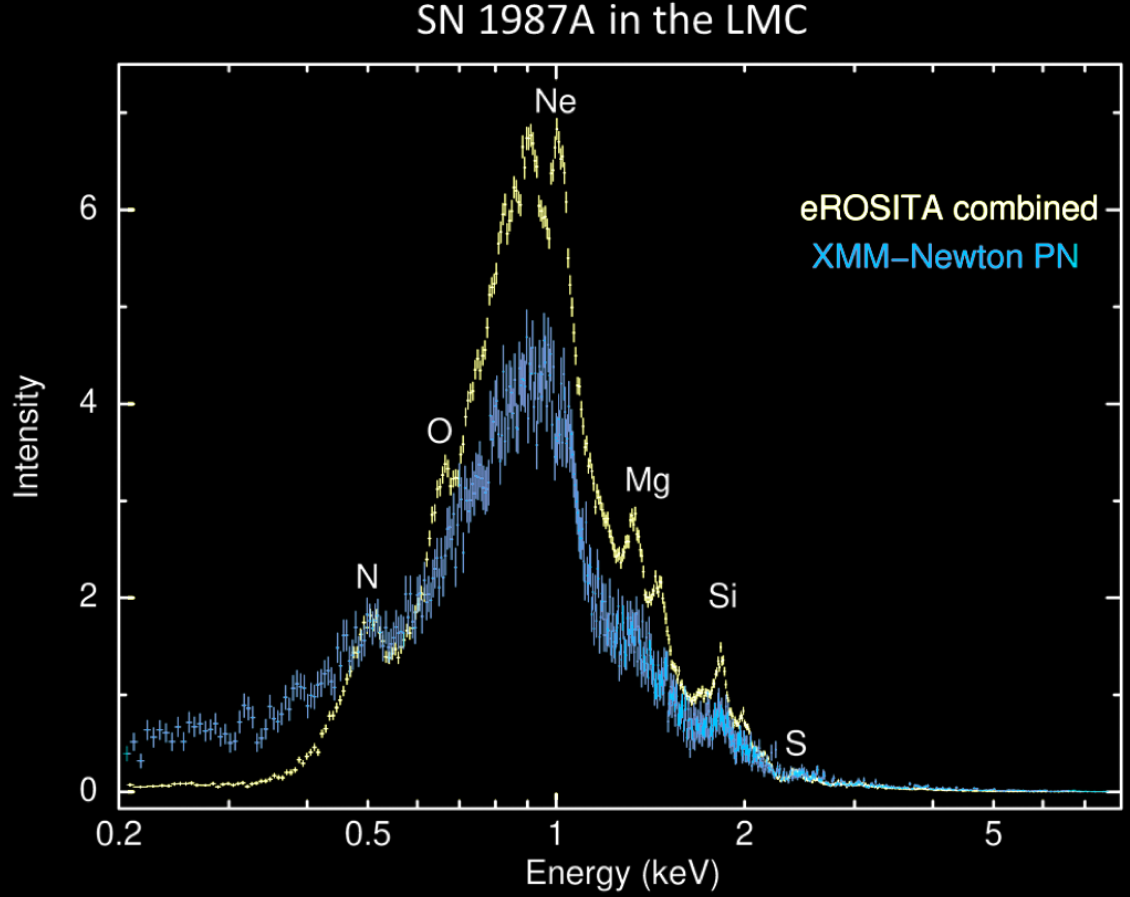

C. Maitra, F. Haberl, MPE/IKI

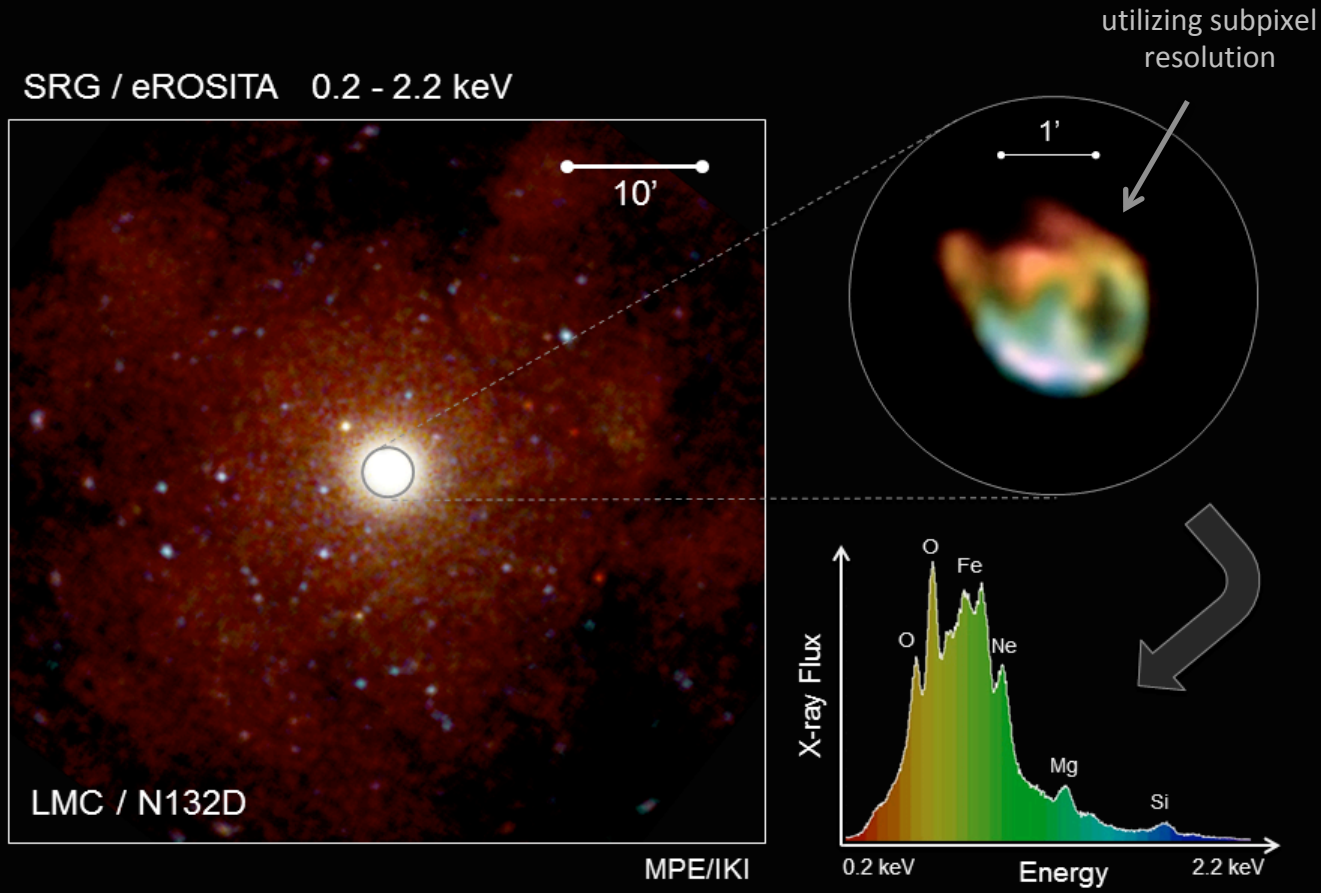
SRG / eROSITA 0.2 - 2.2 keV
10'
LMC / N132D
MPE/IKI
utilizing subpixel resolution
1'
X-ray Flux
O
Fe
O
Ne
Mg
Si
0.2 keV
Energy
2.2 keV

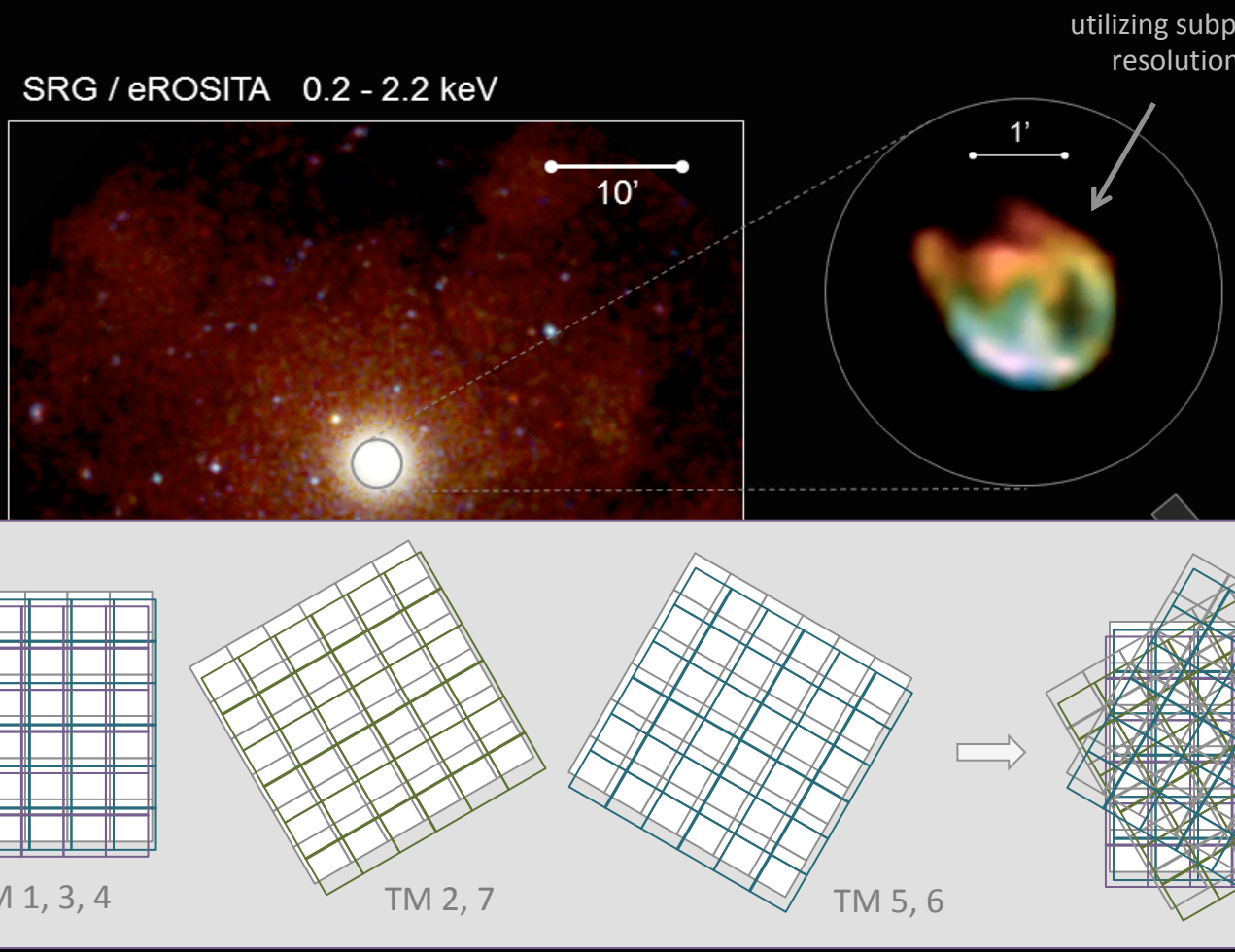
SRG / eROSITA 0.2 - 2.2 keV
10’
utilizing subpixel resolution
1’
TM 1, 3, 4
TM 2, 7
TM 5, 6

Comparison with *XMM-Newton* eRASS:8-like

SRG/eROSITA TM6 0.5-2keV **10-27ks**

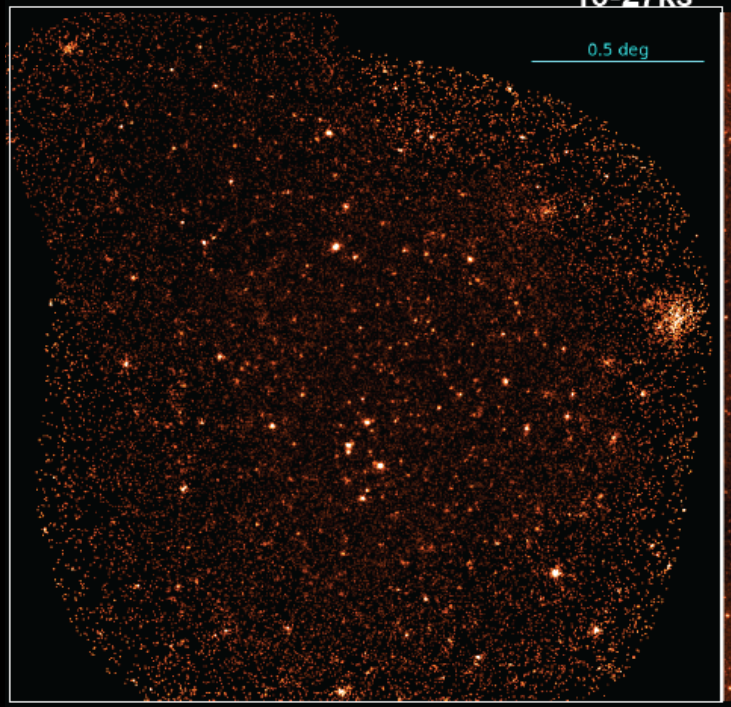

MPE/IKI

10-50ks per pointing *XMM pn+MOS*

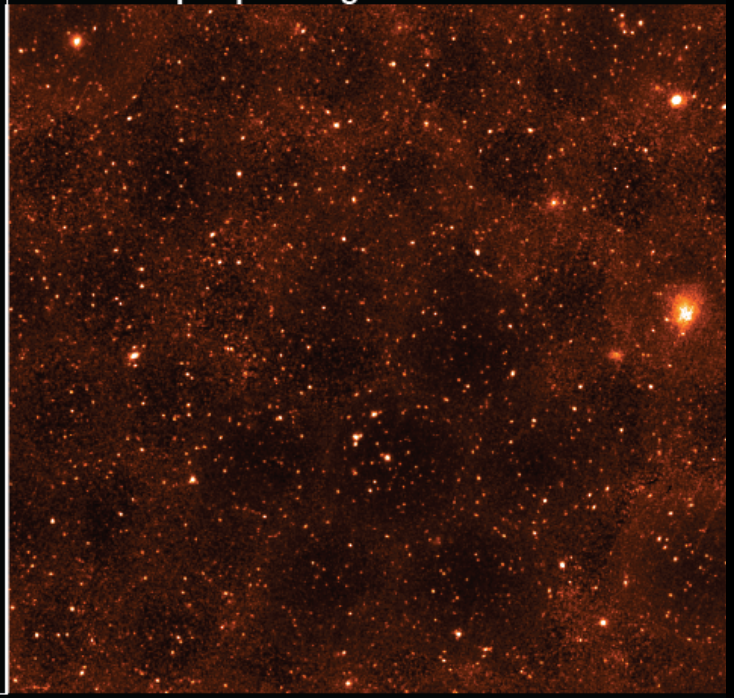

ESA

XXL North Survey field

Image Credit: M. Ramos (MPE)

3 observing modes:

- pointing
- field scan
- survey

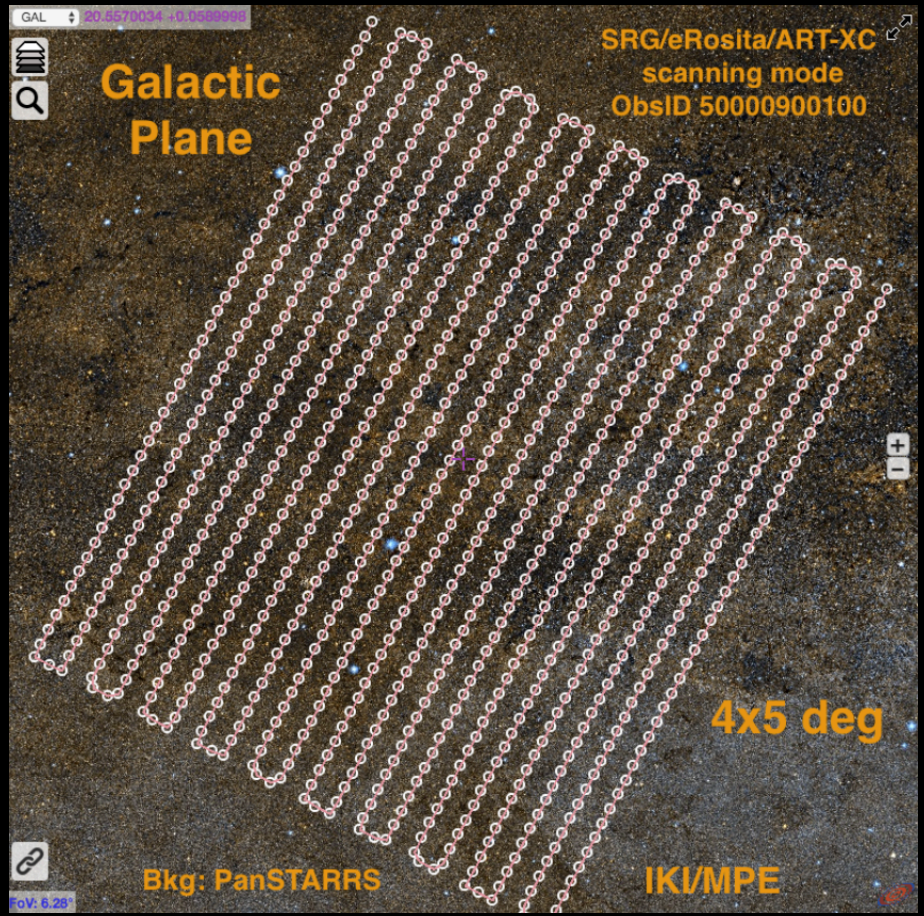

eFEDS: a preview of eRASS:8

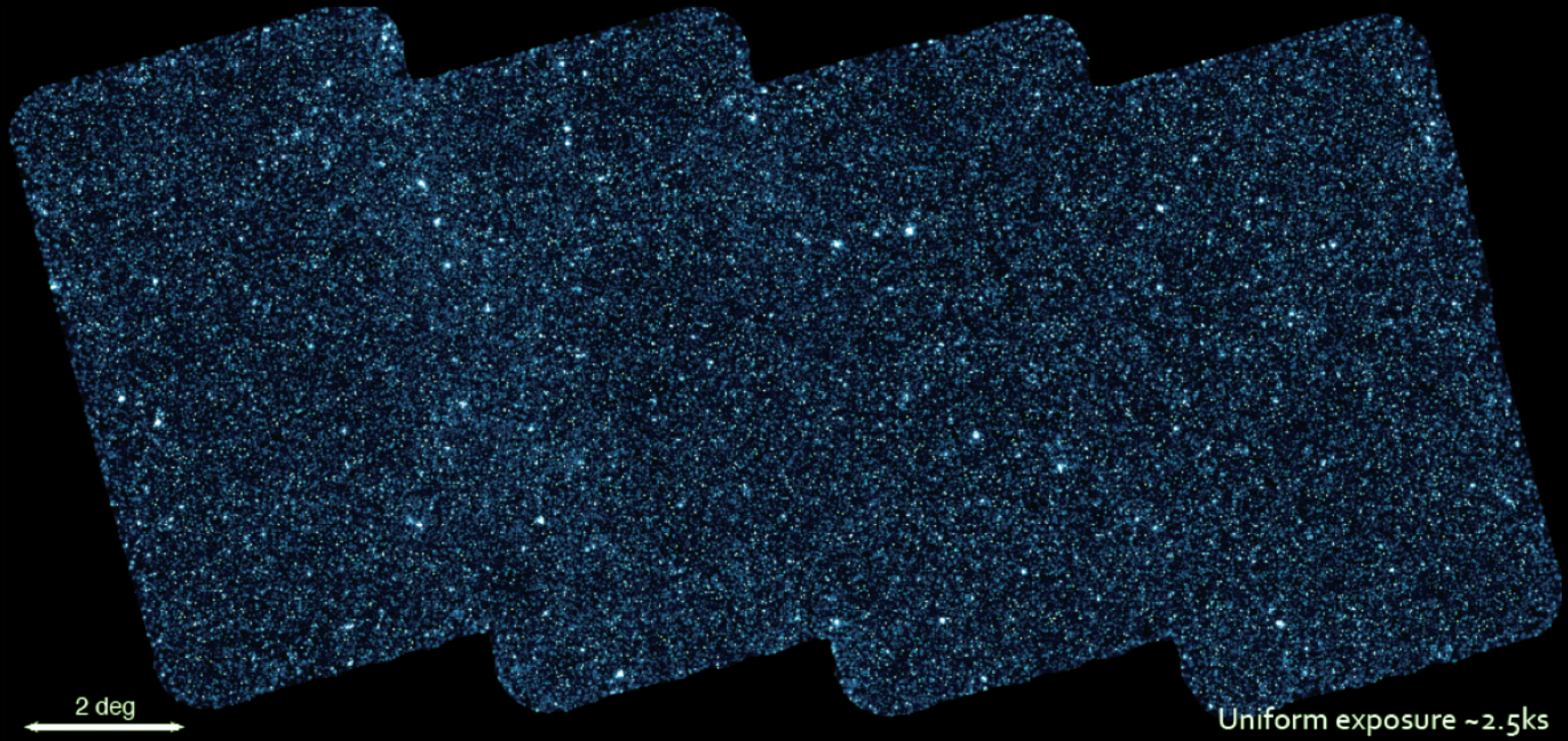

Exposure corrected image in the 0.5 − 2.0 keV band

Credit: H. Brunner, M. Ramos-Ceja

Isolated neutron star PSR B0656+14

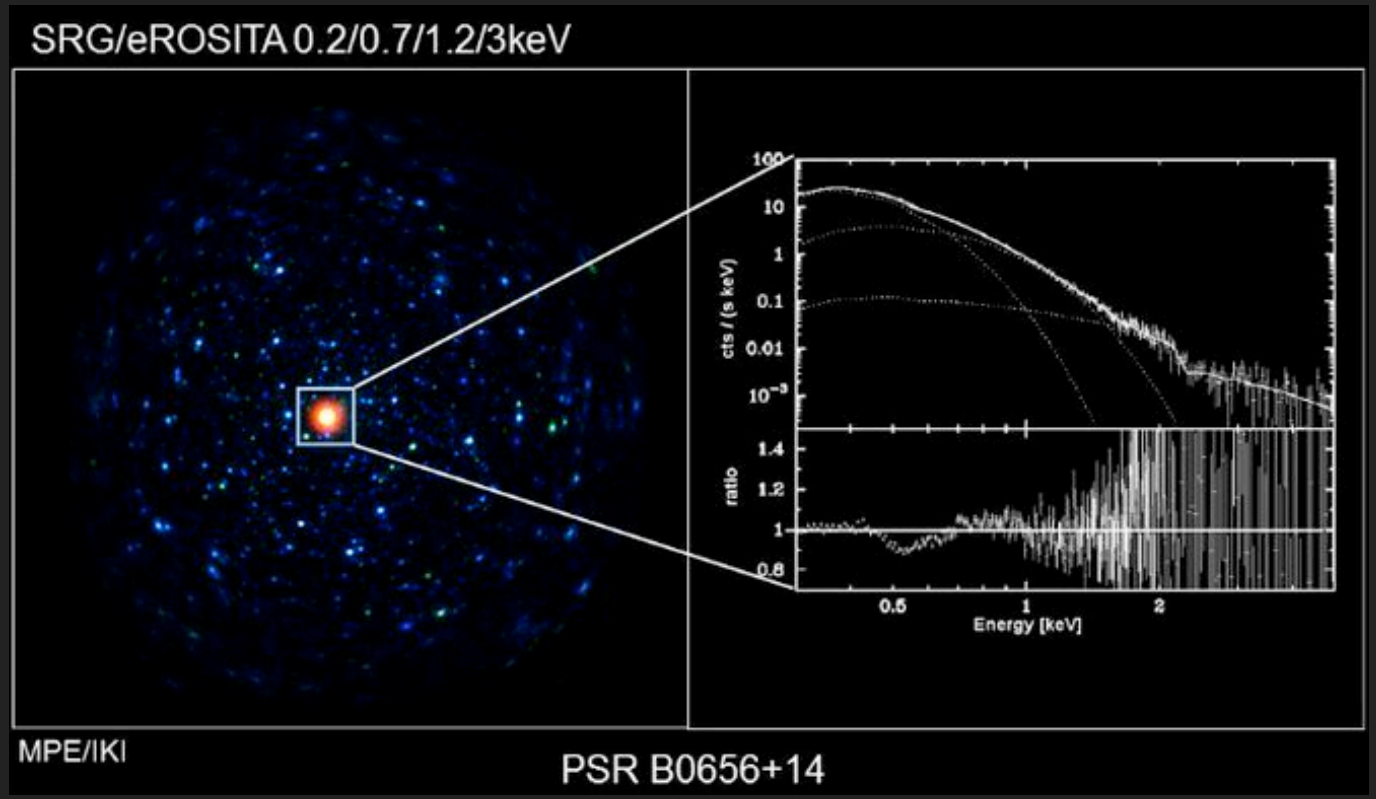

385 ms pulsar, 50 ms time resolution

Isolated neutron star PSR B0656+14

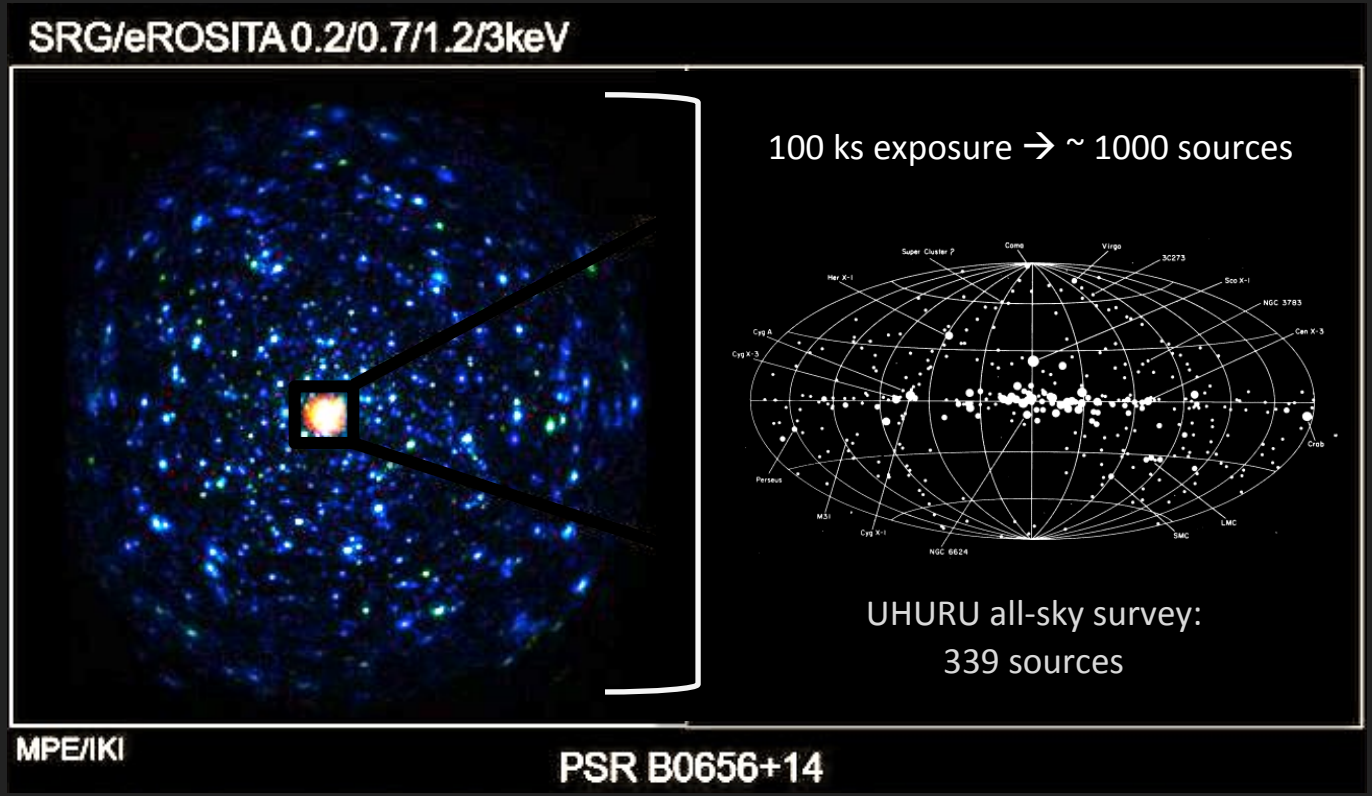

385 ms pulsar, 50 ms time resolution

Abell 3391/3395

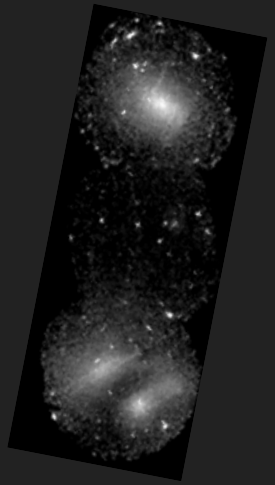

XMM-Newton
0.4 – 1.25 keV

Abell 3391/3395

SRG/eROSITA
0.2-2.0 keV

eROSITA PV phase

T. Reiprich (Univ. Bonn), M. Ramos-Ceja (MPE),
F. Pacaud (Univ. Bonn), D. Eckert (Univ. Geneva),
J. Sanders (MPE), N. Ota (Univ. Bonn),
E. Bulbul (MPE), V. Ghirardini (MPE)

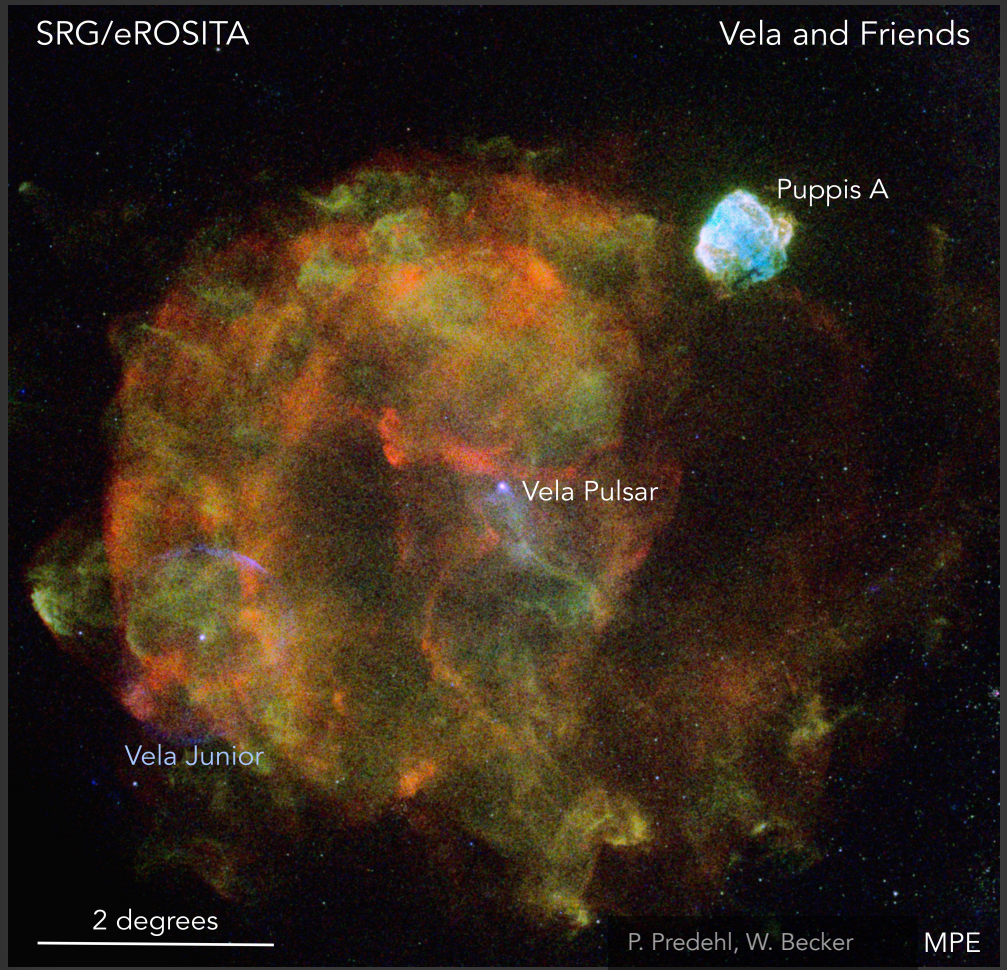
SRG/eROSITA
Vela and Friends
Puppis A
Vela Pulsar
Vela Junior
2 degrees
P. Predehl, W. Becker
MPE

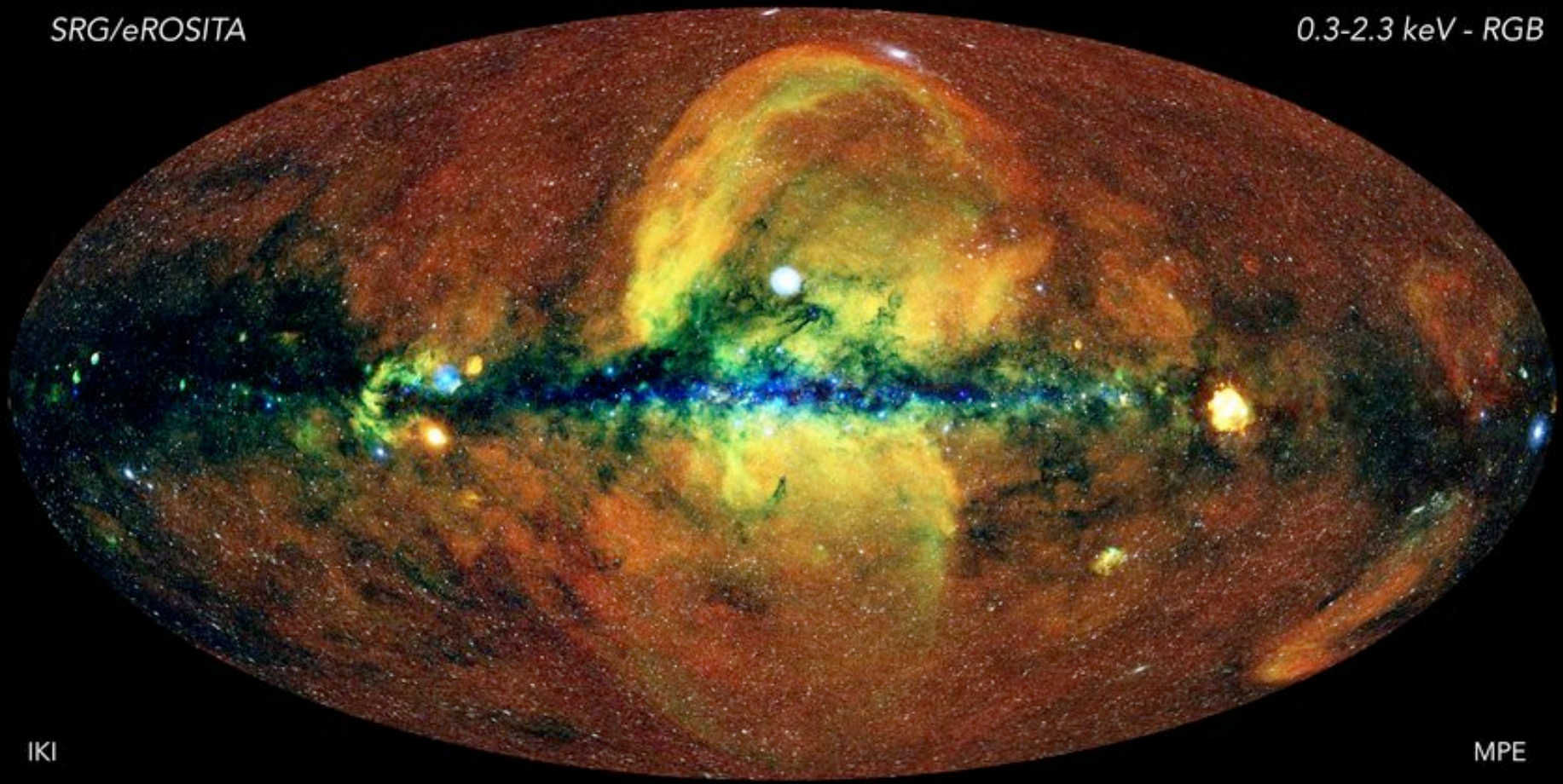
SRG/eROSITA
0.3-2.3 keV - RGB
IKI
MPE

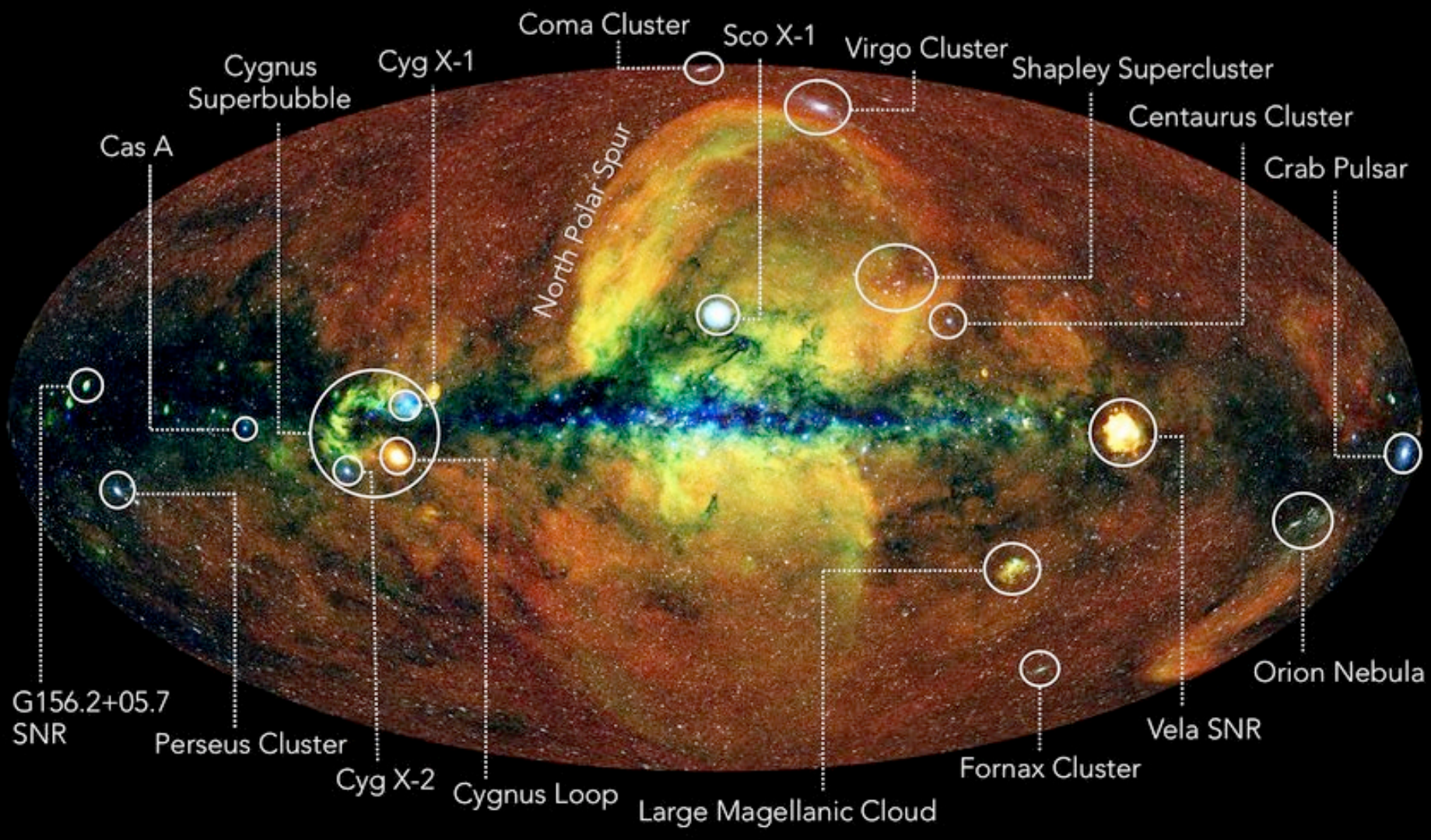
Coma Cluster
Sco X-1
Virgo Cluster
Shapley Supercluster
Centaurus Cluster
Crab Pulsar
Cygnus Superbubble
Cyg X-1
Cas A
North Polar Spur
Orion Nebula
G156.2+05.7 SNR
Perseus Cluster
Cyg X-2
Cygnus Loop
Large Magellanic Cloud
Fornax Cluster
Vela SNR

ROSAT + XMM / EPIC-pn → eROSITA

(extended ROentgen Survey with an Imaging Telescope Array)

eROSITA on SRG (Spectrum-Roentgen-Gamma): Mirror Side

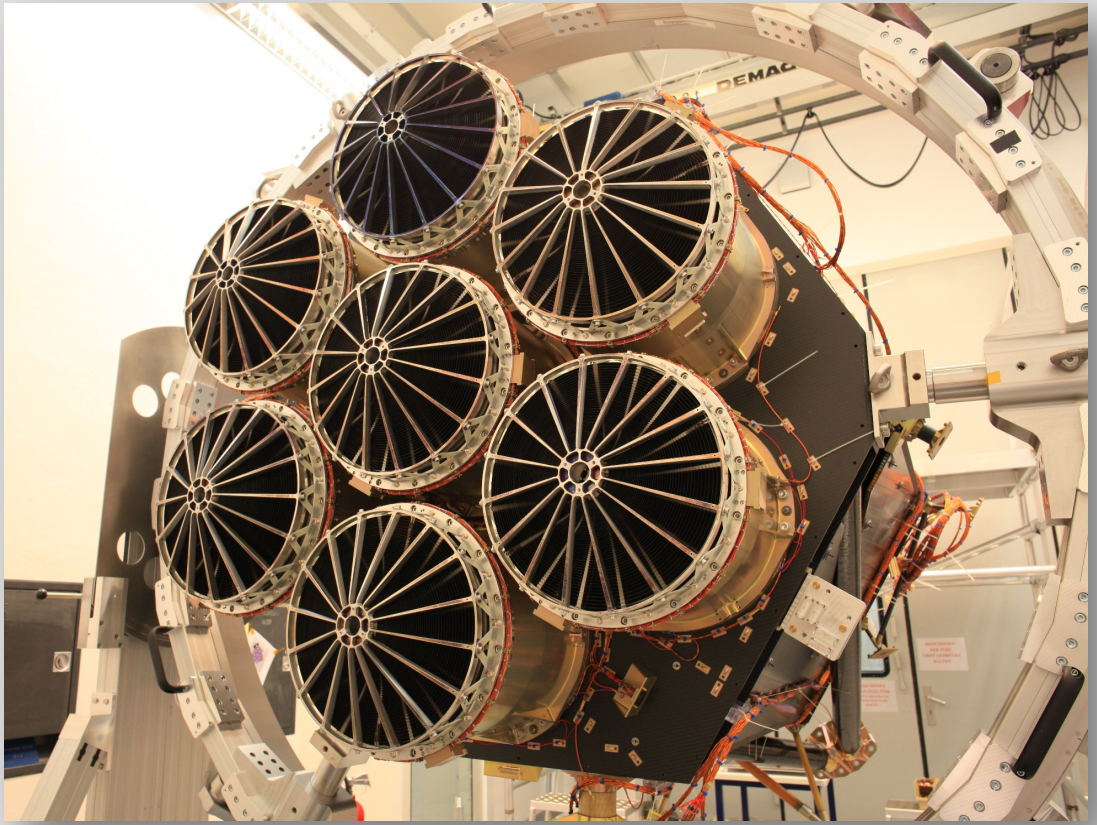

- 7 telescope modules (TM)
- 54 nested gold-coated nickel mirror shells
- focal length: 1600 mm
- field of view: 1 deg diameter
- on-axis HEW: 16“

eROSITA on SRG (Spectrum-Roentgen-Gamma): Detector Side

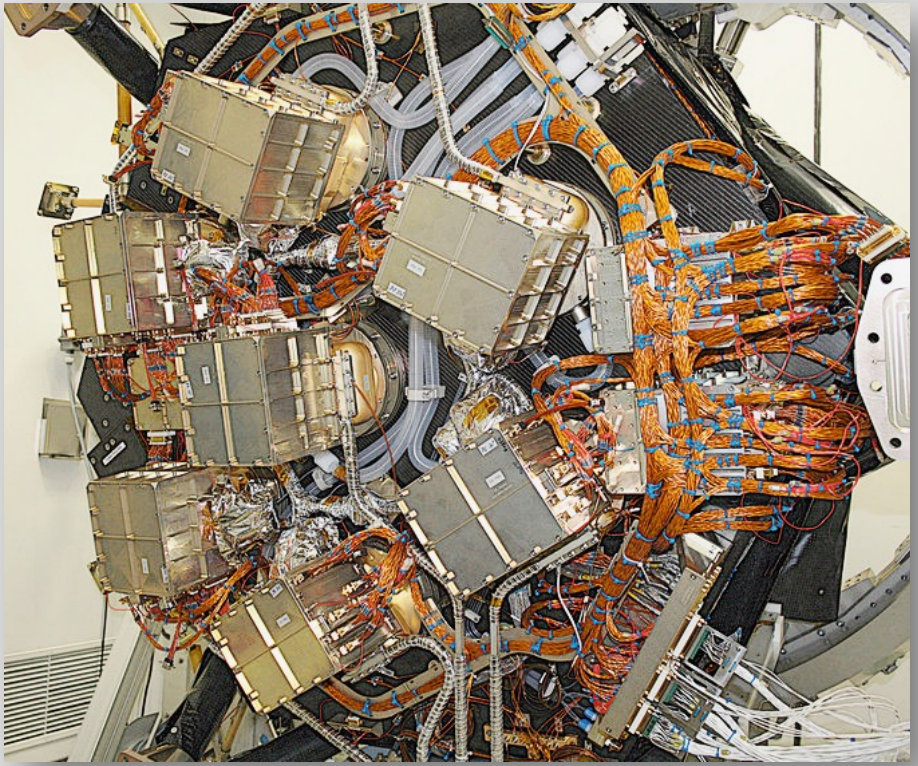

- 7 pn-CCDs with framestore
- 5 CCDs with 200 nm Al filter, 2 without
- 384 x 384 pixels of 75µm x 75 µm
- 50 ms cycle time
- 7 filter wheels with four positions:
  open, closed, ^{55}Fe cal, filter

filter: 5 x 200 nm PI, 2 x 200 nm PI + 100 nm Al

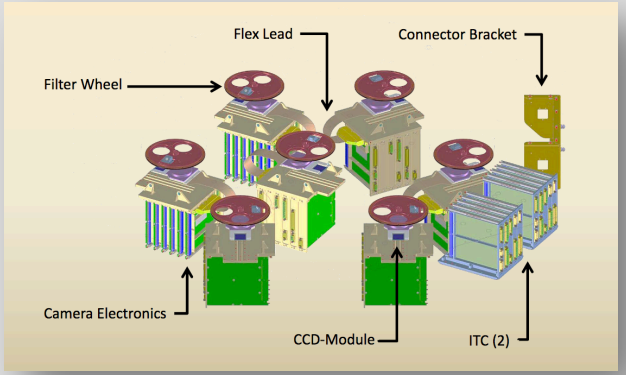

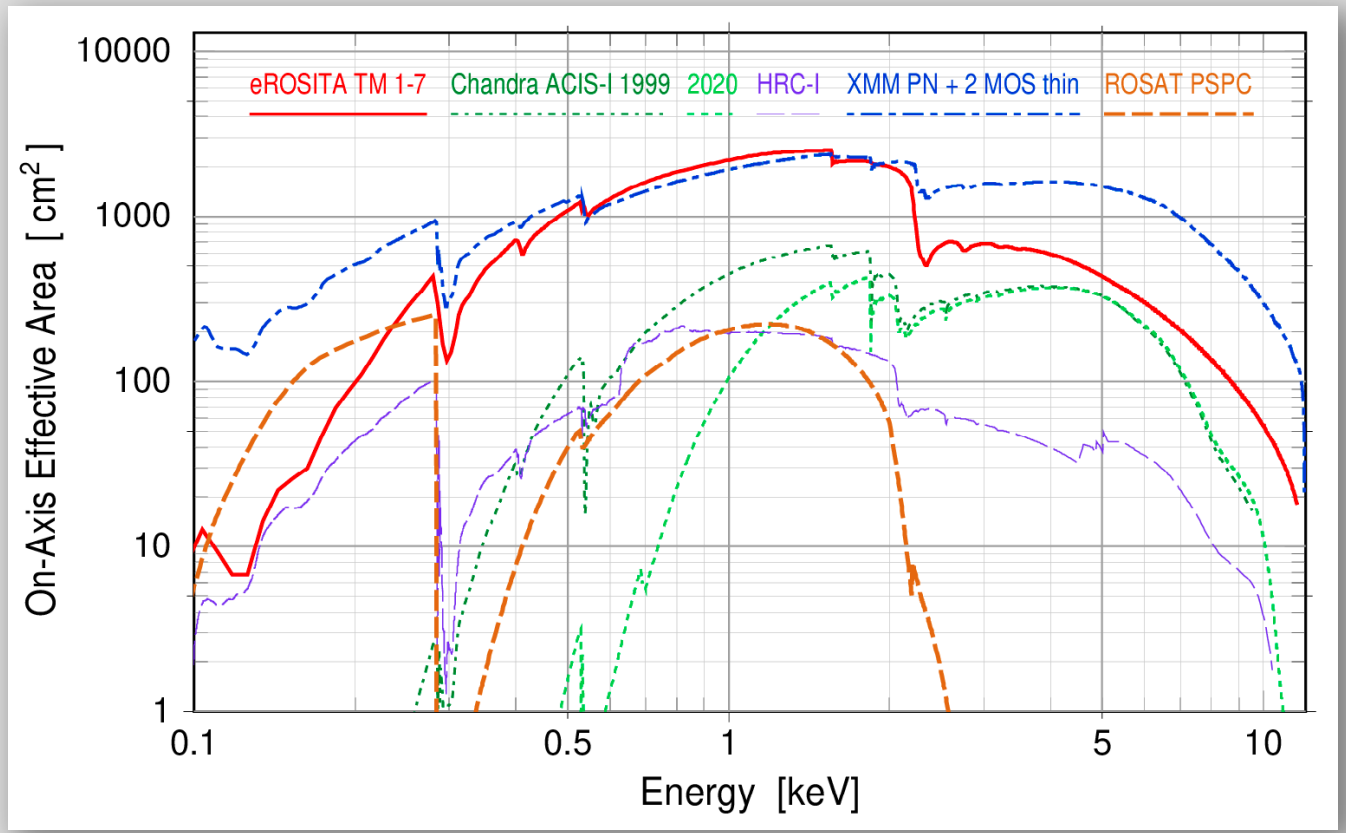

On-Axis Effective Area of eROSITA comparable to XMM-Newton

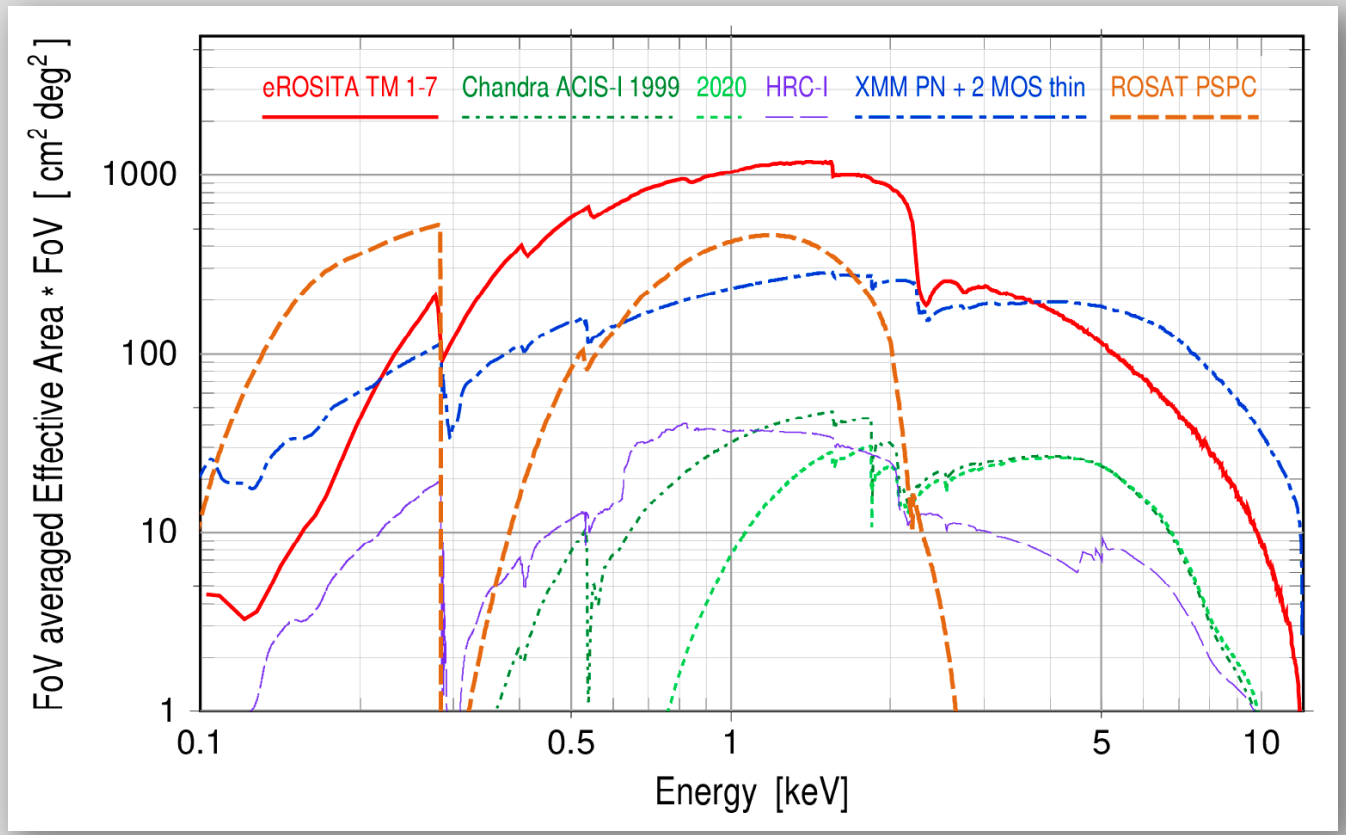

Grasp of eROSITA about 5 times higher than that of XMM-Newton

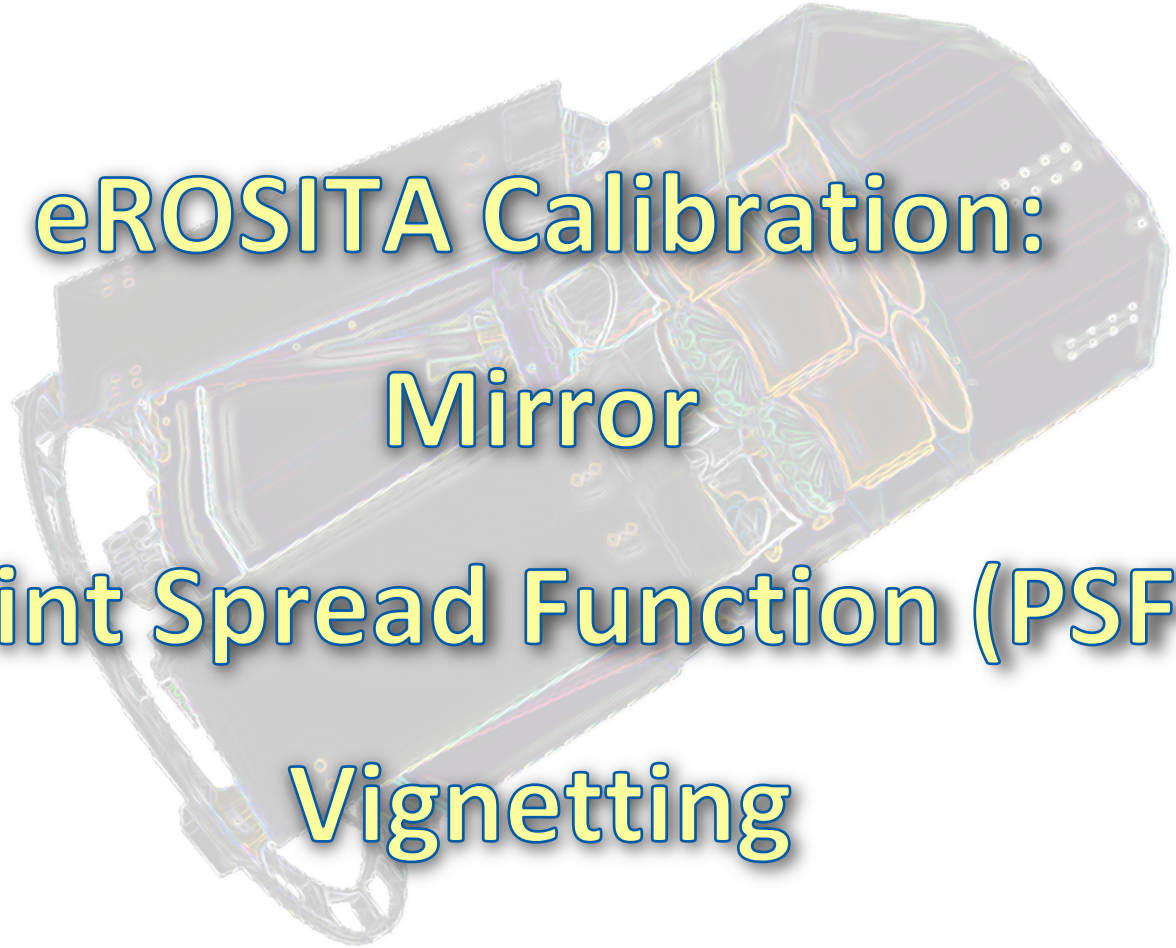

eROSITA Calibration:

Mirror

Point Spread Function (PSF)

Vignetting

X-ray test facility
PANTER
near Munich, Germany

Determination of the eROSITA on-axis PSF

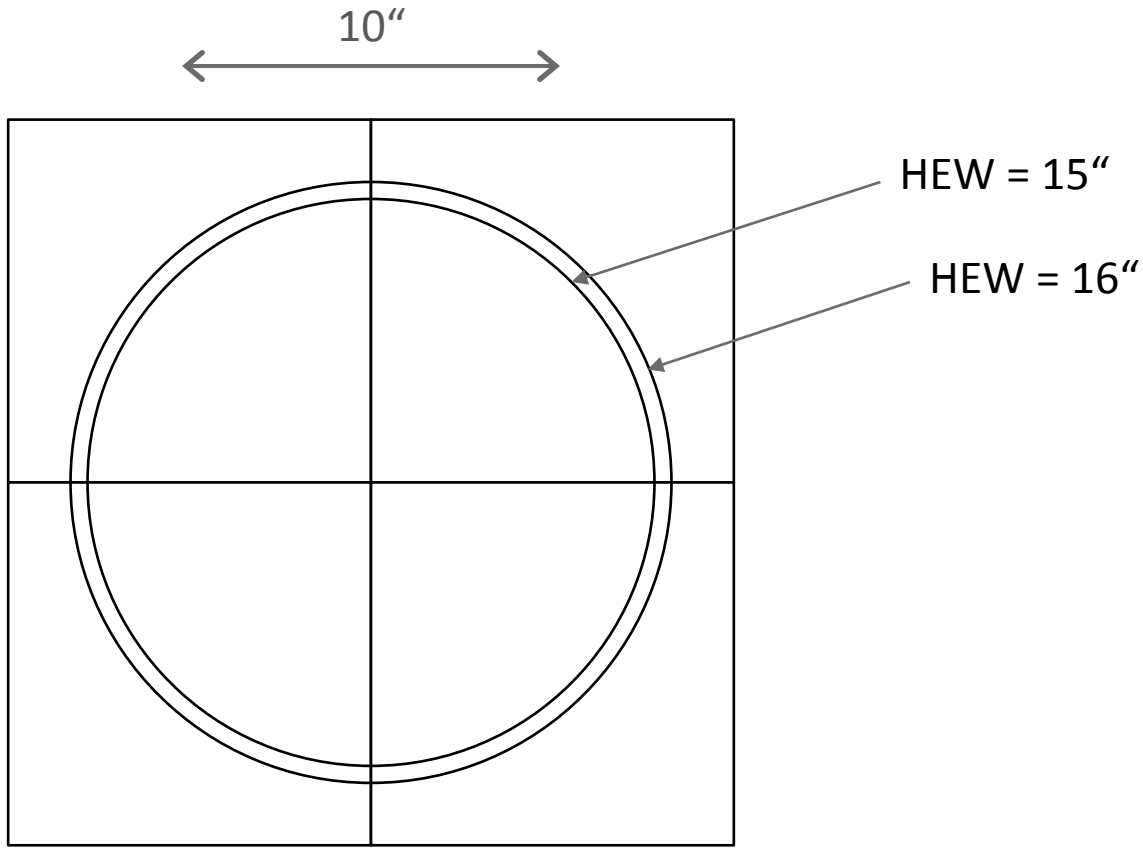

1 px = 9.6“ x 9.6“
= 75 µm x 75 µm

Determination of the eROSITA on-axis PSF

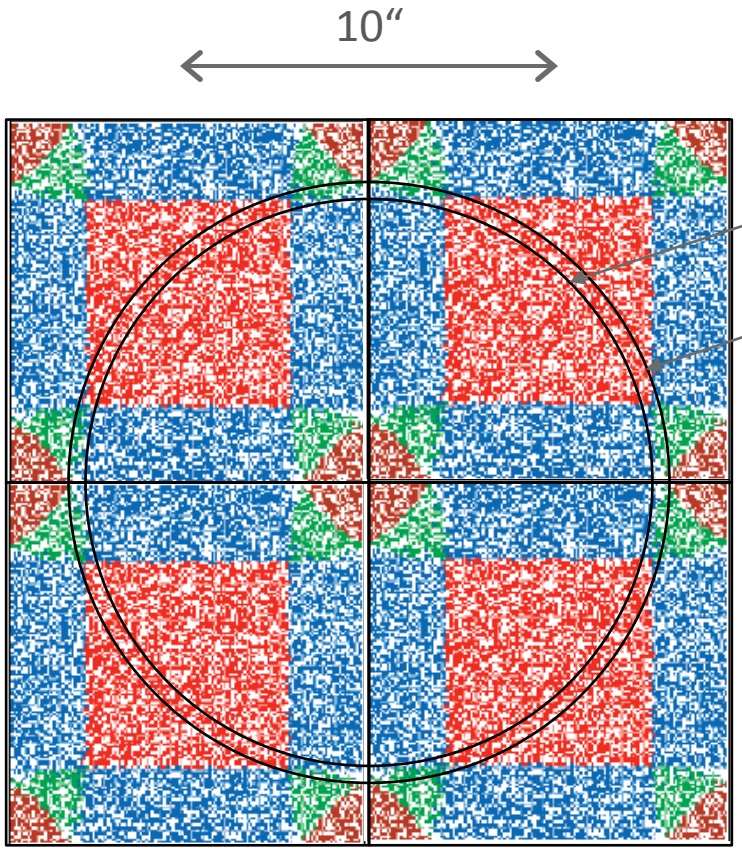

1 px = 9.6“ x 9.6“
= 75 µm x 75 µm

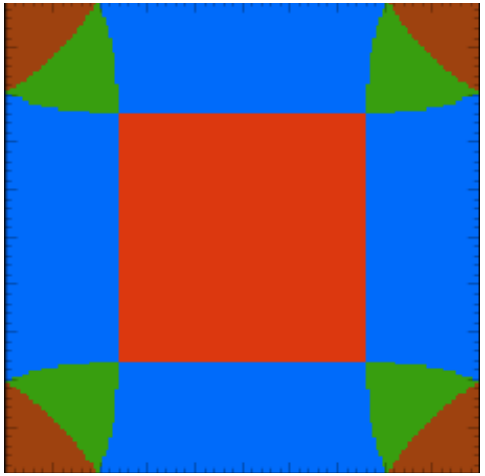

pixel size

using subpixel information for **all valid patterns**

Al-K

12 x 12 raster

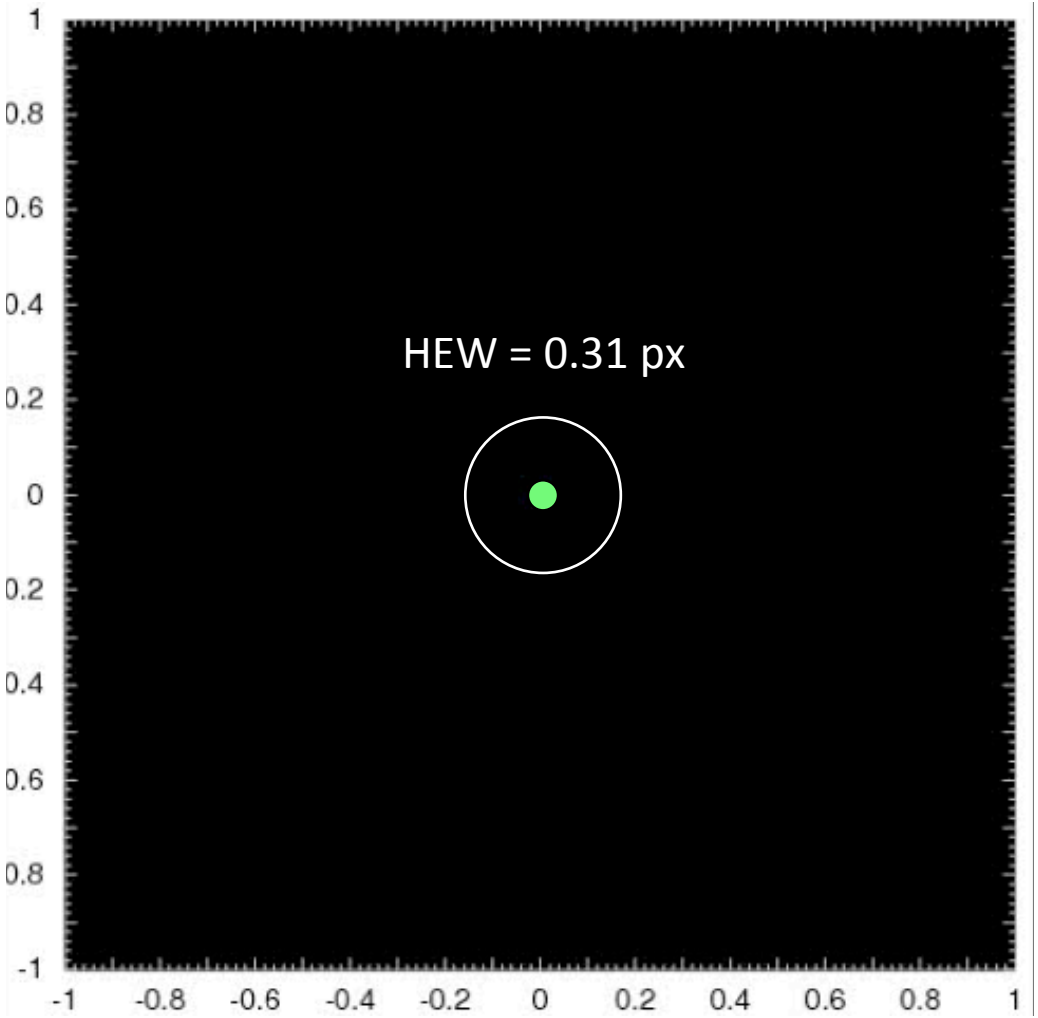

Determination of the eROSITA on-axis PSF

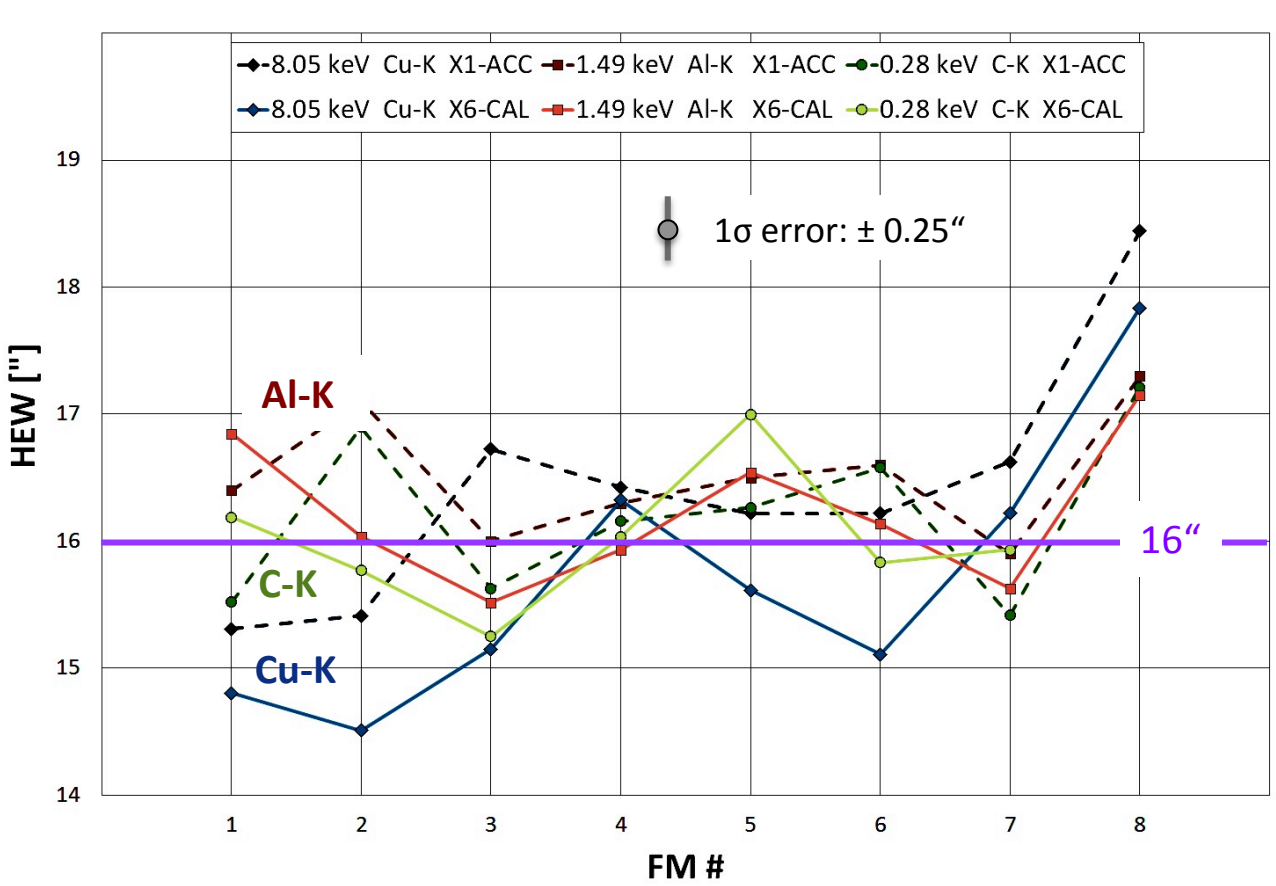

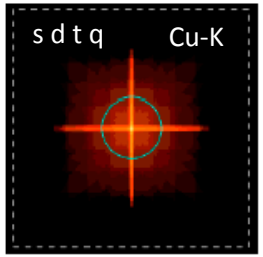

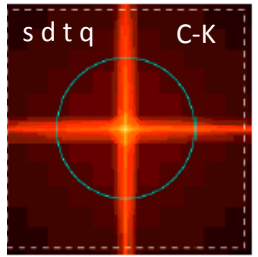

Determination of the eROSITA off-axis PSF

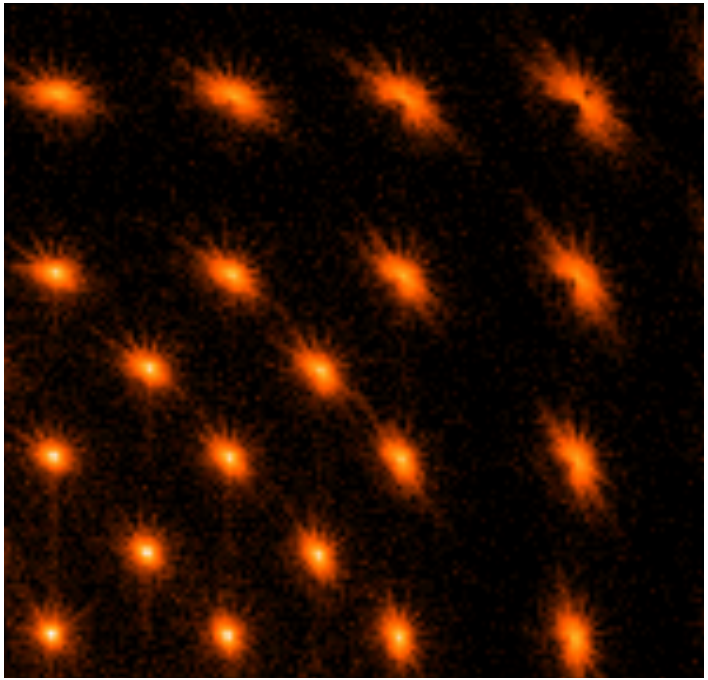

1.5 keV

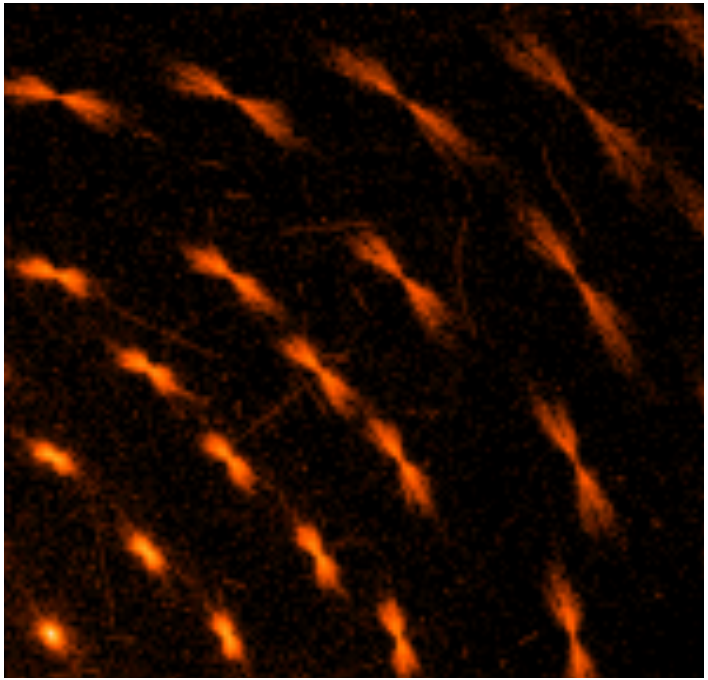

6.4 keV

1 pixel scan takes ~ 6-8 hours: how can we shorten the exposure time ?

Method : operate the CCD in „charge accumulation mode“

1) utilize the fact that the dominant photon energy is known
2) analyse the accumulated charges (challenge: MIP suppression)
3) abandon subpixel resolution (not required for off-axis PSF)

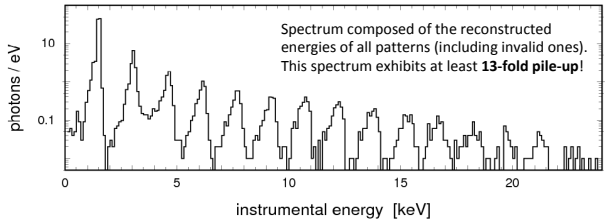

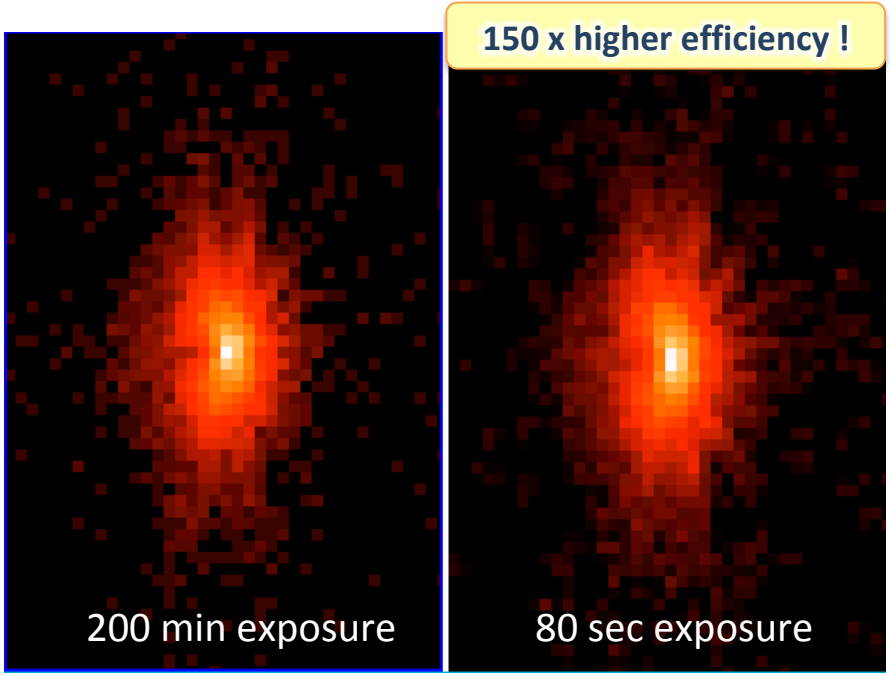

Challenge: MIP suppression

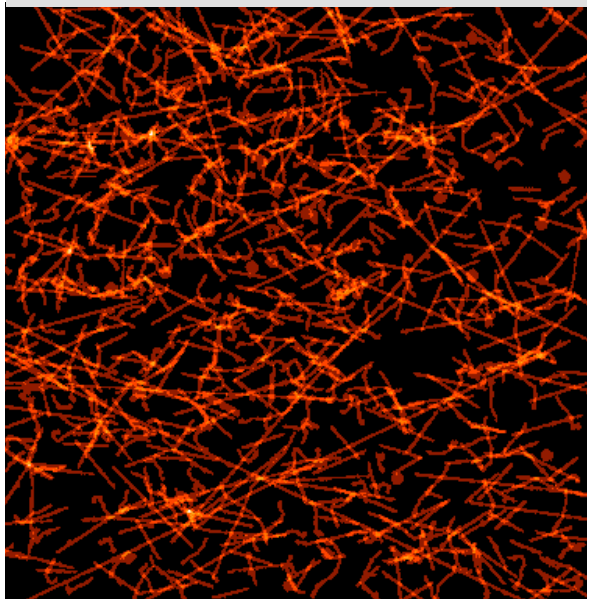

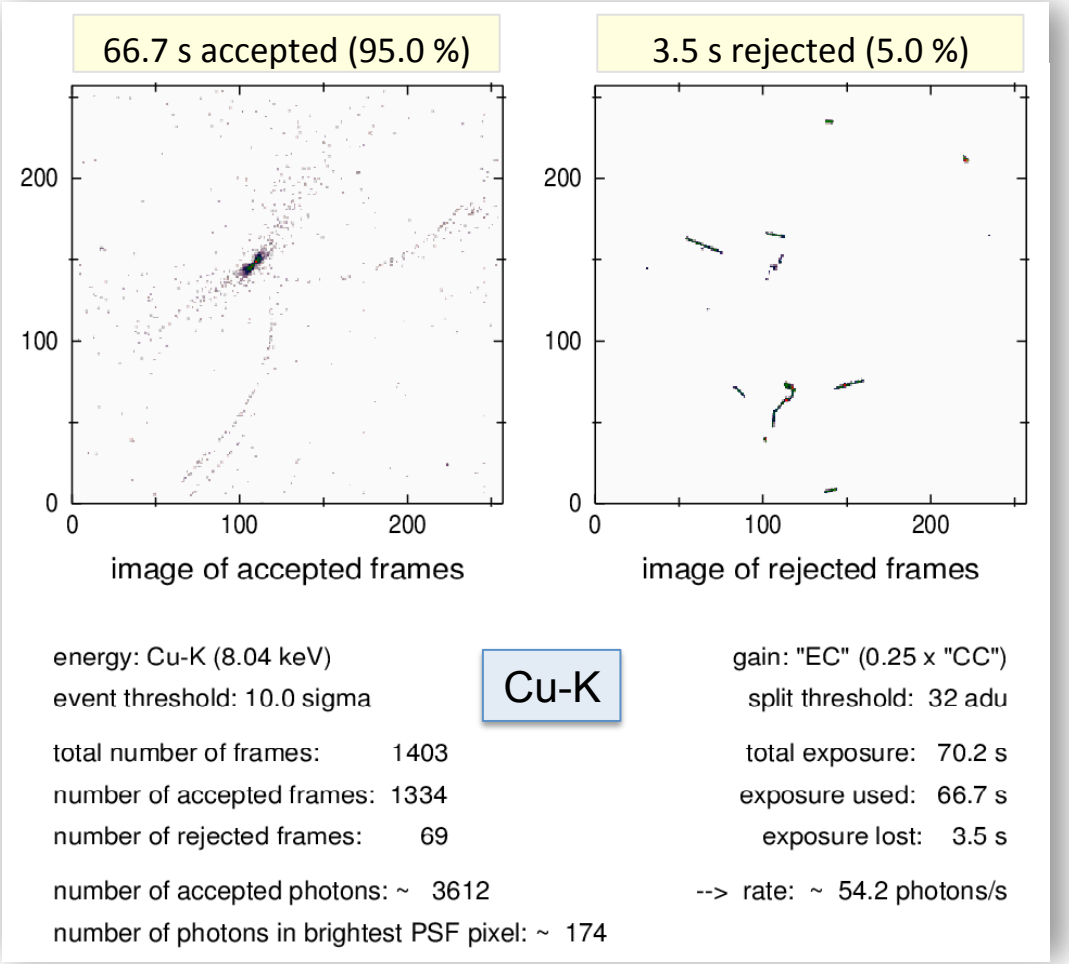

Operating the CCD in „charge accumulation mode“

Challenge: Suppression of MIPs in the case of extreme pile-up

Solution: reject all frames which contain ‚suspicious‘ features

PSF Focal Plane Mapping

PANTER Geometry (overview)

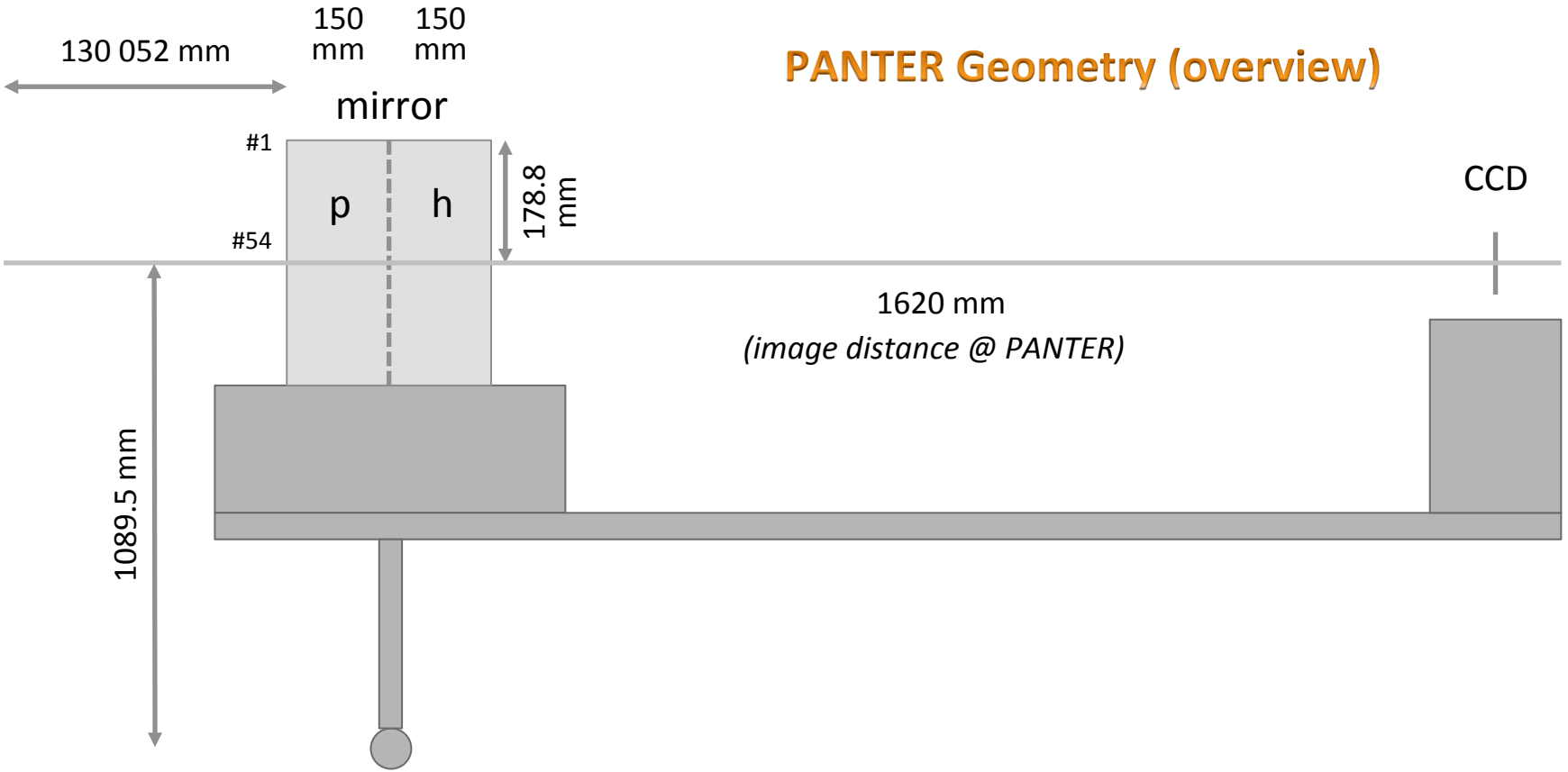

PSF Focal Plane Mapping

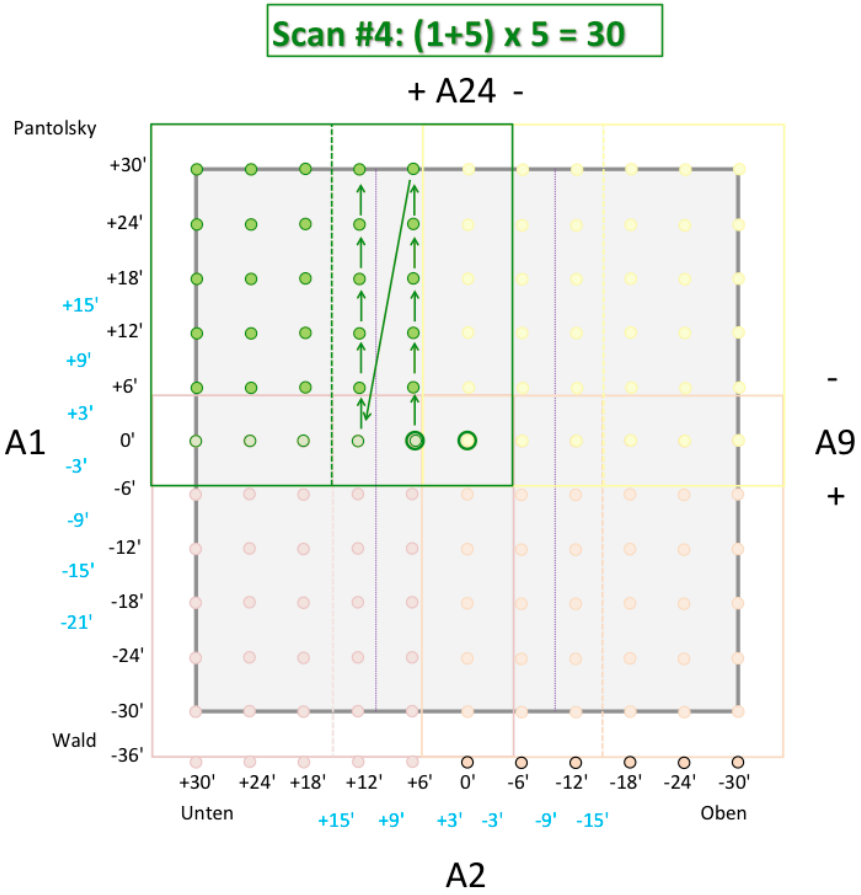

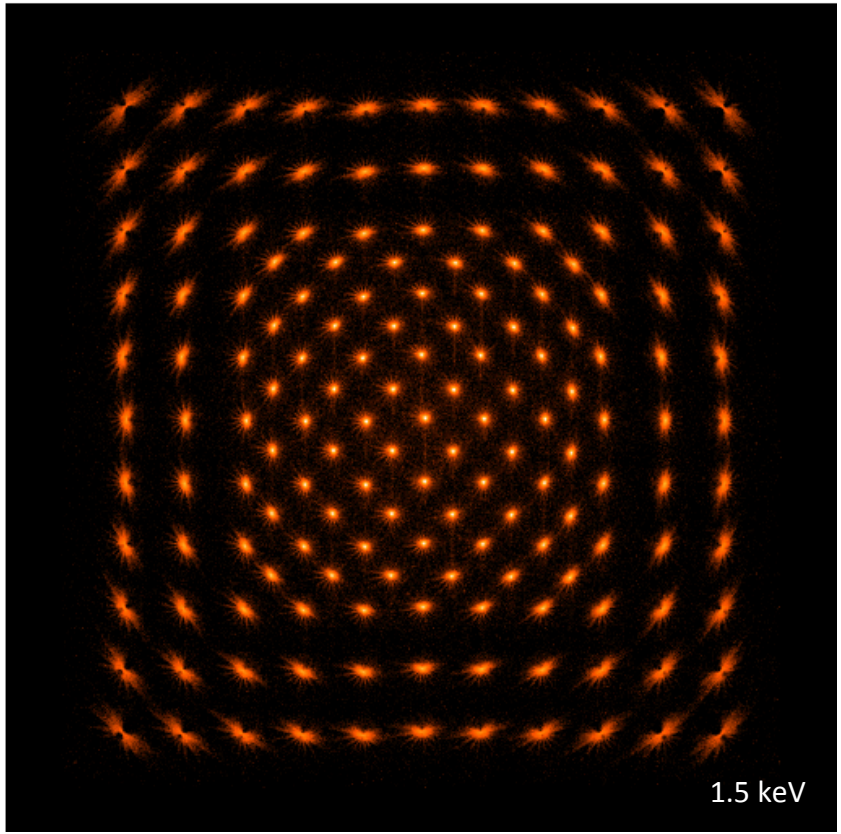

PSF Focal Plane Mapping

PANTER Geometry (details)

X-ray source distance to mirror center: S = 123 822 mm

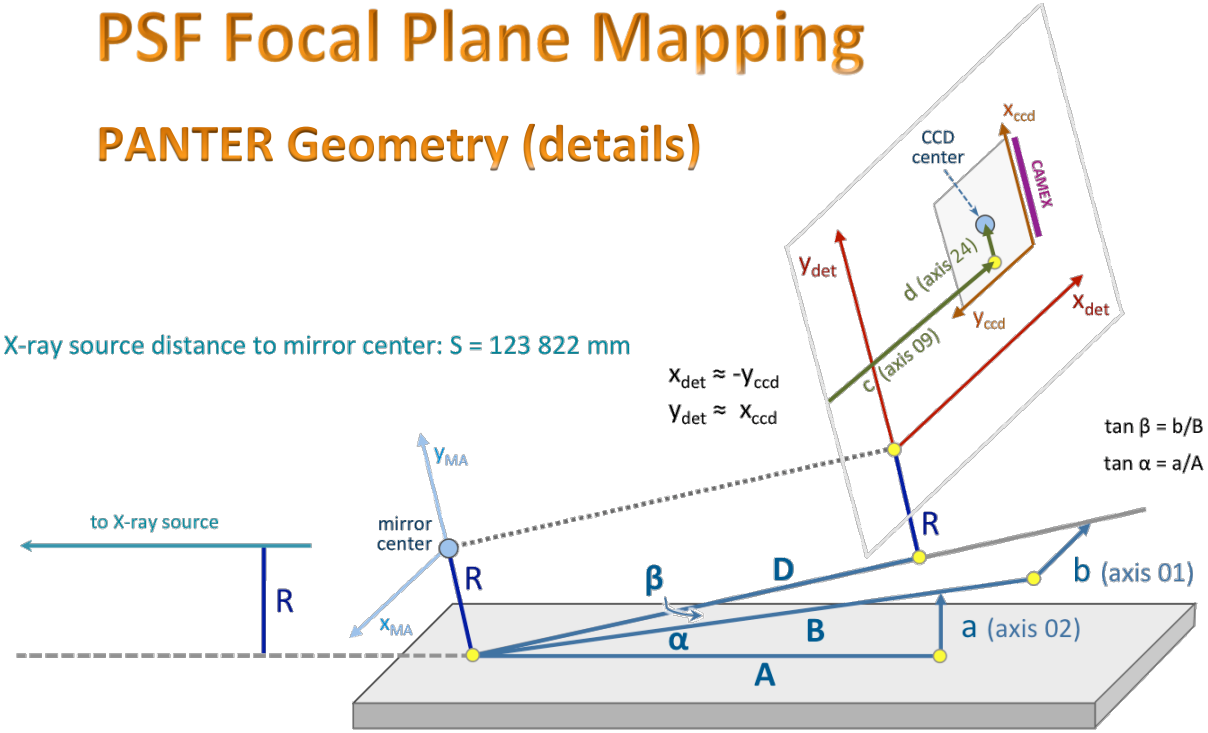

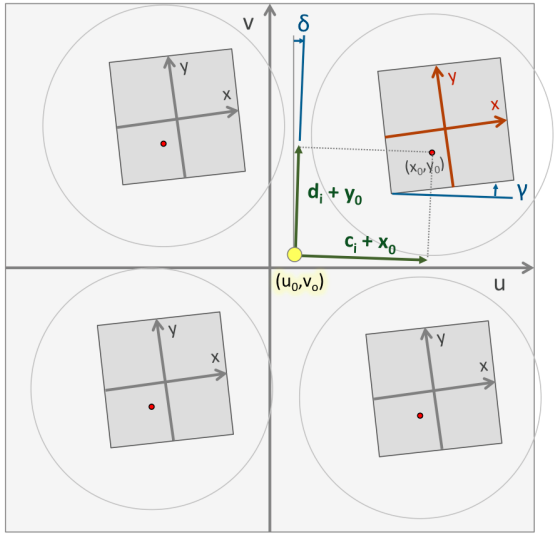

$u_i = c_i + x_0 + (x-x_0) \cos\gamma - (y-y_0) \sin\gamma$
$v_i = d_i + y_0 + (x-x_0) \sin\gamma + (y-y_0) \cos\gamma$

$u_i' = u_0 + (u_i-u_0) \cos\delta - (v_i-v_0) \sin\delta$
$v_i' = v_0 + (u_i-u_0) \sin\delta + (v_i-v_0) \cos\delta$

D = 1622.2 mm
A = 3060.4 mm (62.5 nm/step)
B = 3270.0 mm (1.25 µm/step) (+/- 10mm)
R = 1089.5 mm

1 step = 62.5 nm
4610017 steps → α = 5.37835 deg
→ a = 288.126 mm
→ A = a / tan α = 3060.4 mm

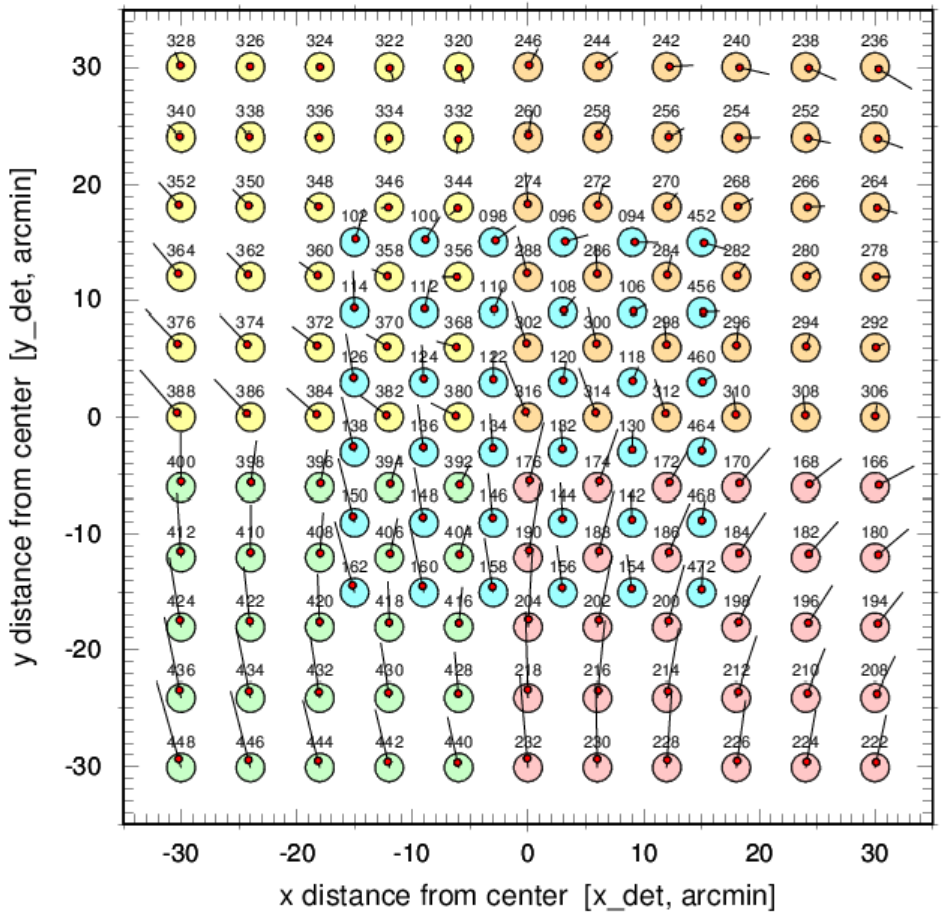

PSF Focal Plane Mapping

without geometric correction

large circles: predicted PSF centers
small circles: corr. measured PSF centers
displacement lines enlarged by factor 10.0

A = 3060.4 mm, B = 3270.0 mm, C = 1621.0 mm
gamma = 0.0 arcmin, delta = 0.0 arcmin
x = (128.0 - y_ccd) , y = (x_ccd - 128.0)

mean positional 1σ deviation: 20.6“

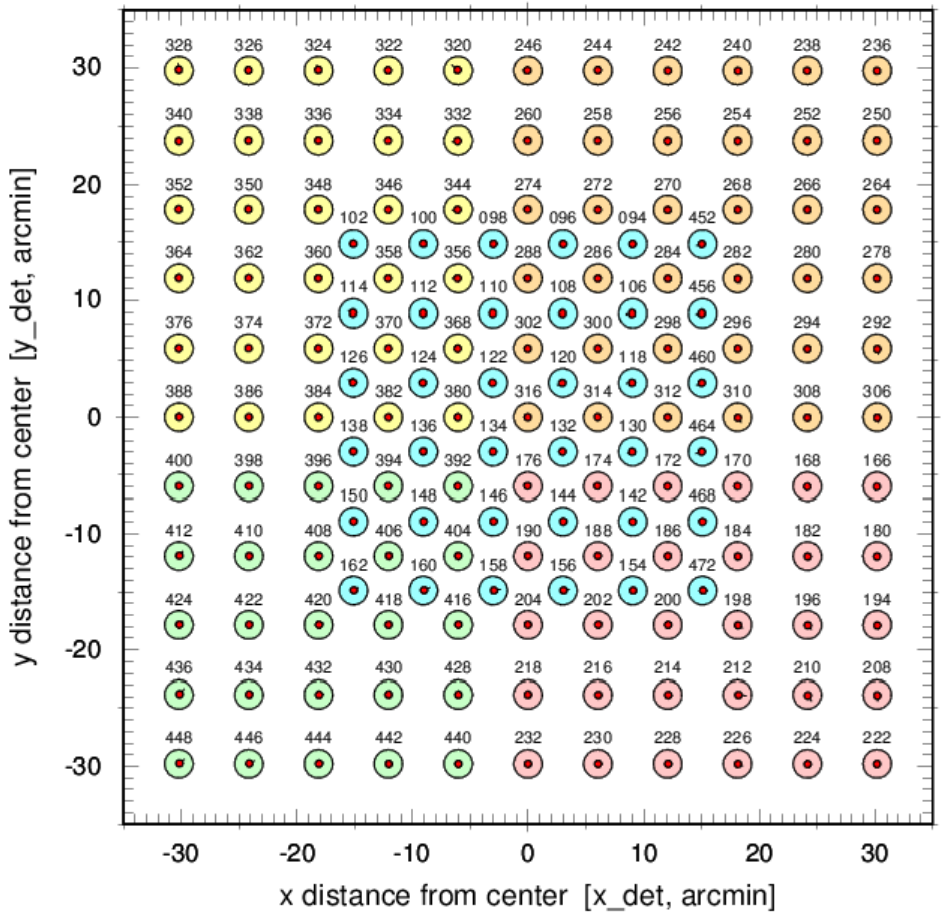

PSF Focal Plane Mapping

Result of geometrical fit with 7 parameters:
A, B, D, γ, δ, x_0, y_0

large circles: predicted PSF centers
small circles: corr. measured PSF centers
displacement lines enlarged by factor 10.0

A = 3095.3 mm, B = 3252.7 mm, D = 1622.2 mm
gamma = 46.4 arcmin, delta = -9.9 arcmin
x = (127.8 - y_ccd) , y = (x_ccd - 129.7)

mean positional 1σ deviation: 2.1“

PSF Focal Plane Mapping: additional challenges

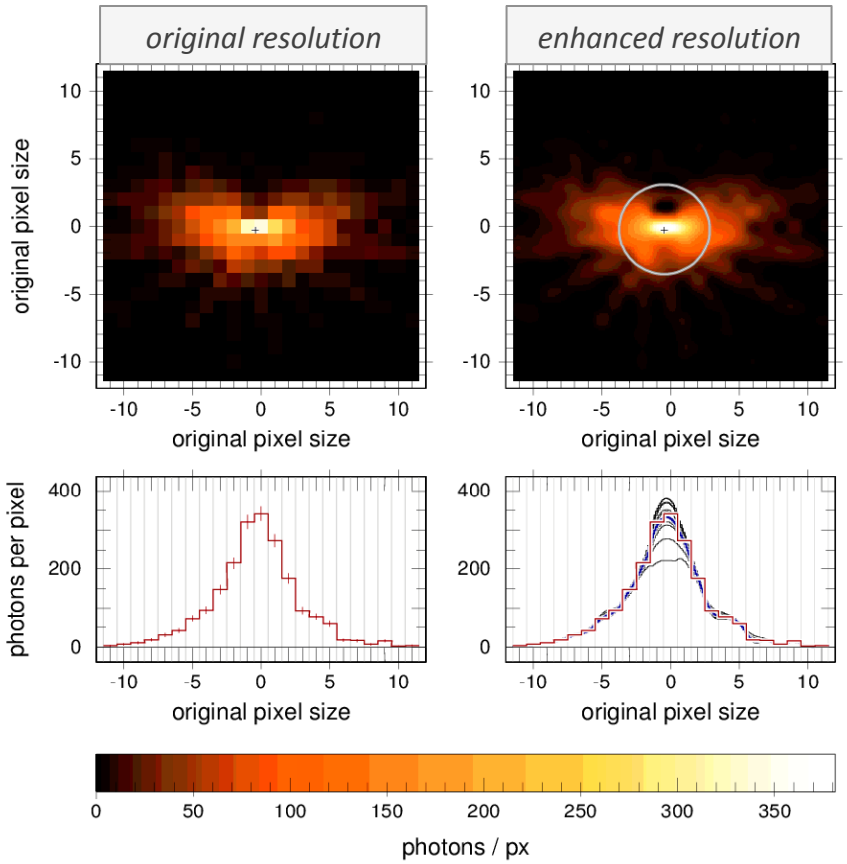

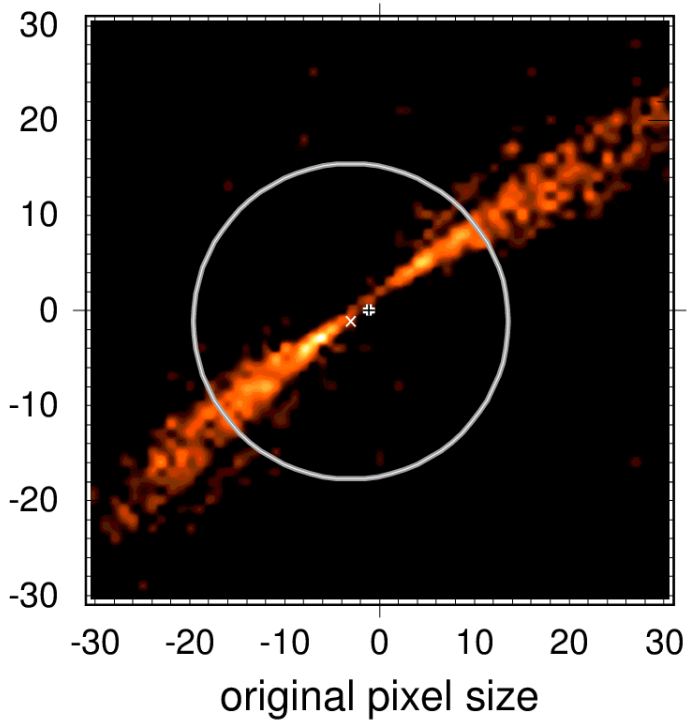

where is the PSF center ?

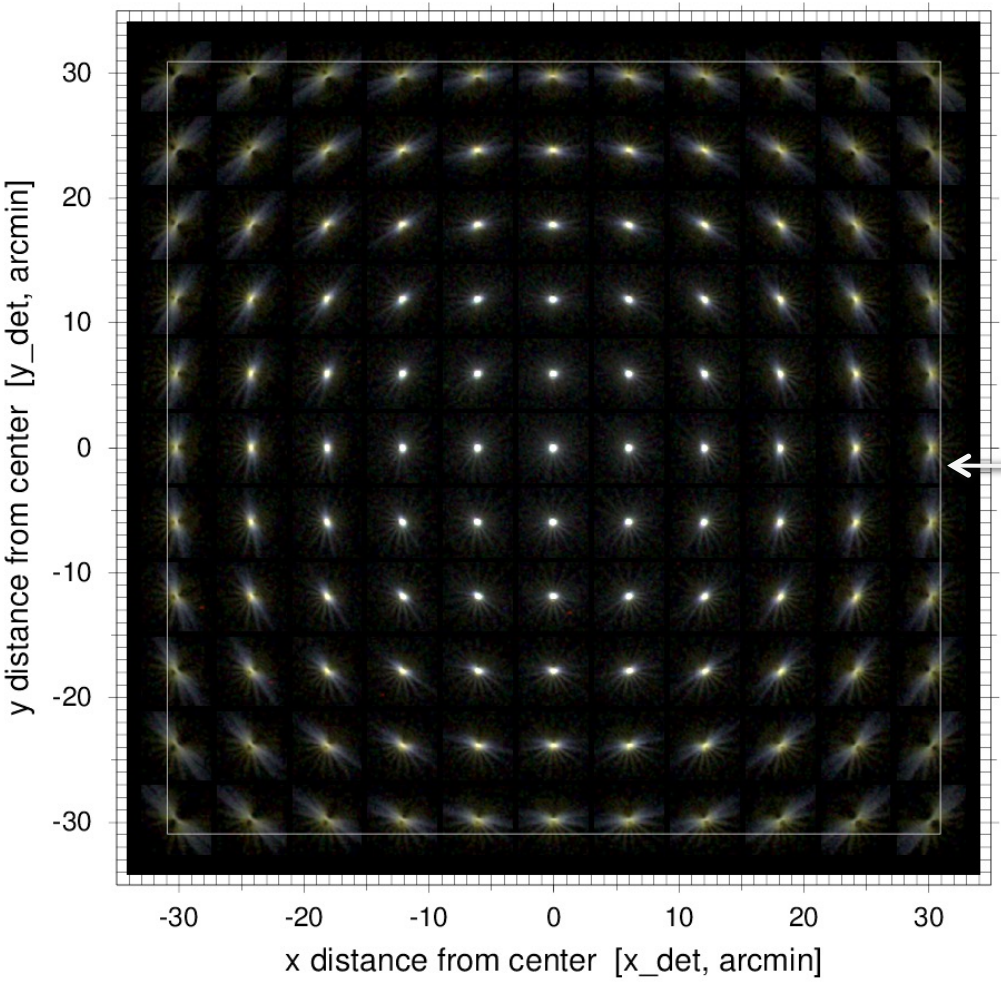

PSF Focal Plane Mapping: RGB images

eROSITA FoV

121 PSFs from scans 1 – 4, each composed of 3 energies

brightest pixel of all PSFs at each energy normalized to 1.0

transfer function: $f(z) = z^{0.4}$, zoomed to [0.0, 0.4]

selected RGB energies

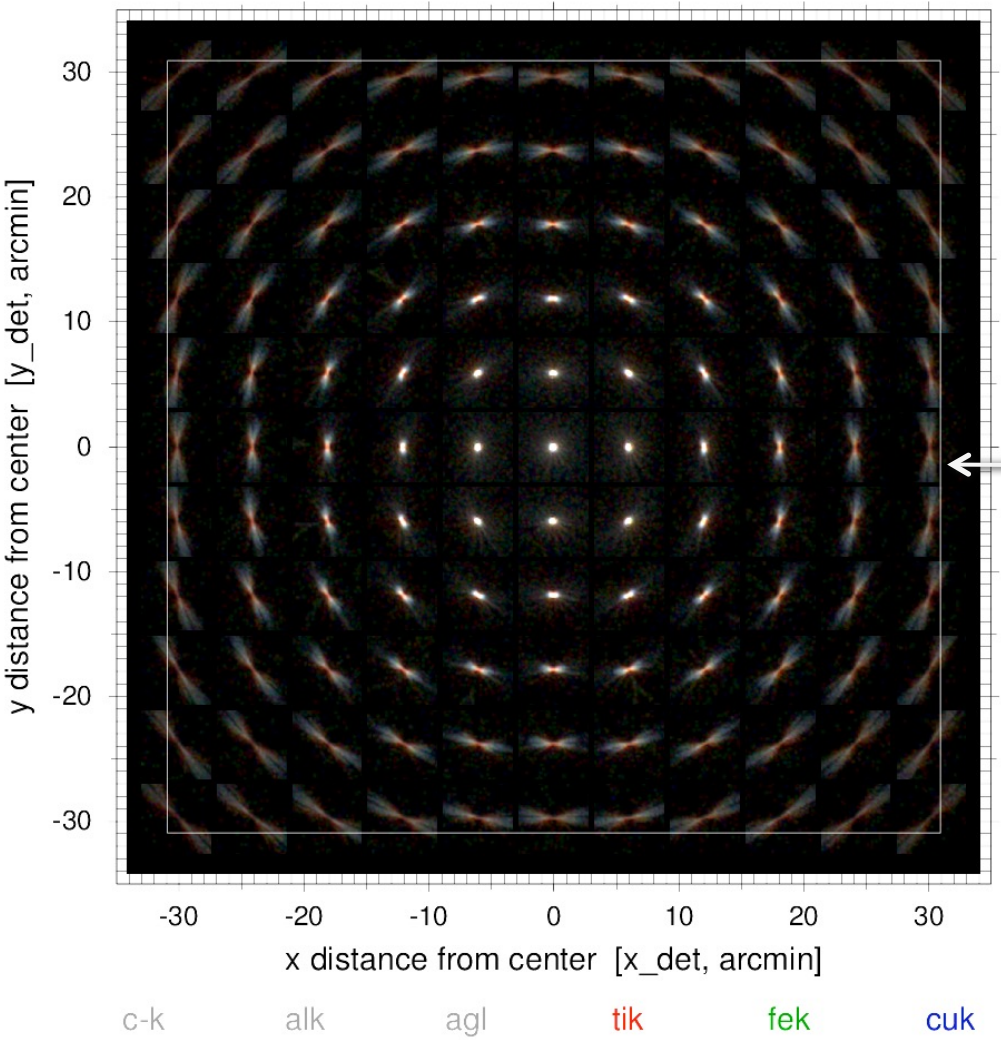

PSF Focal Plane Mapping: RGB images

eROSITA FoV

121 PSFs from scans 1 – 4, each composed of 3 energies

brightest pixel of all PSFs at each energy normalized to 1.0

transfer function: $f(z) = z^{0.4}$, zoomed to [0.0, 0.4]

selected RGB energies

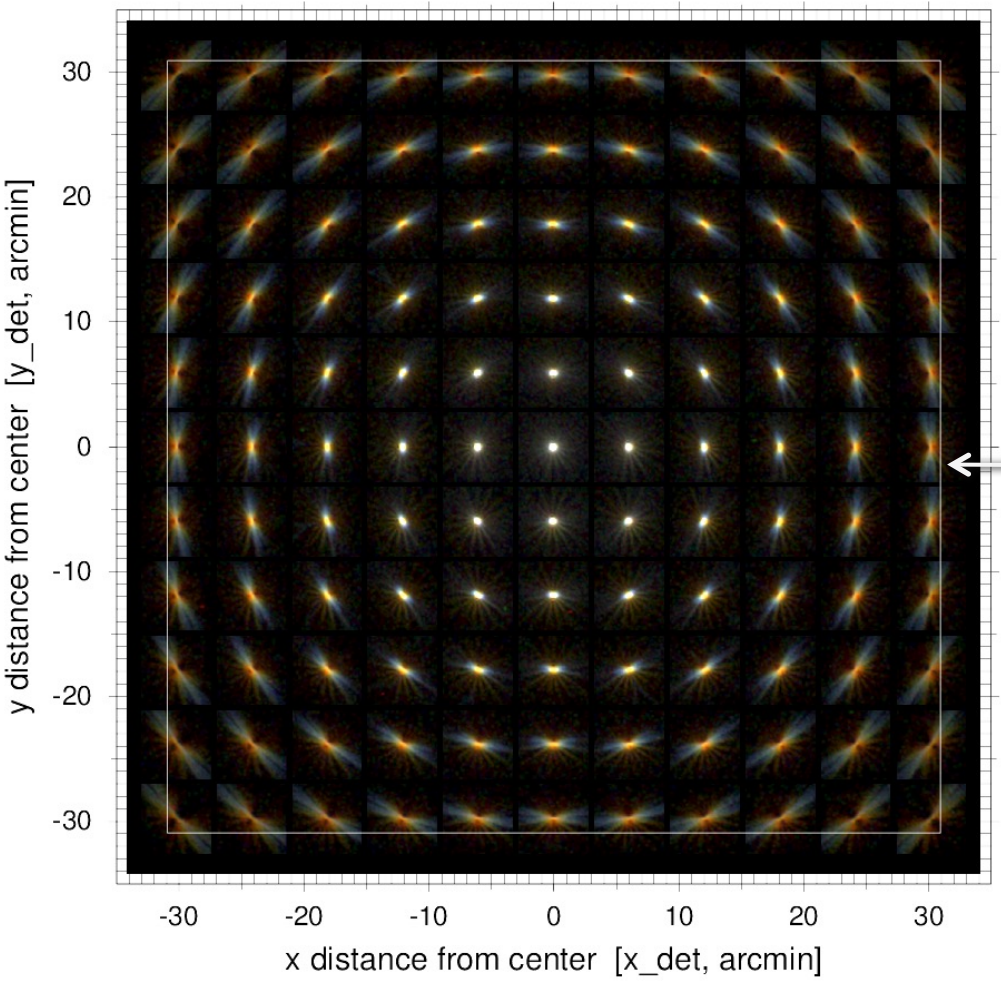

PSF Focal Plane Mapping: RGB images

eROSITA FoV

121 PSFs from scans 1 – 4, each composed of 6 energies

brightest pixel of all PSFs at each energy normalized to 1.0

transfer function: $f(z) = z^{0.4}$, zoomed to [0.0, 0.4]

selected RGB energies

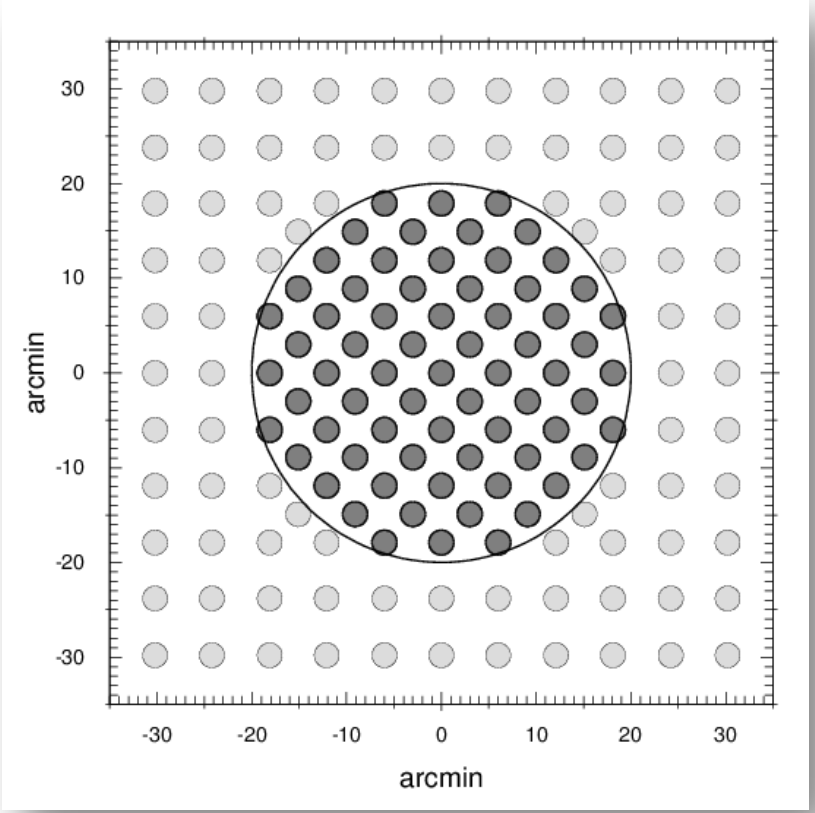

inner FoV (40 arcmin diameter)

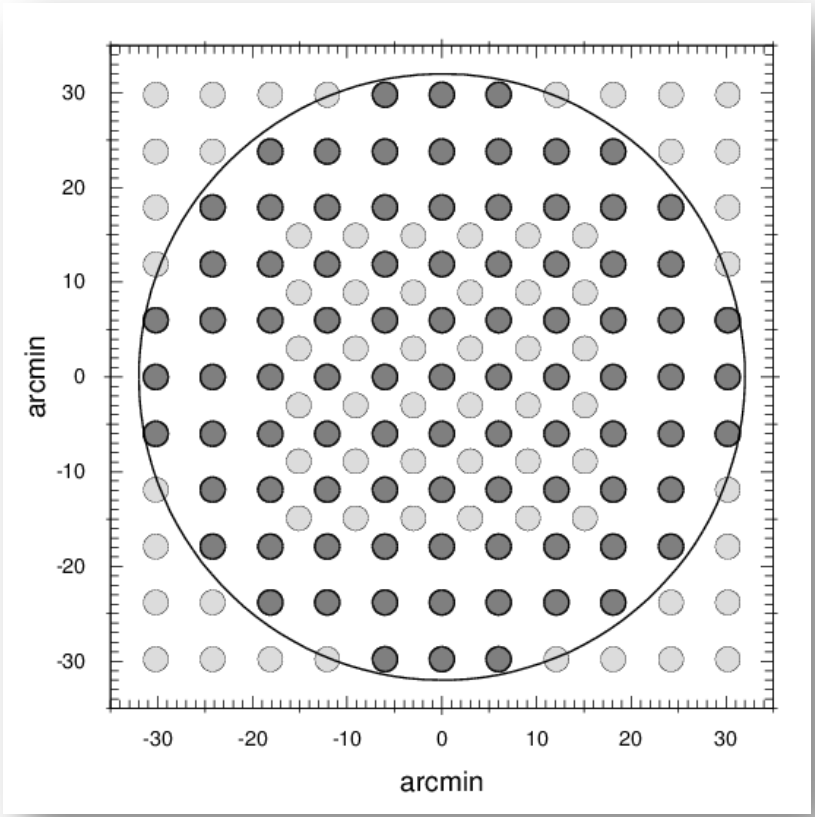

full FoV (60 arcmin diameter)

C-K

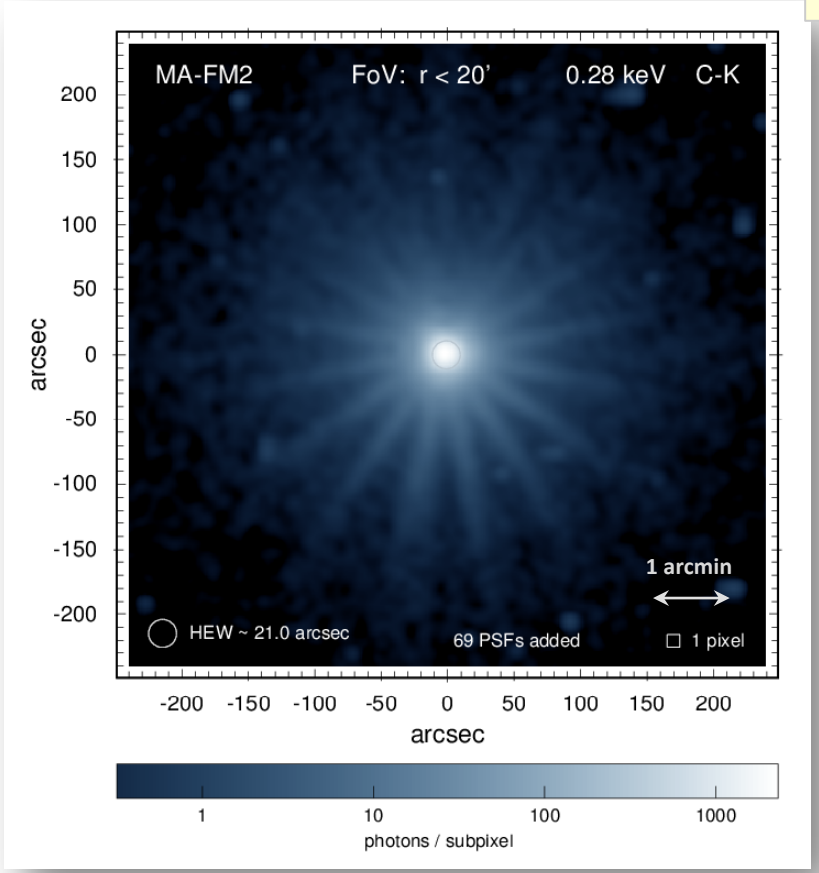

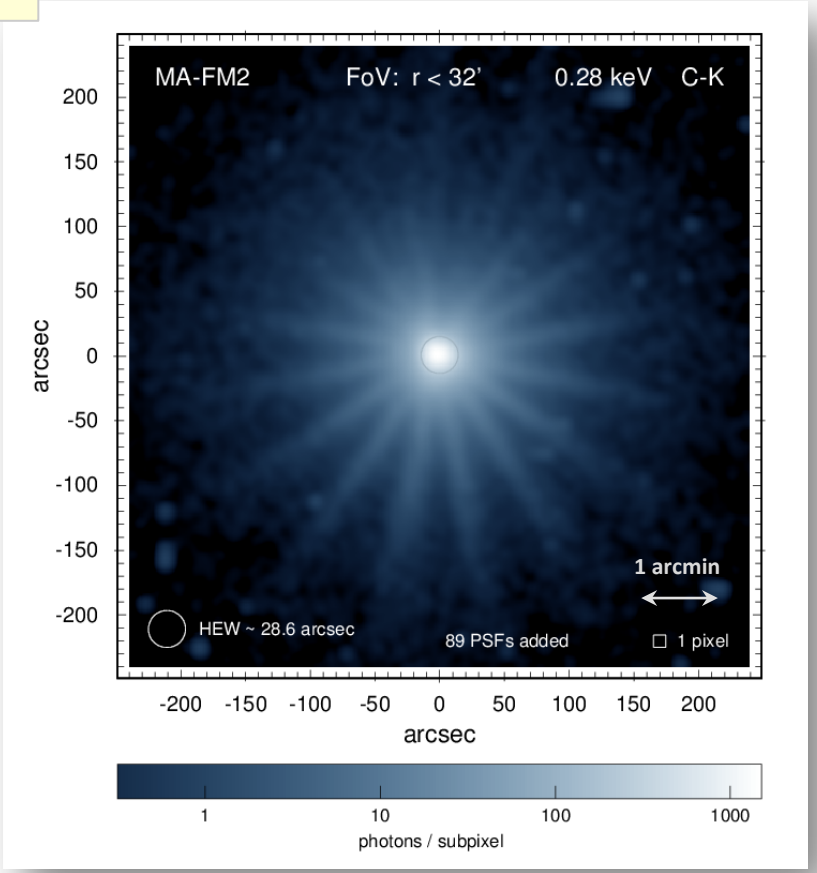

inner FoV (40 arcmin diameter)

full FoV (60 arcmin diameter)

Cu-K

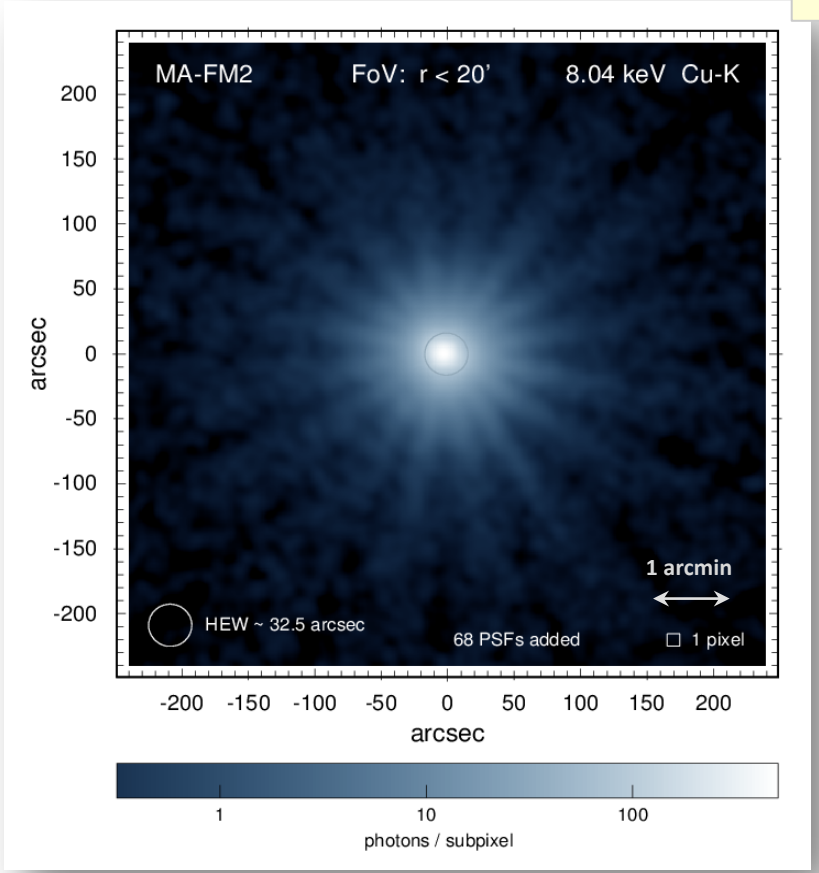

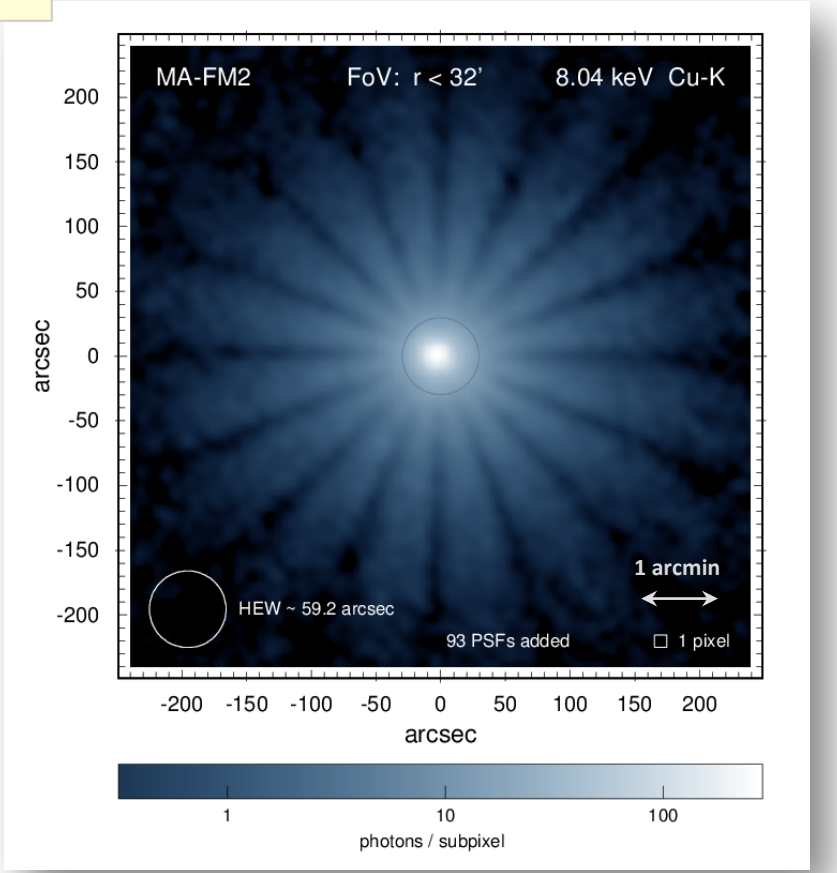

inner FoV (40 arcmin diameter)

full FoV (60 arcmin diameter)

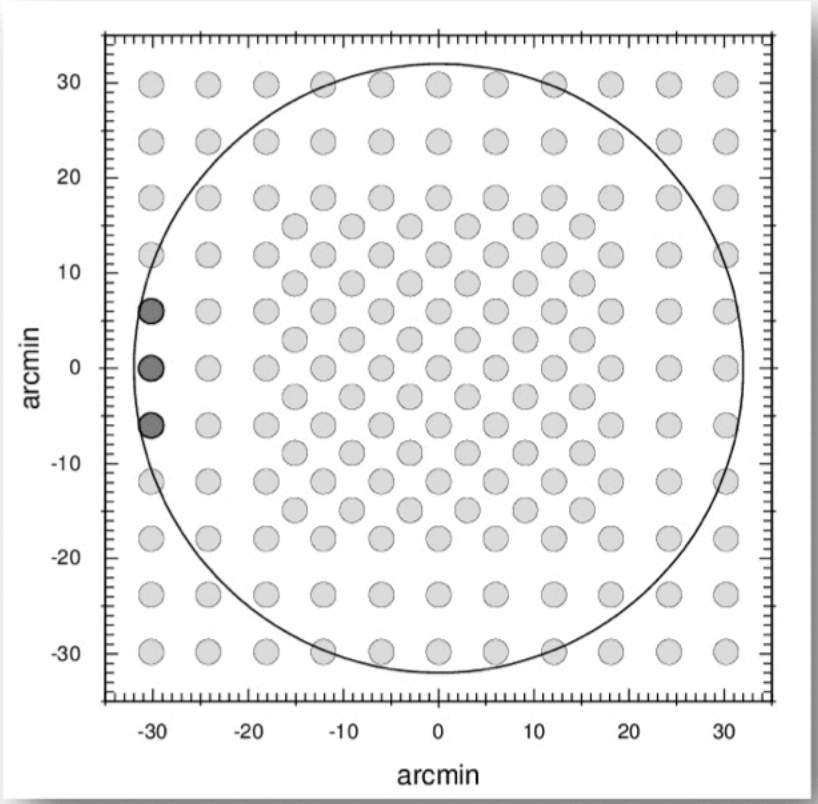

scan at -30 arcmin

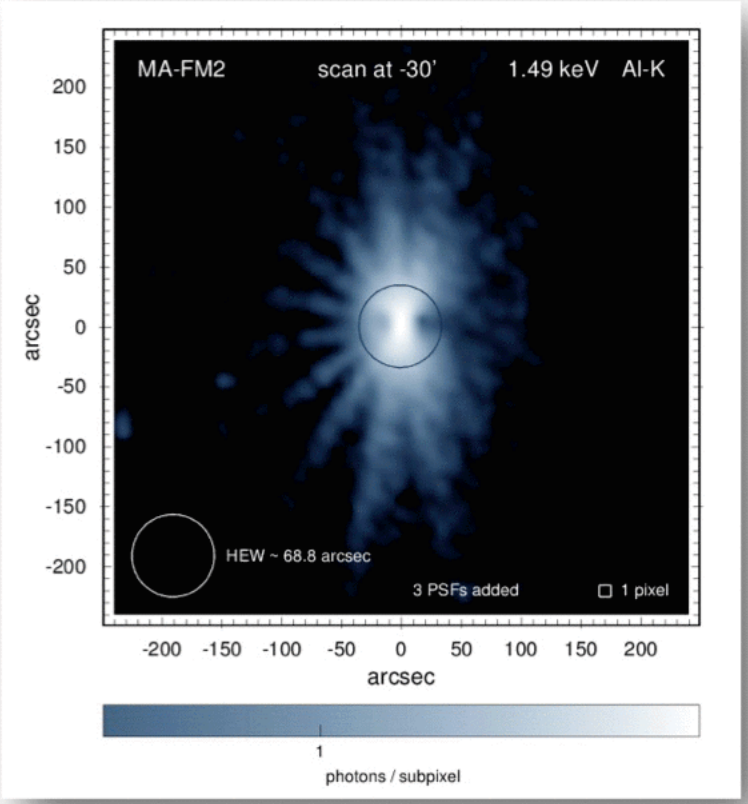

Al-K, 1.49 keV

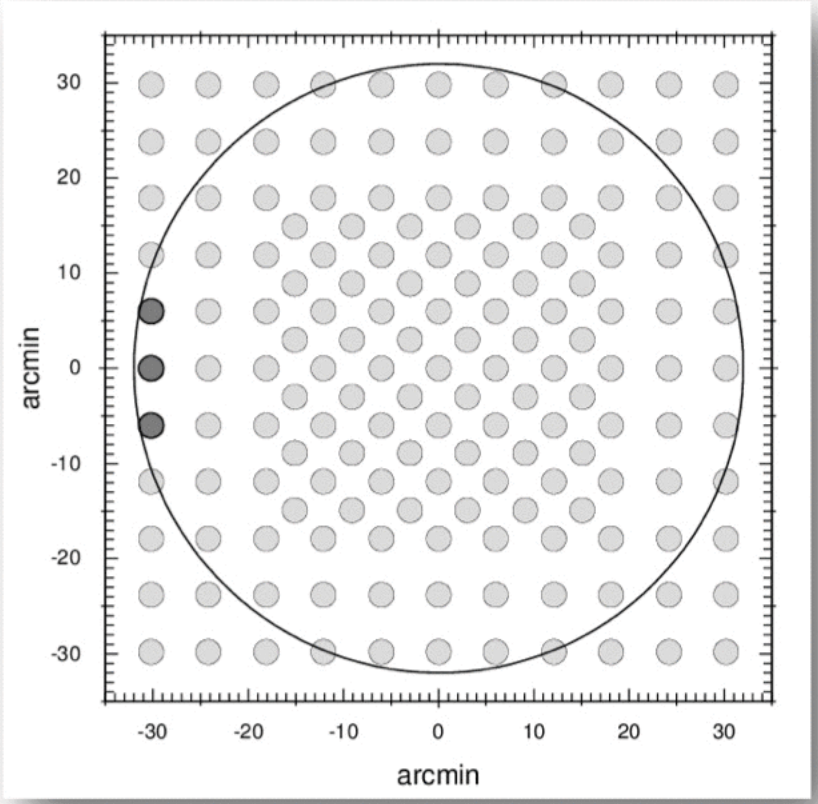

scan at -30 arcmin

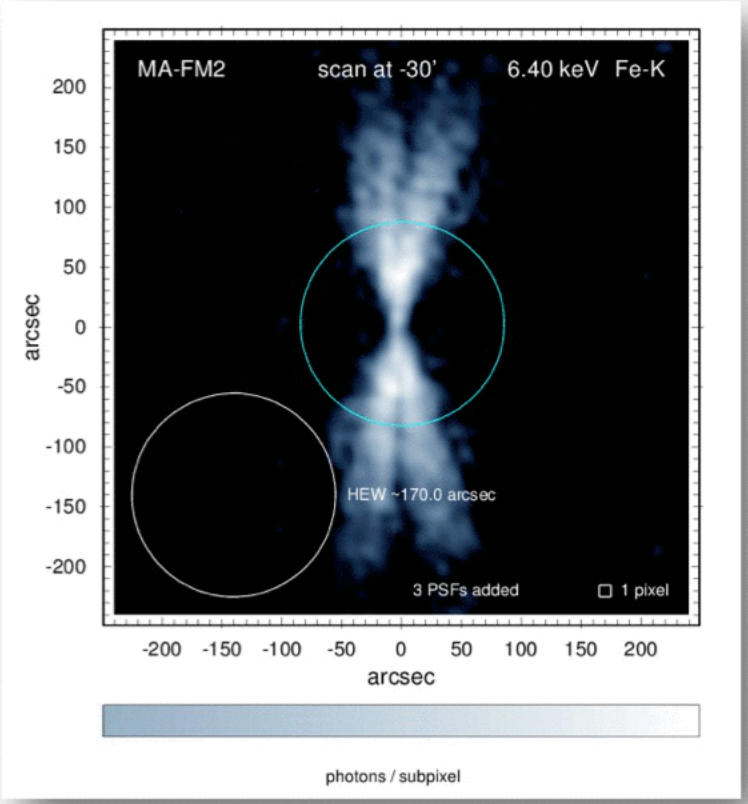

Fe-K, 6.40 keV

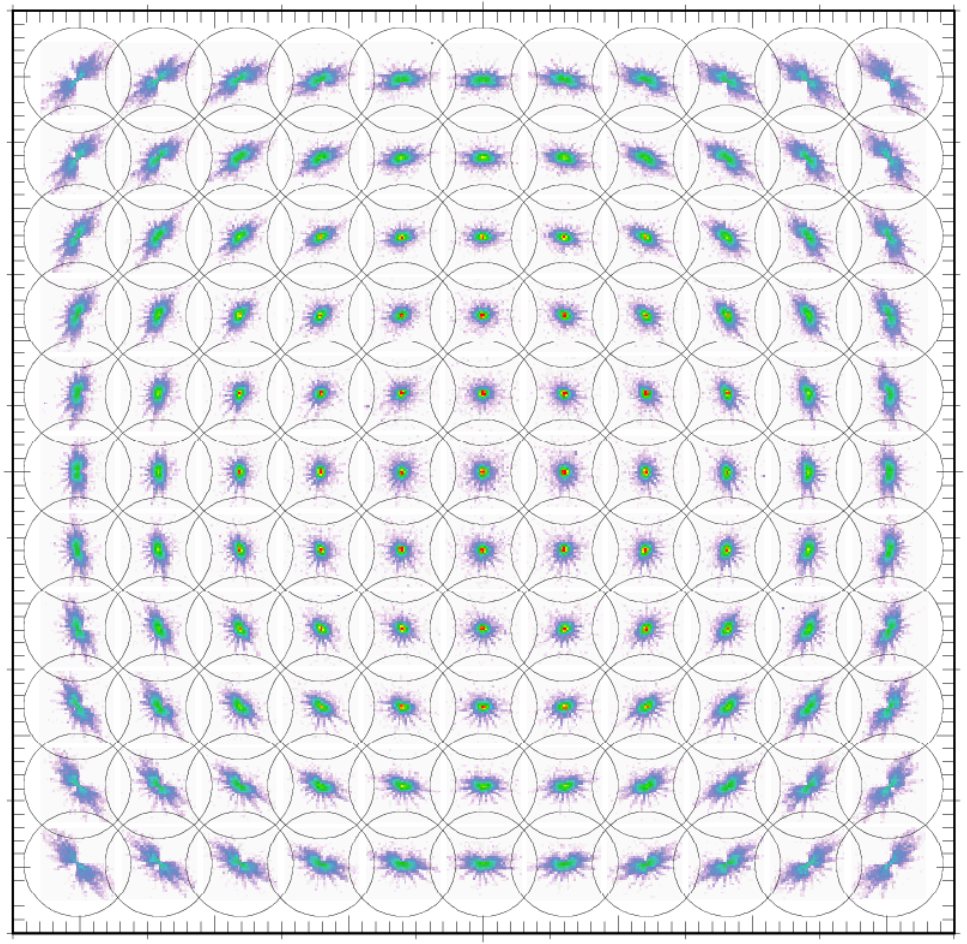

FM2, Al-K

PSF Focal Plane Mapping

after geometry correction

extraction radius: 4 arcmin

→ vignetting

PSF Focal Plane Mapping

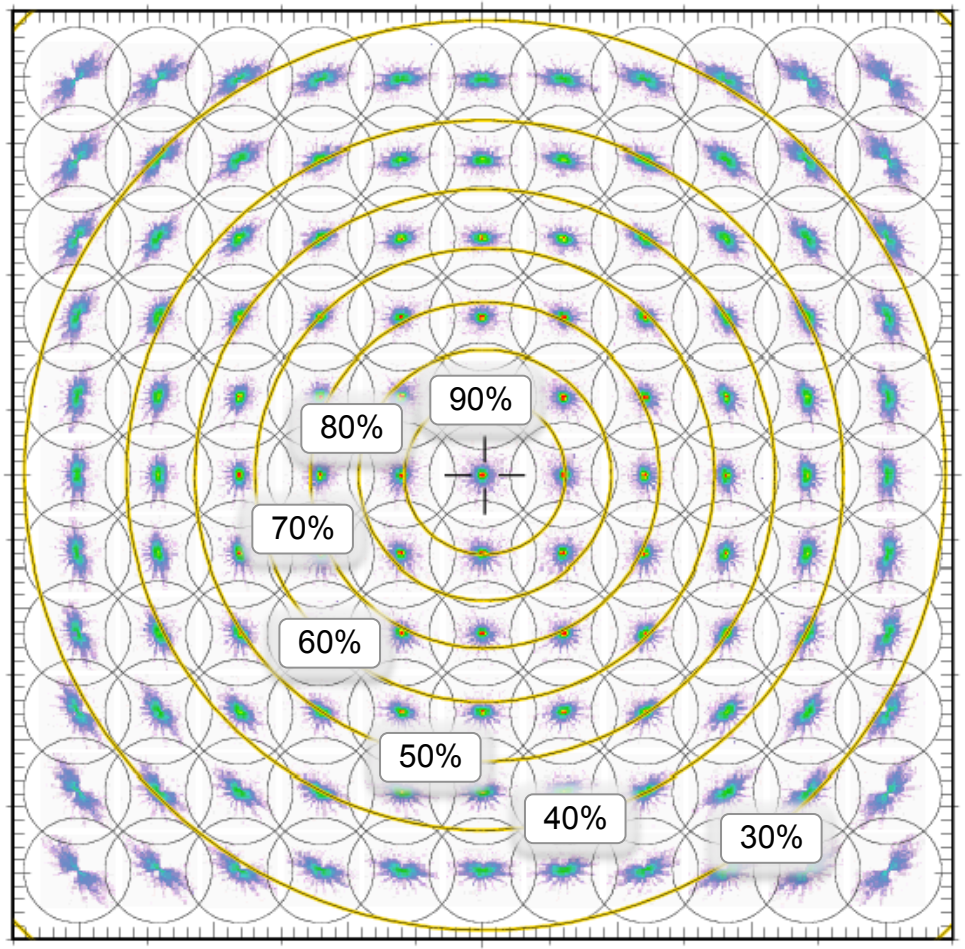

FM2, Al-K

after geometry correction

extraction radius: 4 arcmin

→ vignetting

PSF Focal Plane Mapping: vignetting curves

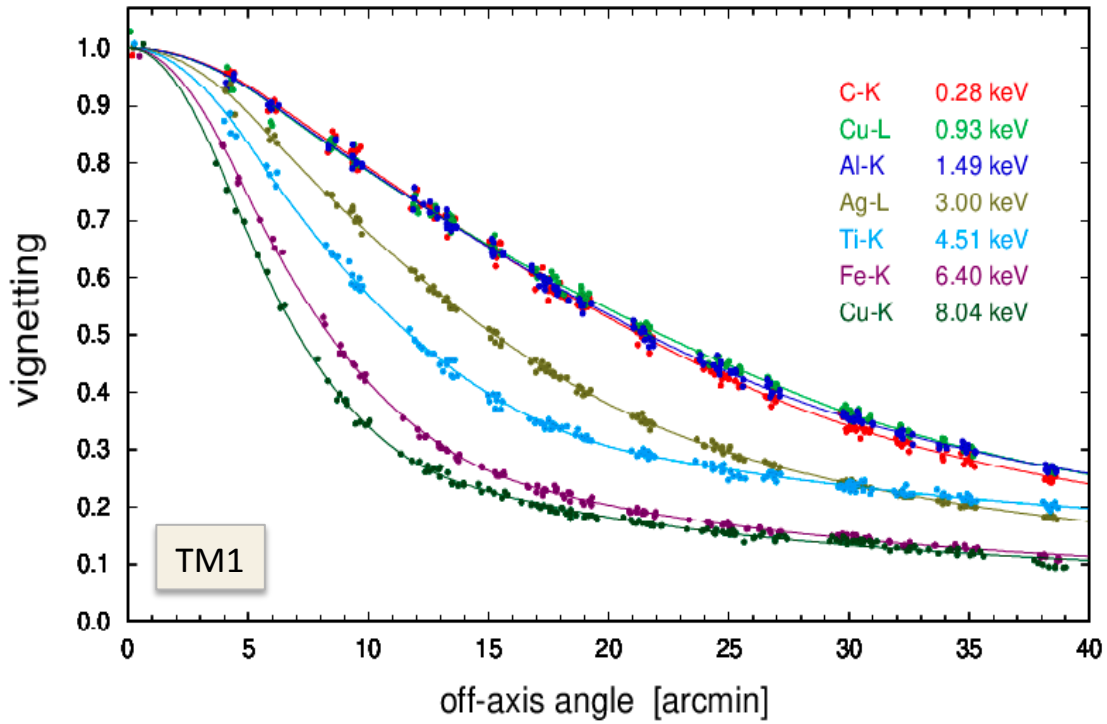

vignetting defined here as the relative encircled flux within r = 4.0 arcmin for a point source

derived from **1073 PSFs** covering the focal plane

empirical curves were determined together with the vignetting center

only assumption: azimuthal symmetry in vignetting

Calibration observations during the CalPV phase

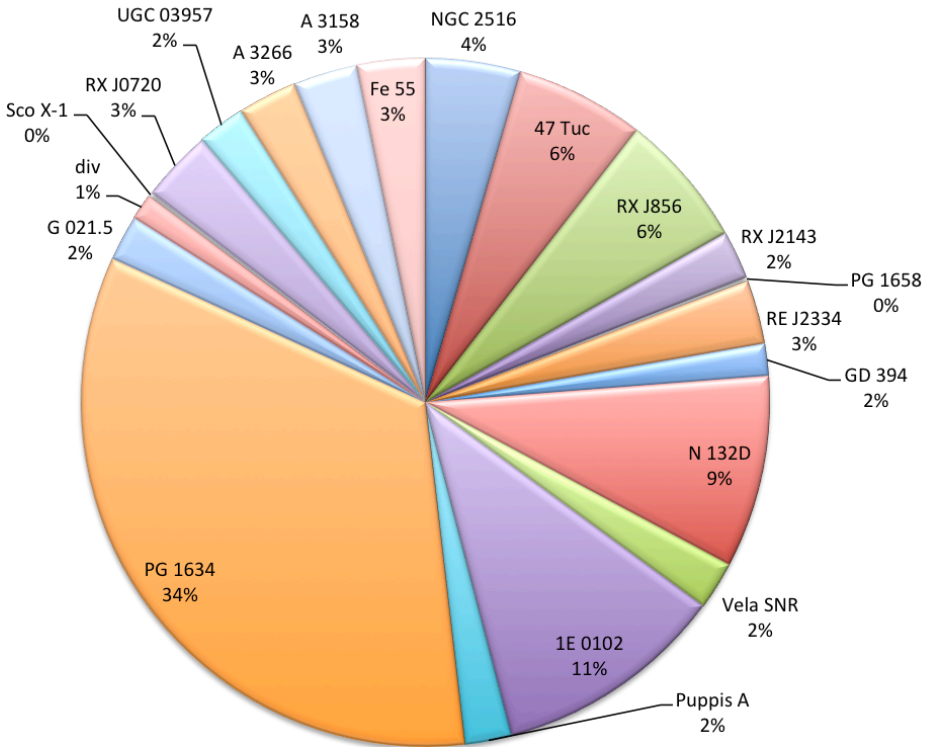

The segments scale with the average exposure time per TM

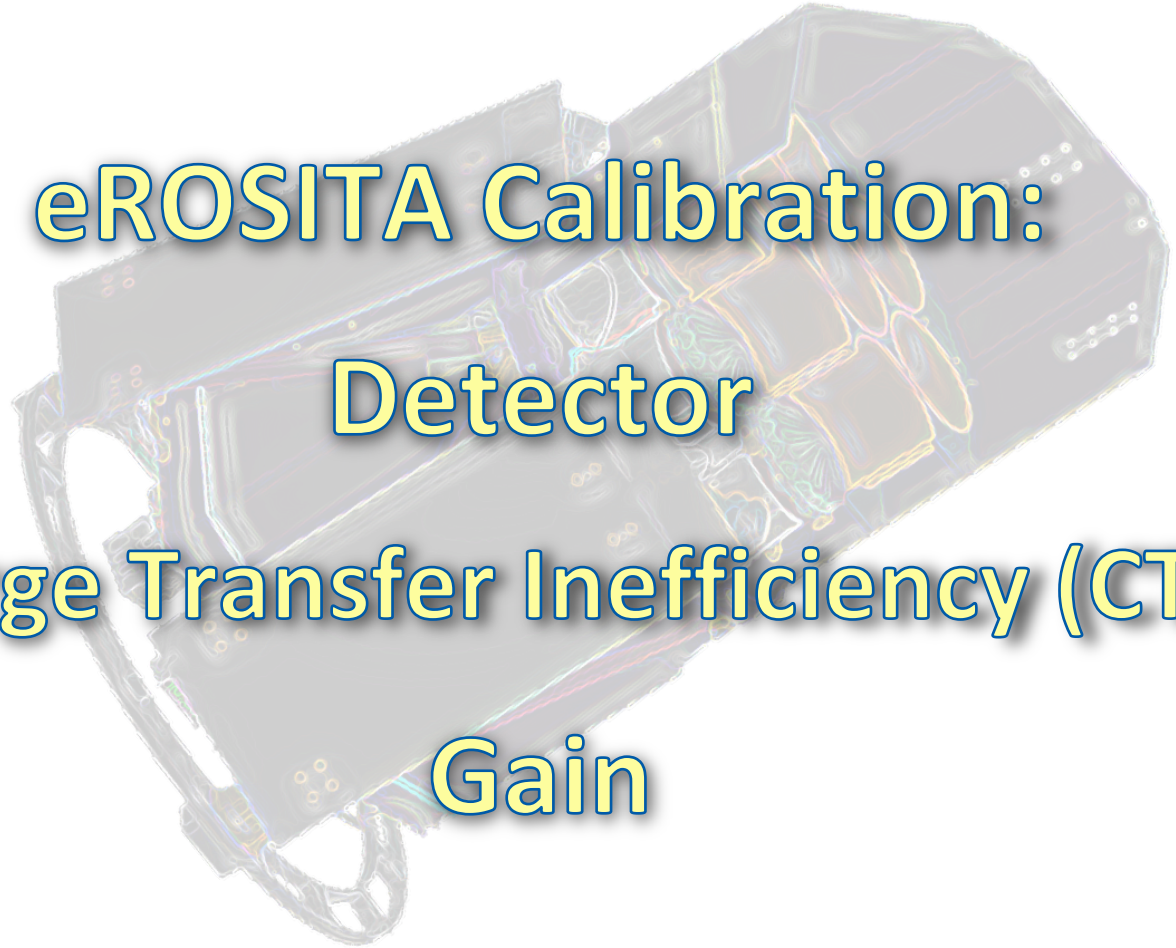

eROSITA Calibration:

Detector

Charge Transfer Inefficiency (CTI),

Gain

extent of charge cloud & 75 µm pixel size
→ 4 pattern types

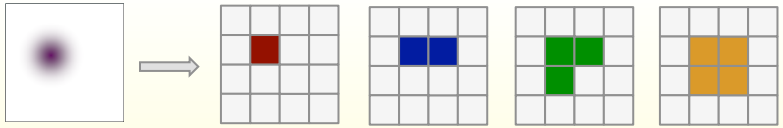

reconstructed spectral distributions

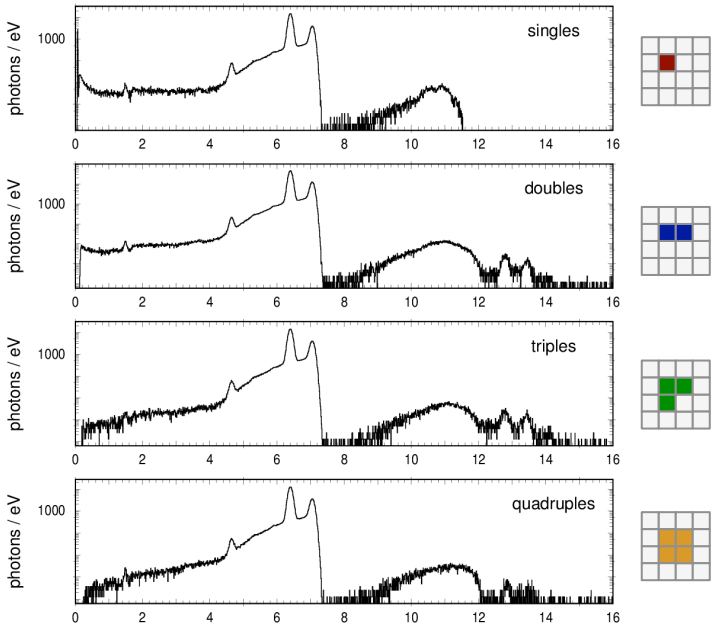

instrumental energy [„keV“]

- charge splitting over several pixels
- charge transfer losses (CTI)
- gain differences between CCD columns

observed pulse height distribution

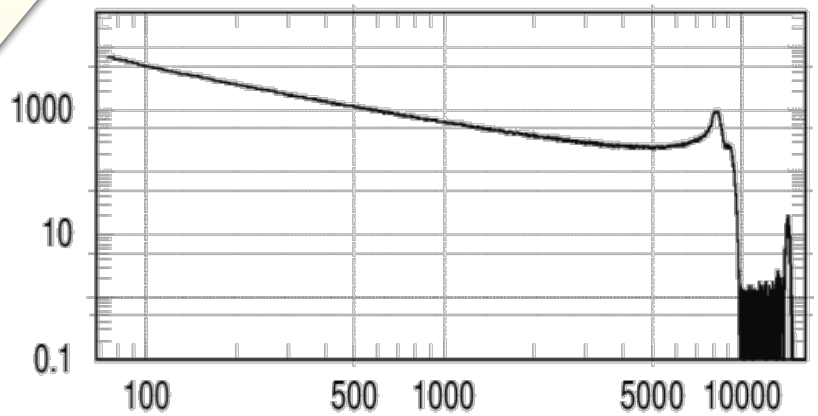

analog-digital-unit [adu]

example: Fe-K, measured with FM4

Reconstructing the spectral distribution requires

- **pattern** recognition
- correction for **gain** variations between CCD channels
- correction for charge transfer loss **(CTI)**

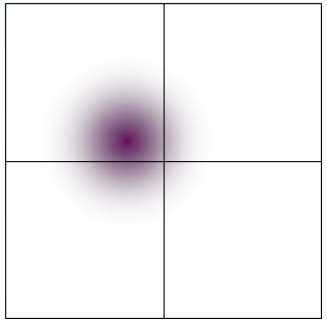

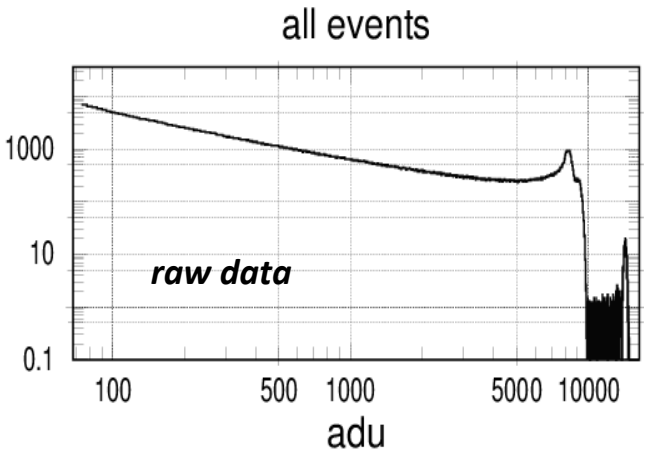

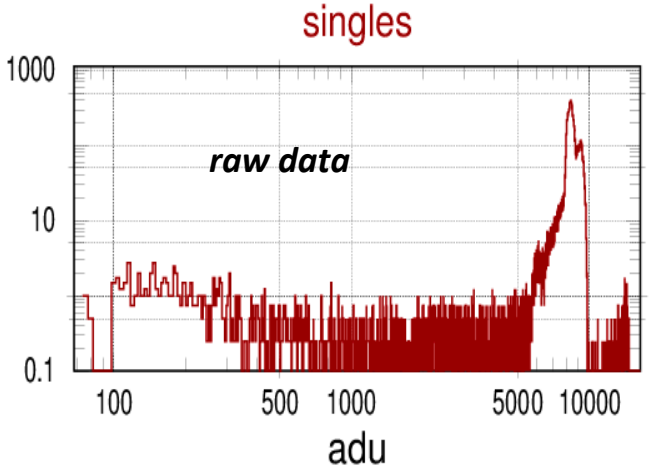

pattern recognition

Reconstructing the spectral distribution requires

- **pattern** recognition
- correction for **gain** variations between CCD channels
- correction for charge transfer loss **(CTI)**

gain determination

example:
Fe-K, measured with FM4

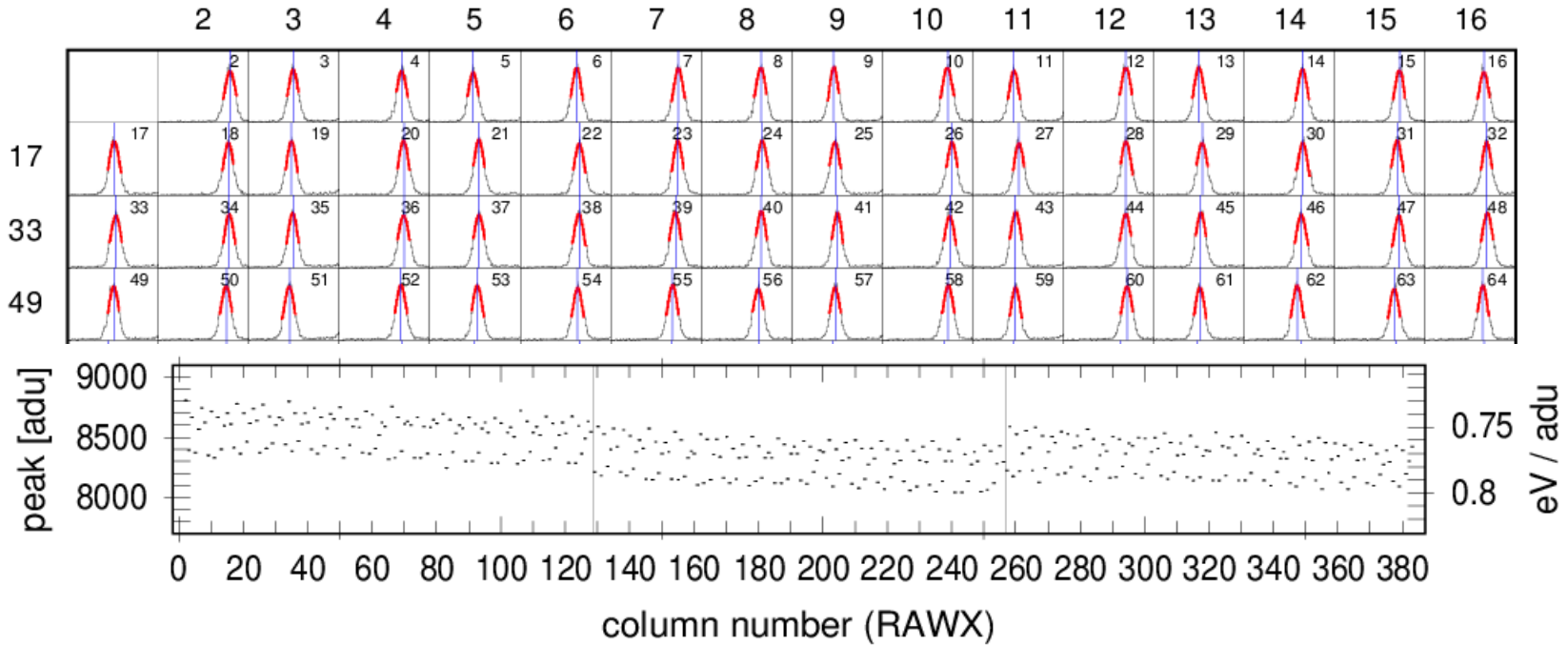

CTI determination

Reconstructing the spectral distribution requires
- **pattern** recognition
- correction for **gain** variations between CCD channels
- correction for charge transfer loss **(CTI)**

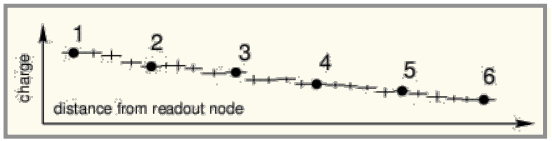

CCD column 240 (arbitrary choice)

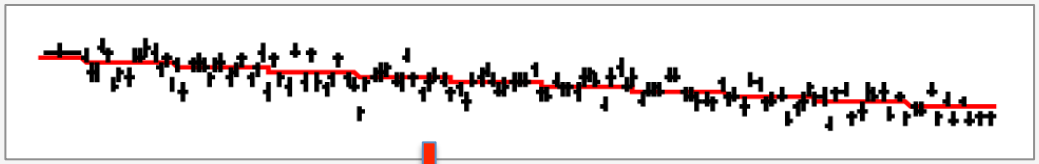

CTI = 2.1 x 10^{-5}

emission line determined in 130 (adaptively computed) macro pixels containing a minimum of 30 first singles around the line

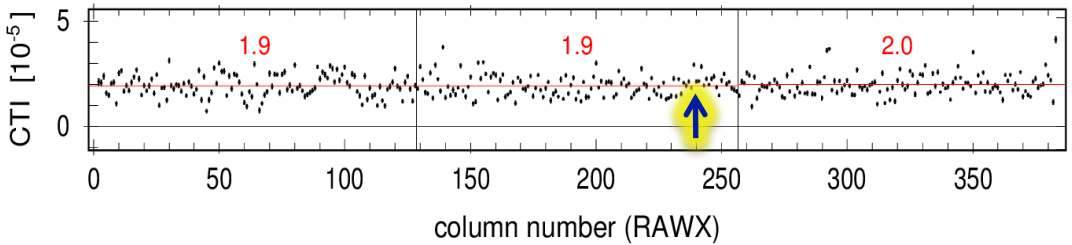

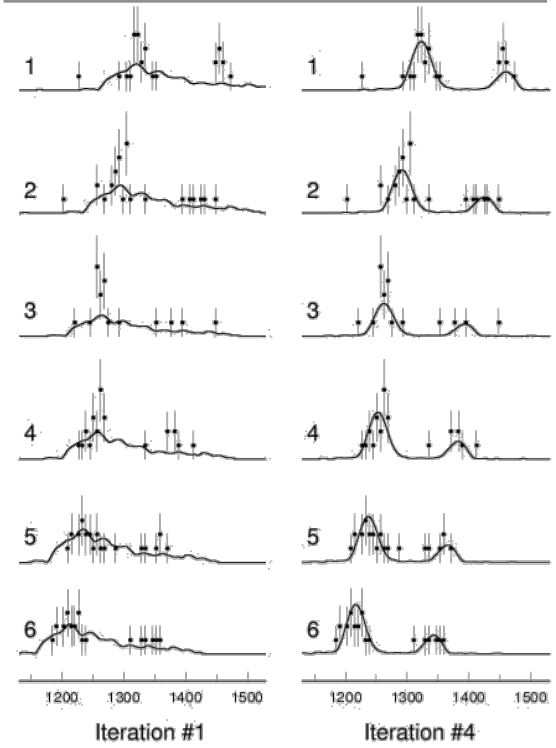

CTI determination

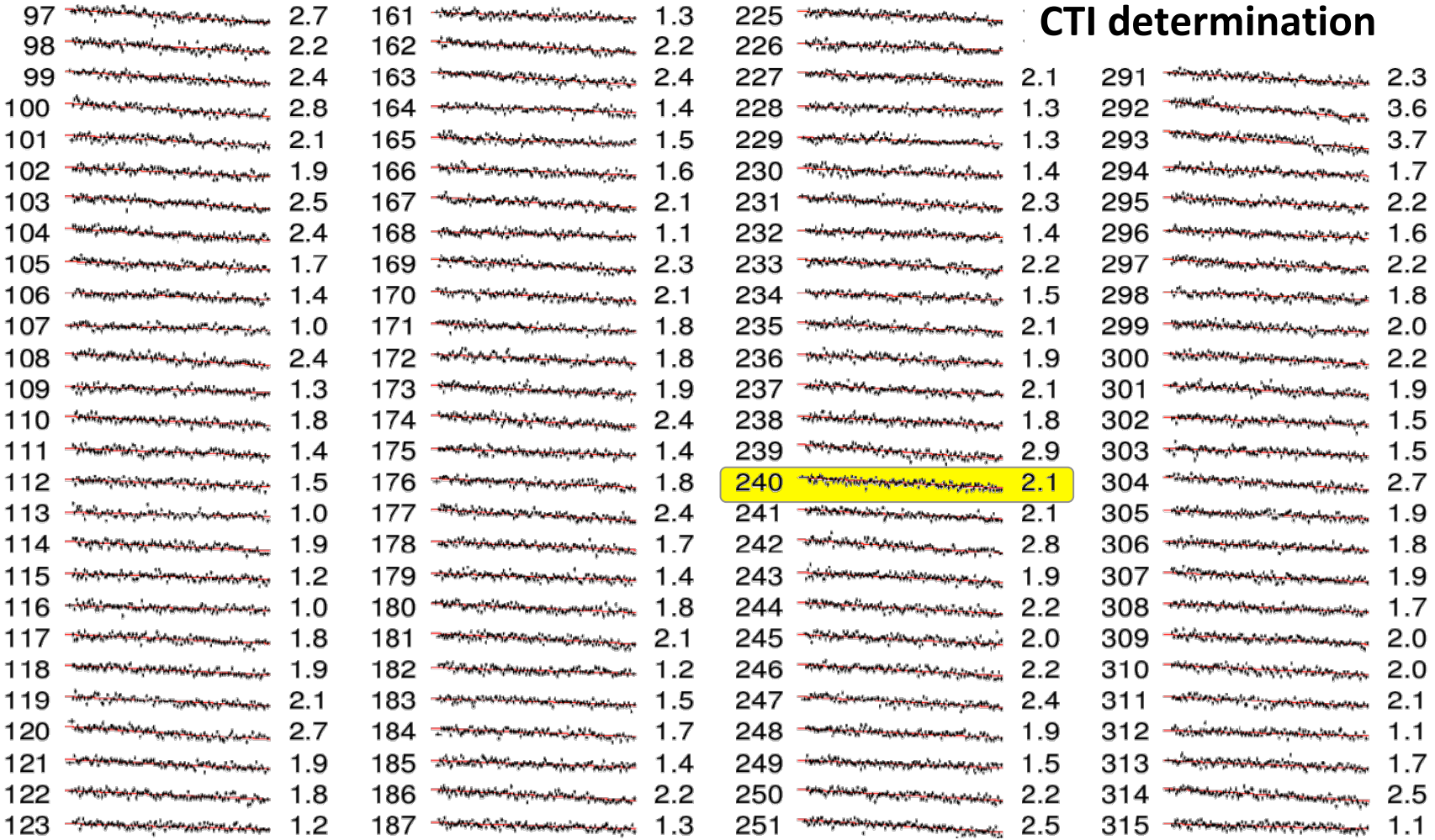

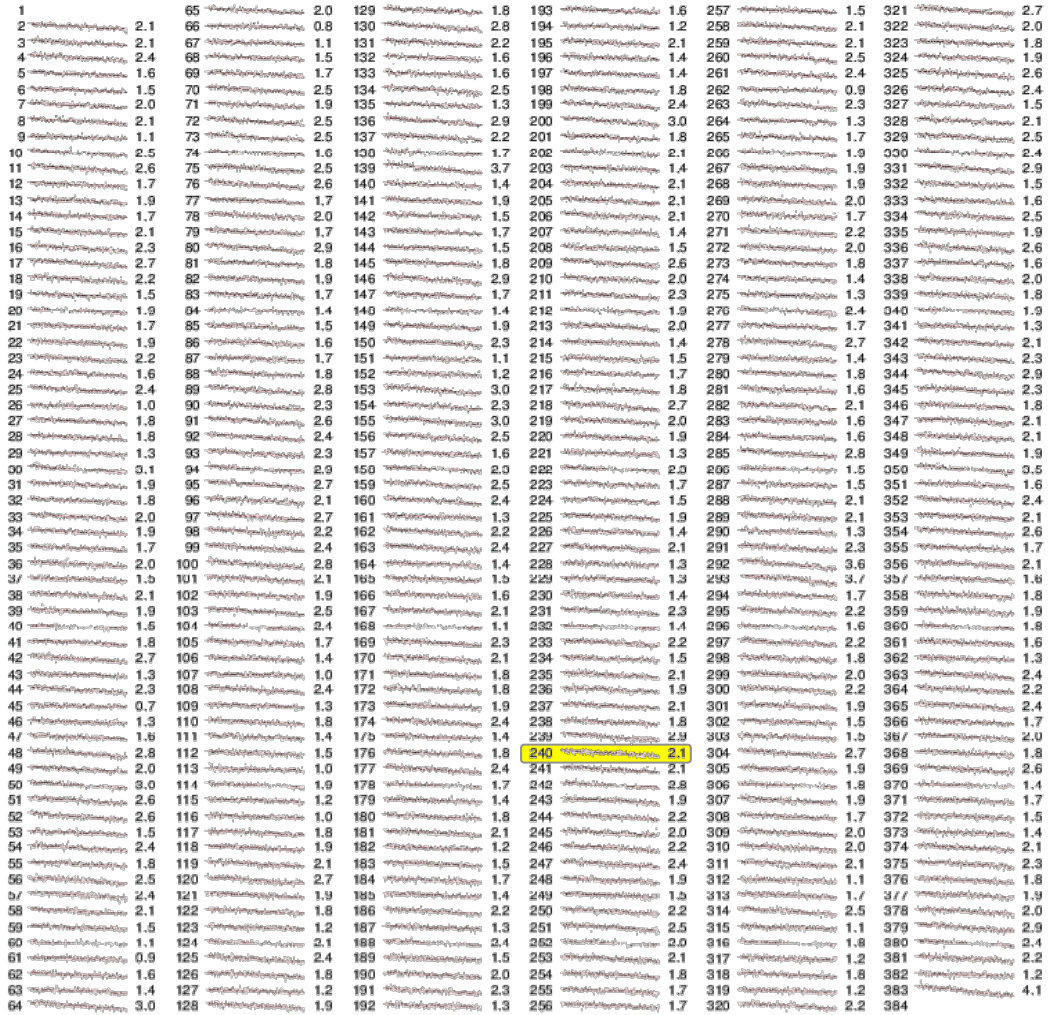

CTI determination

example:
Fe-K, measured with FM4

plot contains
47 267 data points

each data point is the result of several iterative template fits

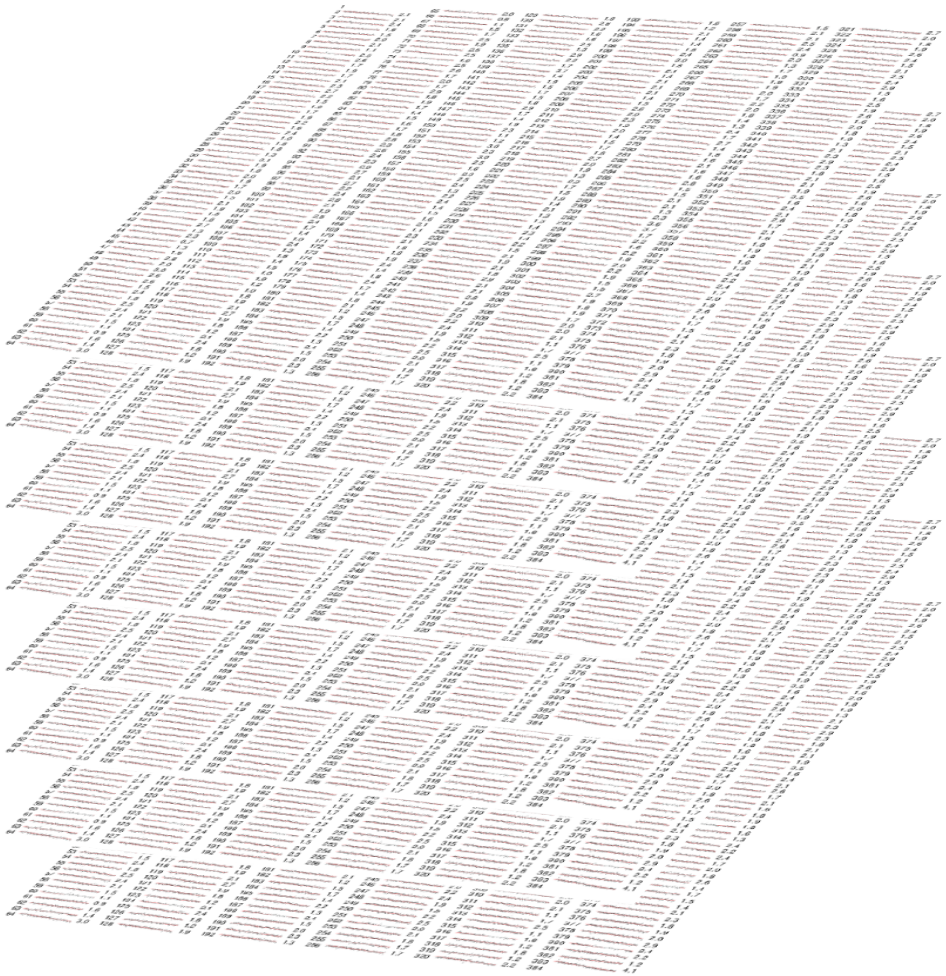

CTI determination

8 calibration energies

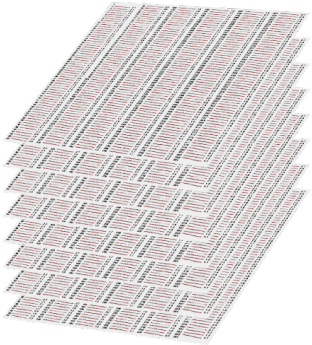
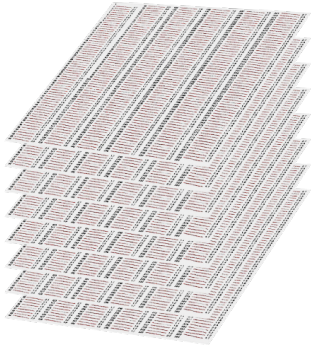
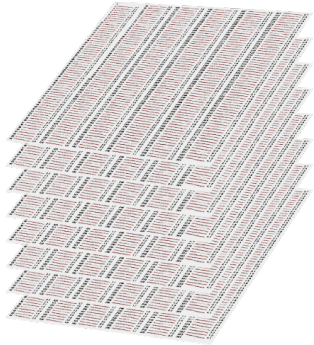
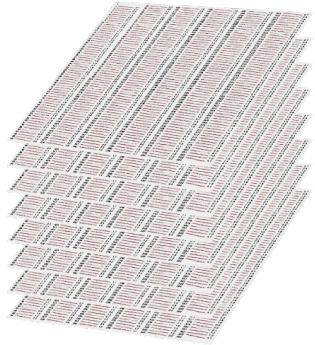
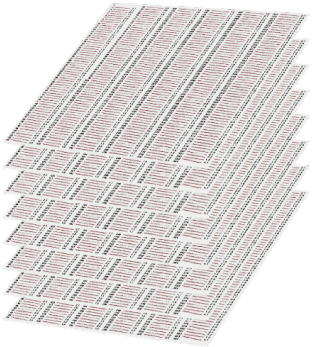
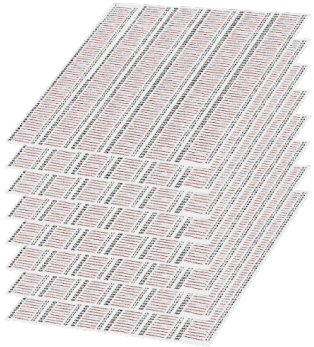
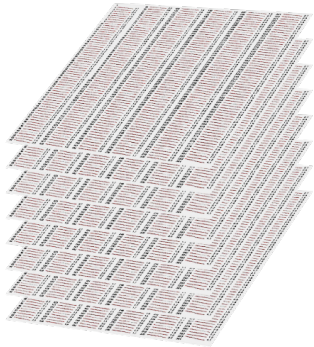

8 energies

7 CCDs

all 7 CCDs calibrated with 3.3 billion events

Energy interpolation of the CTI and gain

CTI

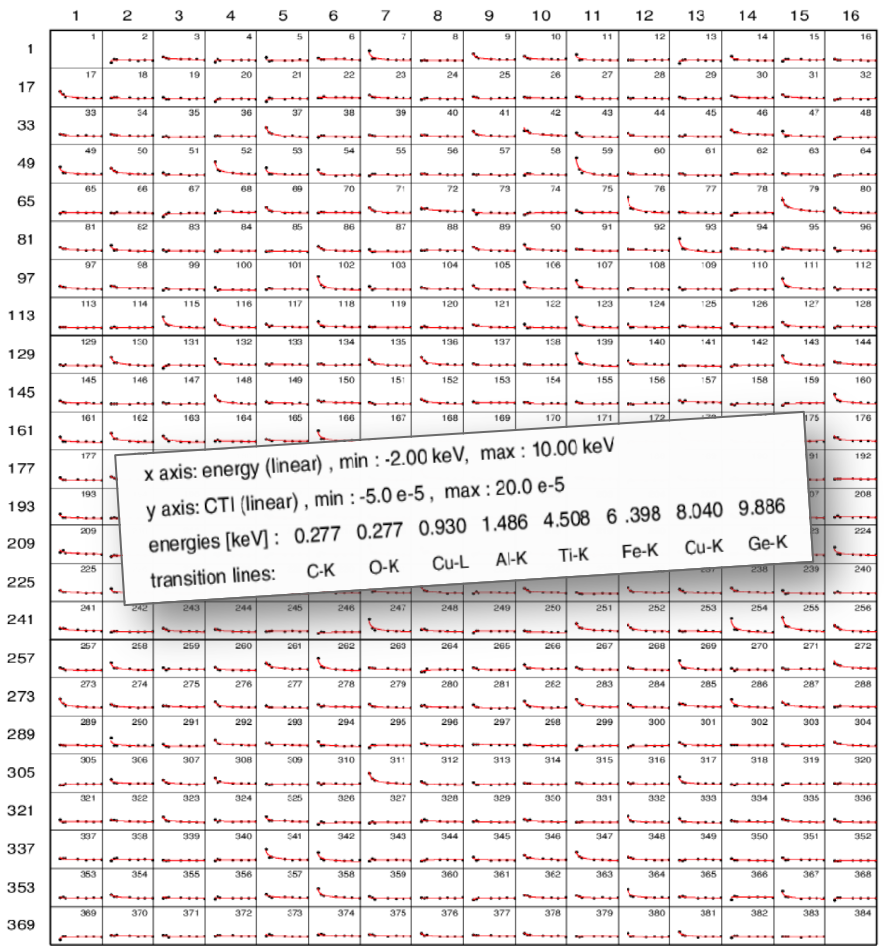

gain

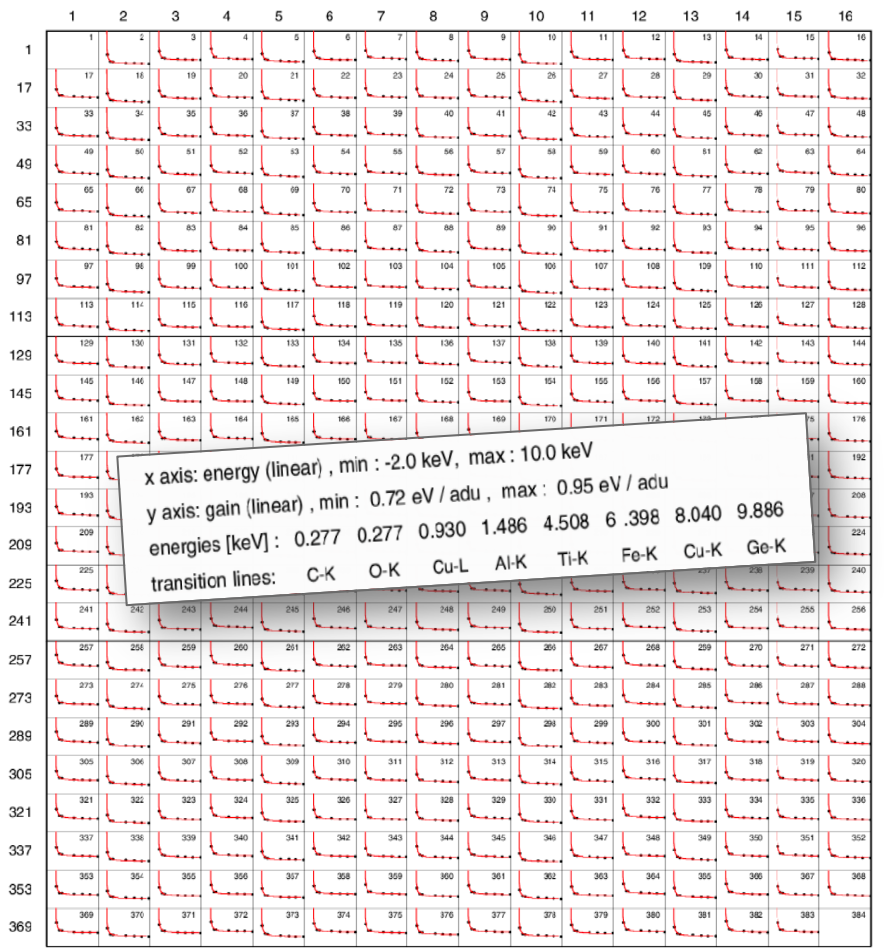

Reconstructing the spectral distribution requires

- **pattern** recognition
- correction for **gain** variations between CCD channels
- correction for charge transfer loss **(CTI)**

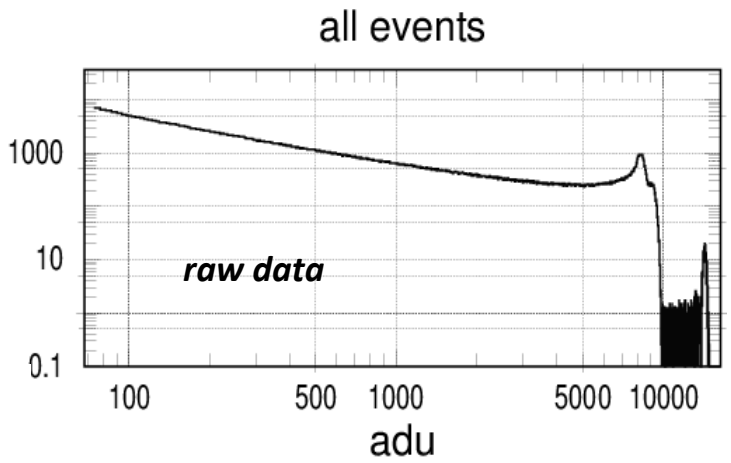

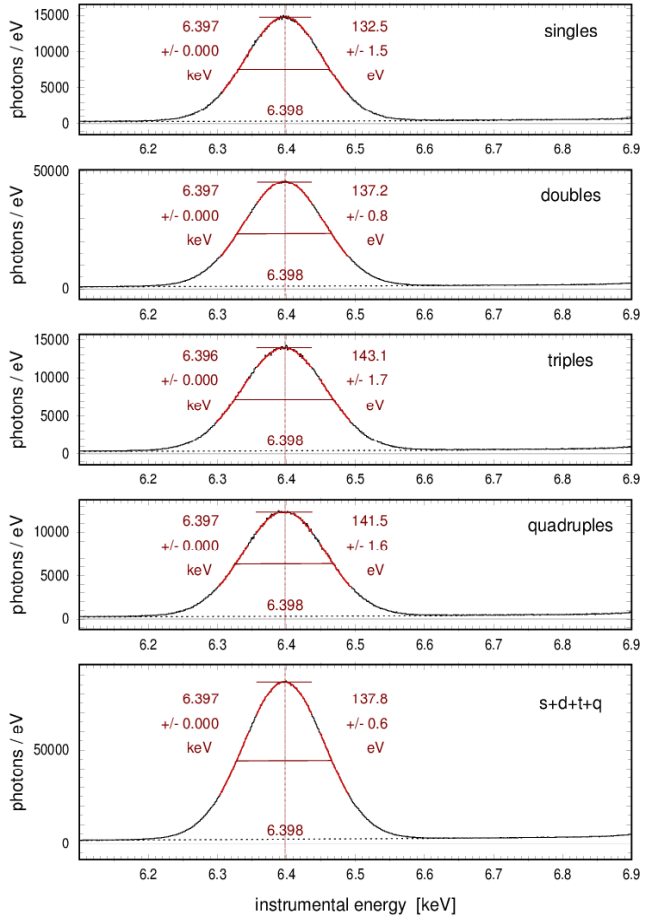

reconstructed spectral distribution

example: Fe-K, measured with FM4

FWHM = 132.5 – 143.1 eV, all photons: FWHM = 137.8 eV

accuracy of absolute energy scale: ± 2 eV (± 0.03%)

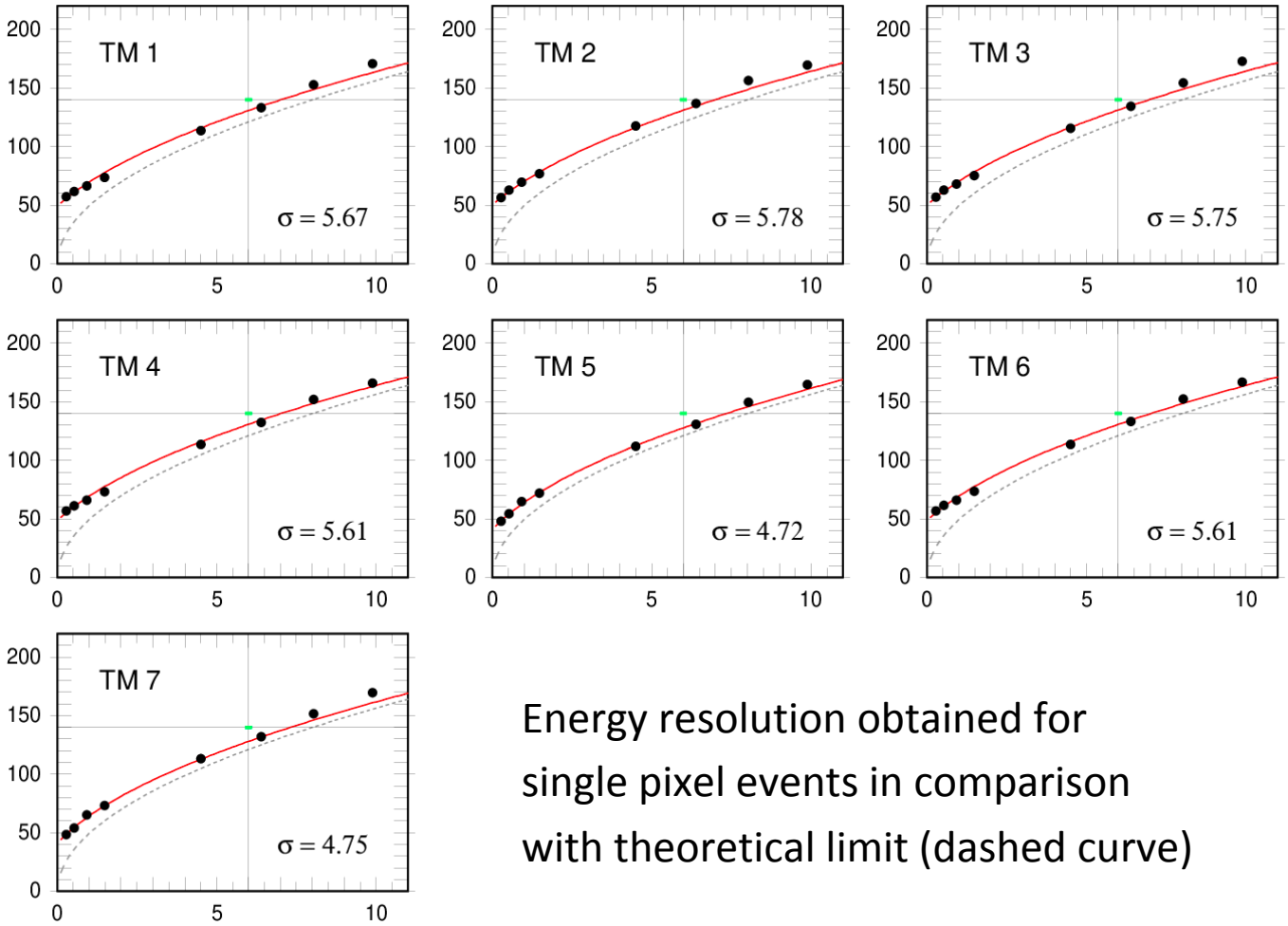

Energy resolution obtained for single pixel events in comparison with theoretical limit (dashed curve)

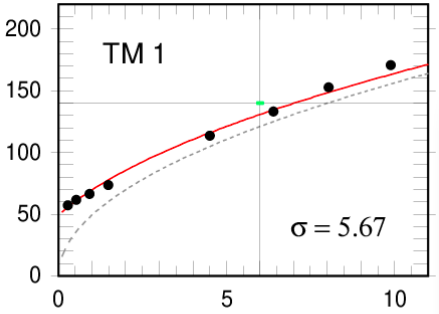

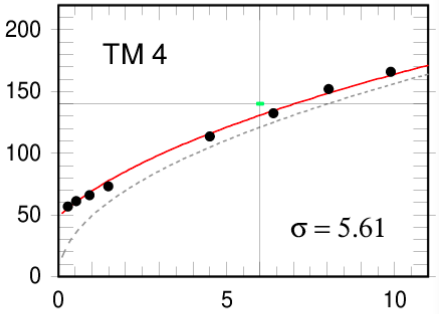

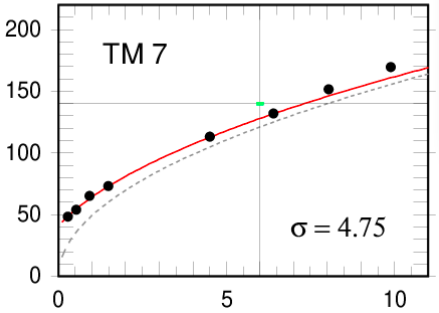

Spectrum of Boron and Carbon emission lines

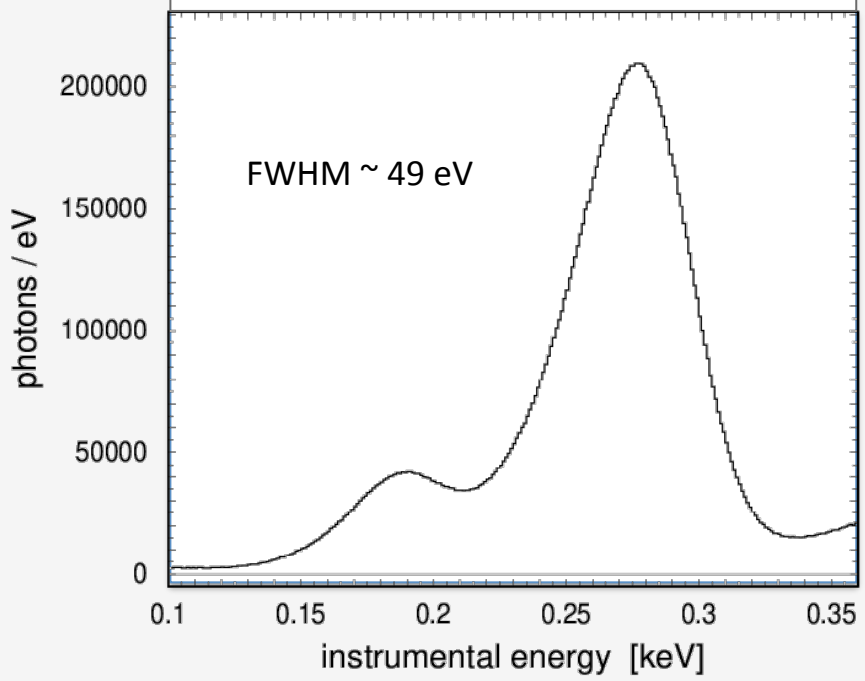

Energy calibration with the internal ^{55}Fe source

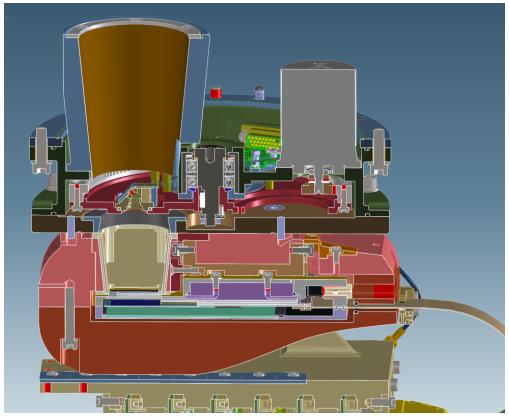

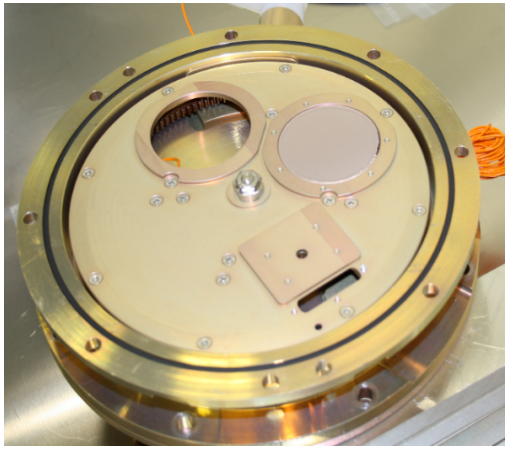

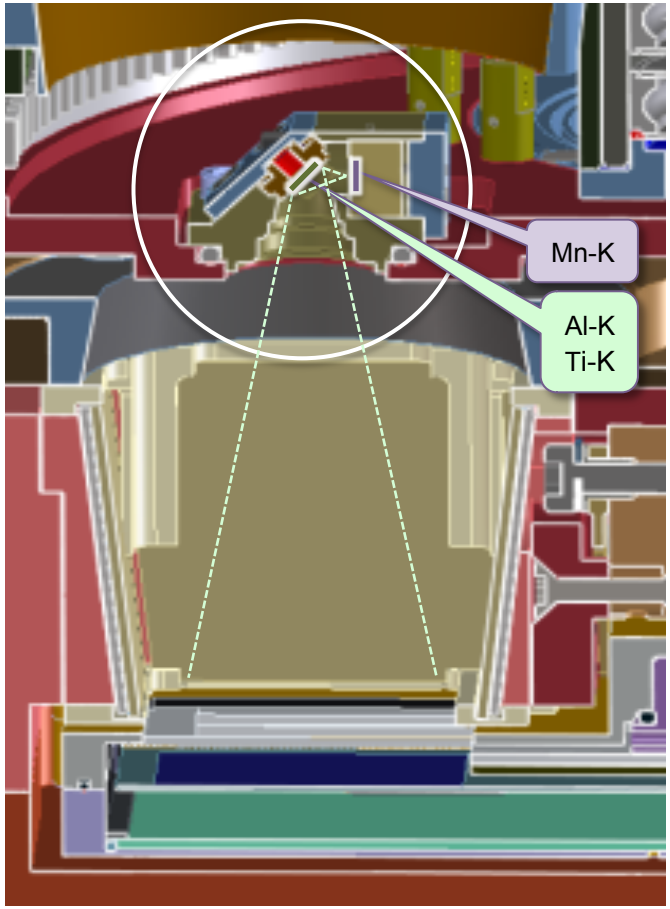

Energy Calibration: internal calibration source

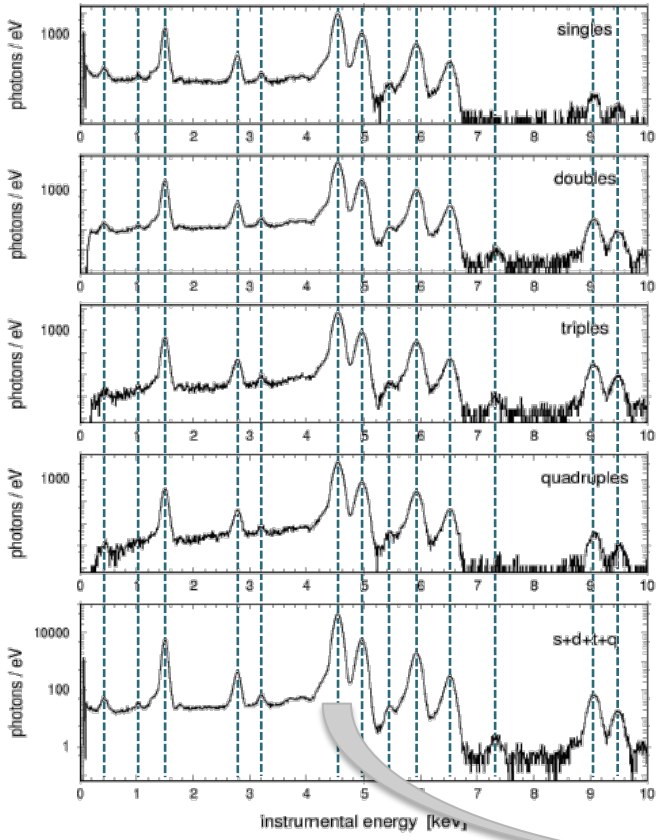

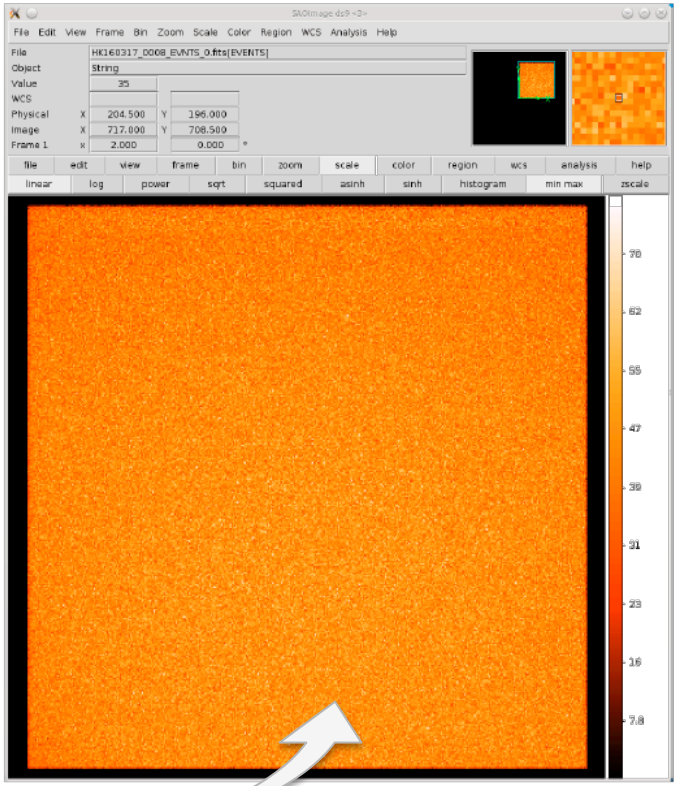

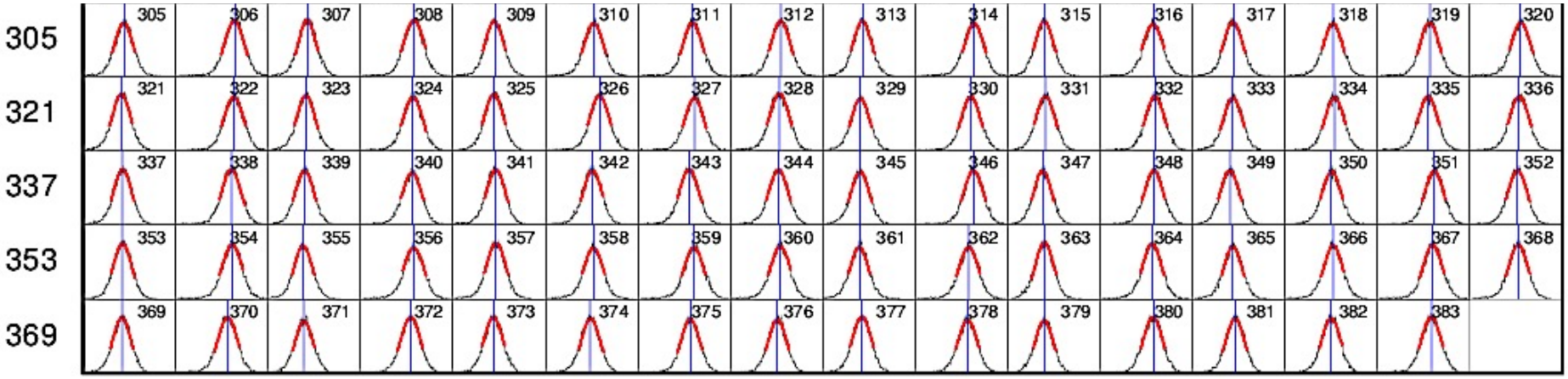

CTE correction applied energy: 1.486 keV split threshold: 46 adu

selection: first singles, amplitude range: 1700 .. 2100 adu, intensity range: 0.0 - 513.5 counts / bin

minimum counts per macro pixel: 90 binning: 4 precursor energy threshold: 100 adu

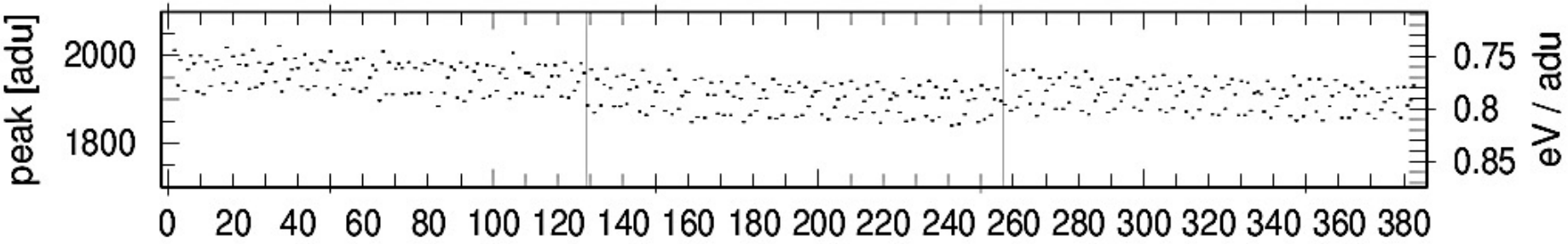

Gain: TM 4, Al-K

ground calibration

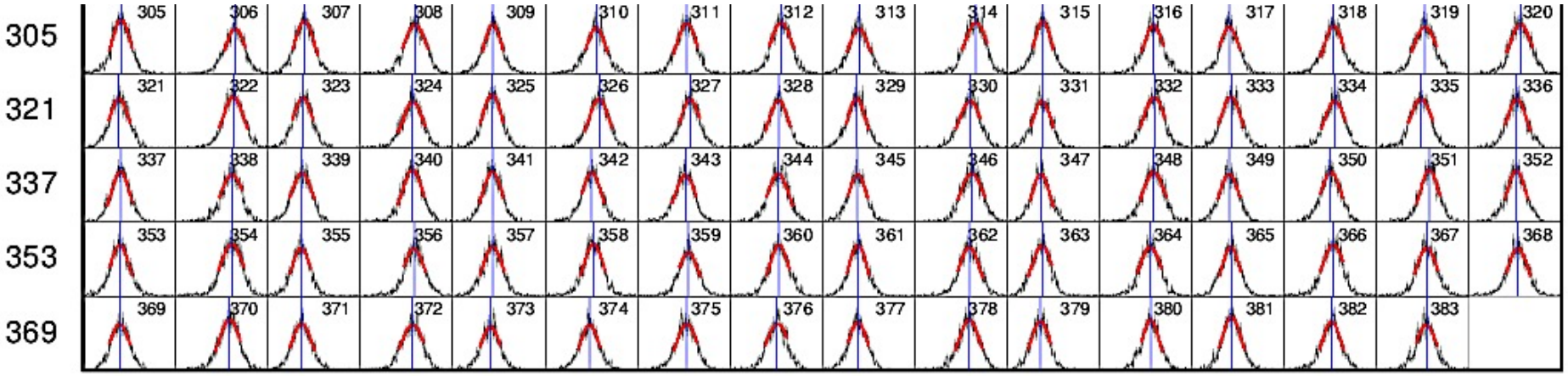

CTE correction applied energy: 1.486 keV split threshold: 60 adu

selection: first singles, amplitude range: 1700 .. 2100 adu, intensity range: 0.0 - 101.4 counts / bin

minimum counts per macro pixel: 90 binning: 4 precursor energy threshold: 100 adu

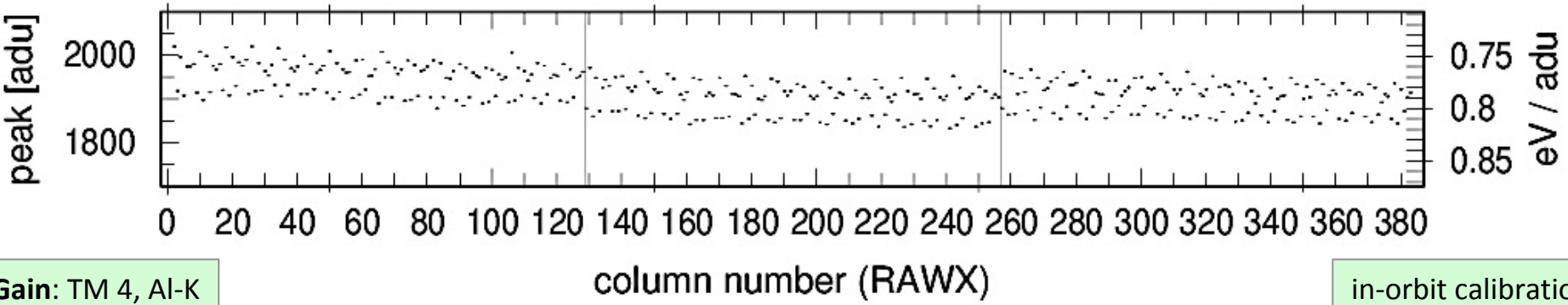

Gain: TM 4, Al-K

in-orbit calibration

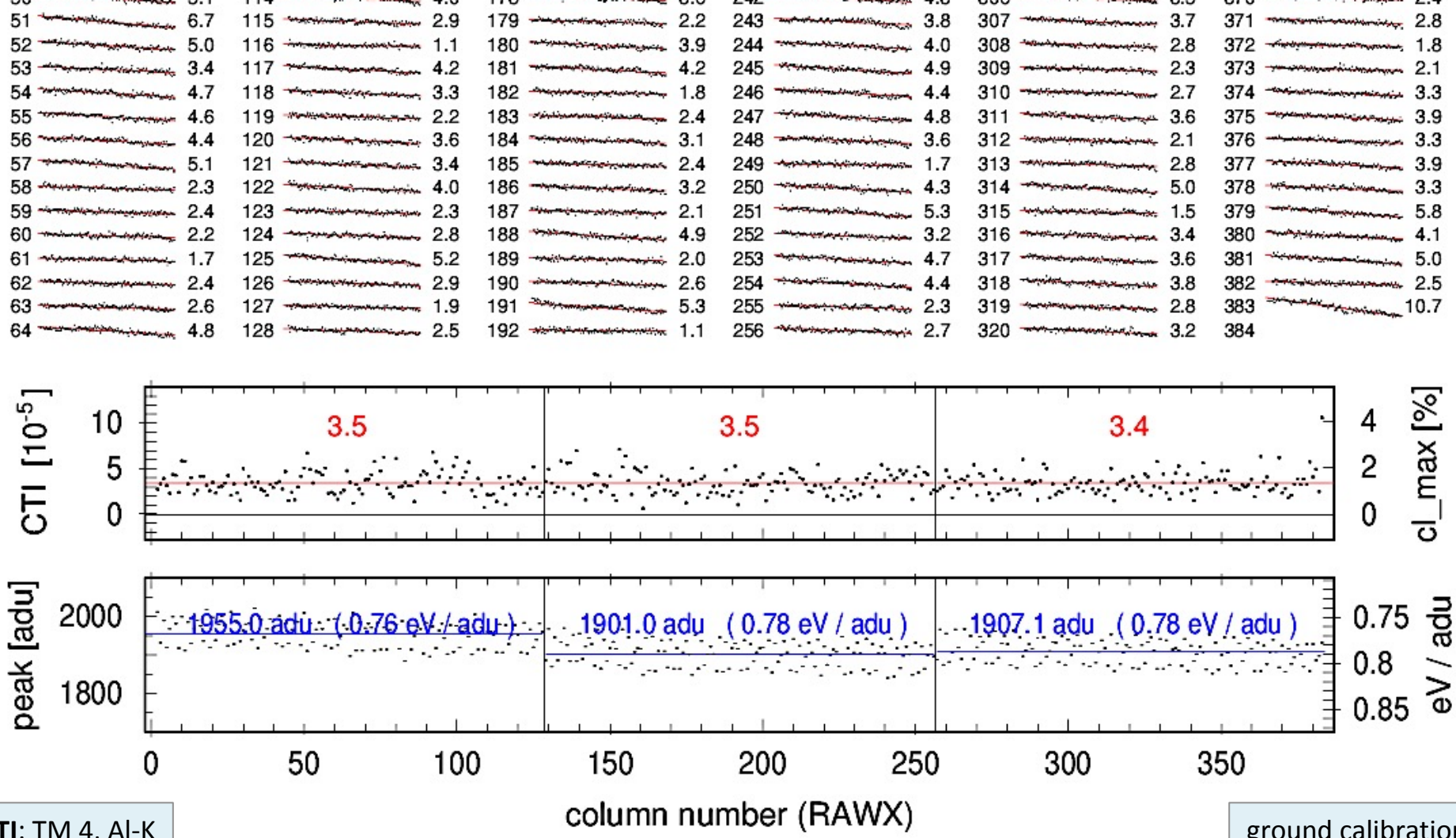

CTI: TM 4, Al-K

ground calibration

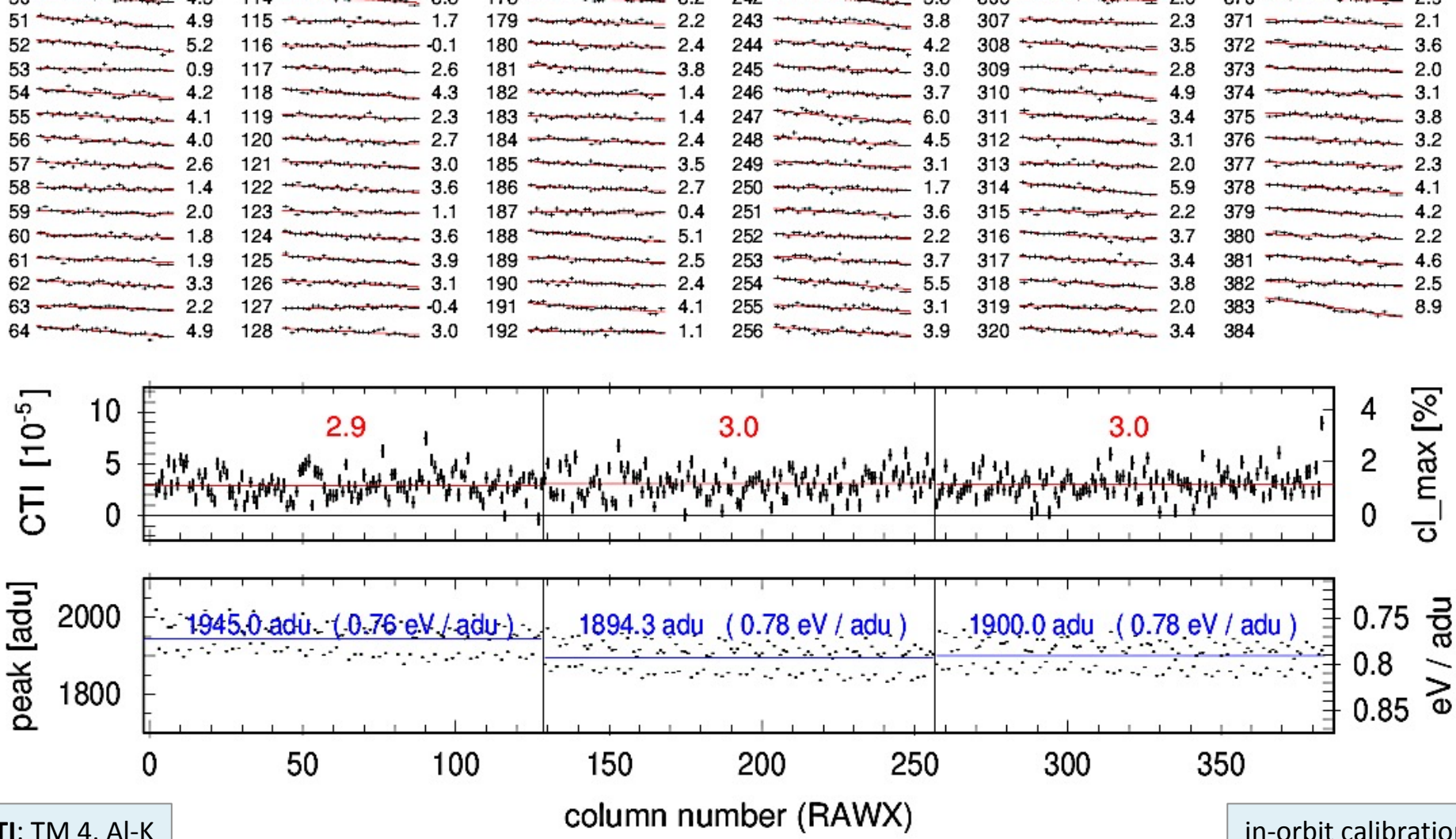

CTI: TM 4, Al-K

in-orbit calibration

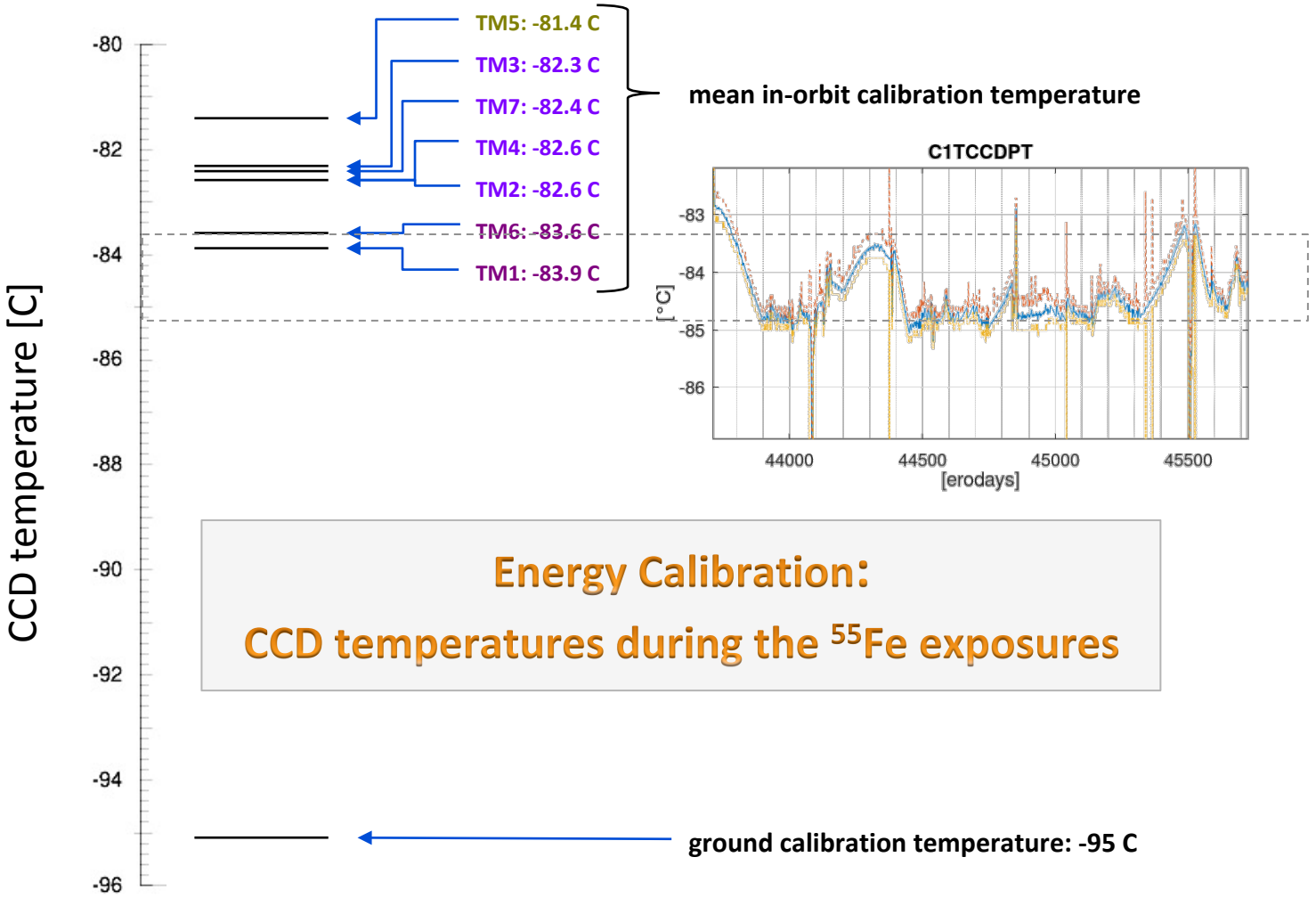
CCD temperature [C]
-80
-82
-84
-86
-88
-90
-92
-94
-96
TM5: -81.4 C
TM3: -82.3 C
TM7: -82.4 C
TM4: -82.6 C
TM2: -82.6 C
TM6: -83.6 C
TM1: -83.9 C
mean in-orbit calibration temperature
C1TCCDPT
-83
-84
-85
-86
[°C]
44000
44500
45000
45500
[erodays]
Energy Calibration:
CCD temperatures during the 55Fe exposures
ground calibration temperature: -95 C

CCD temperature induced energy drifts

Al-K

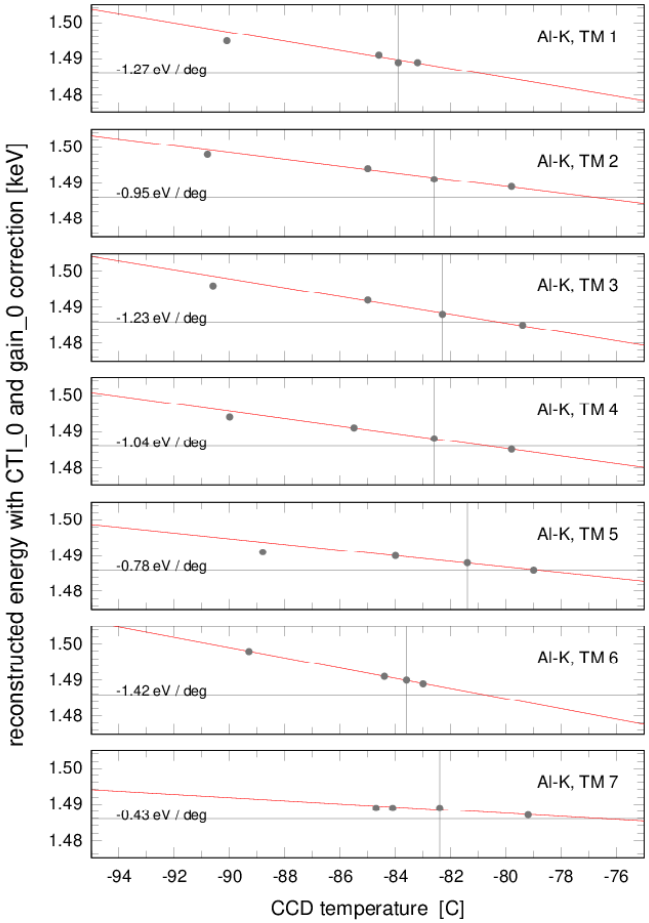

Ti-K

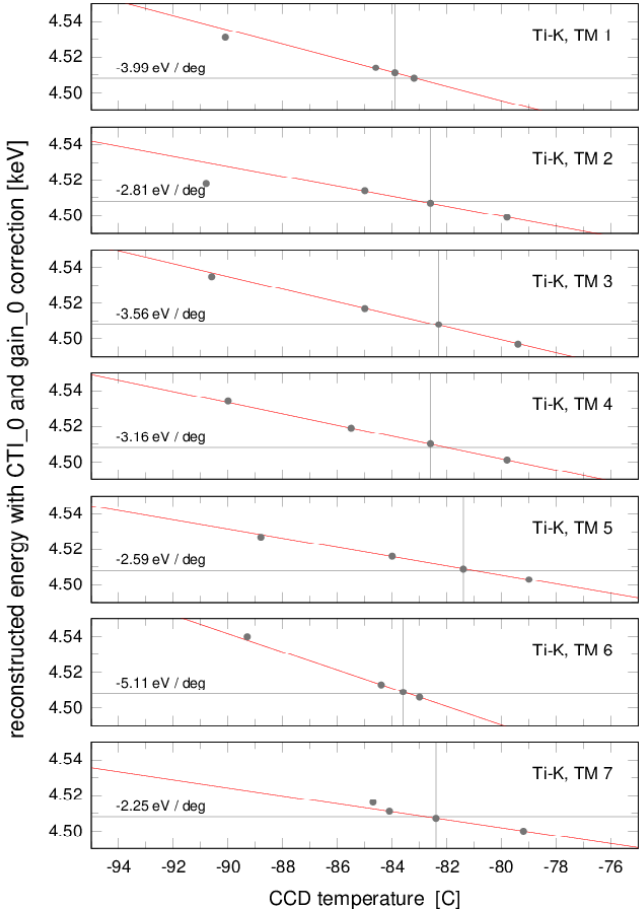

Effect of the temperature dependent gain

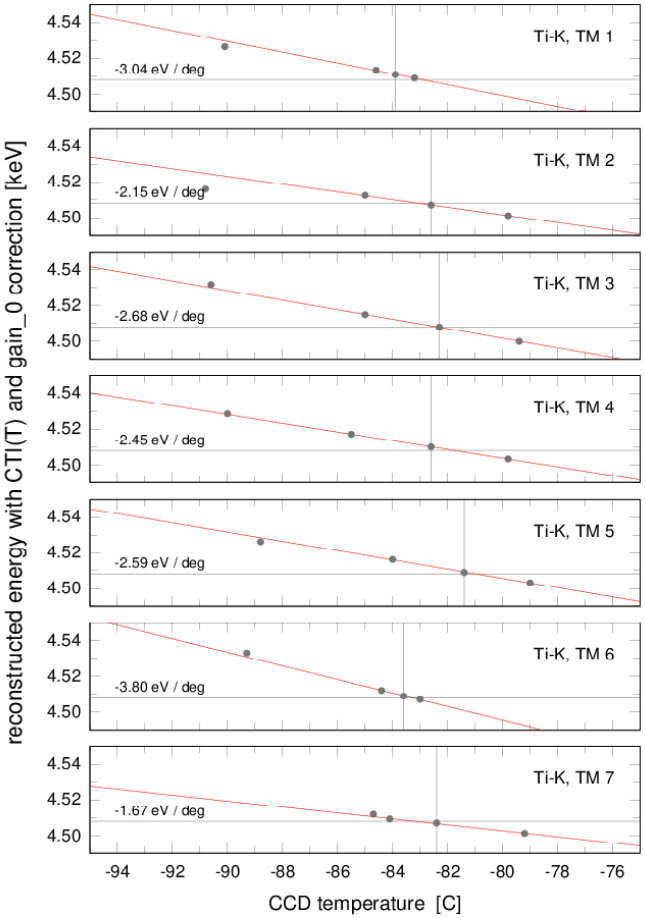

Ti-K

Effect of the temperature dependent CTI

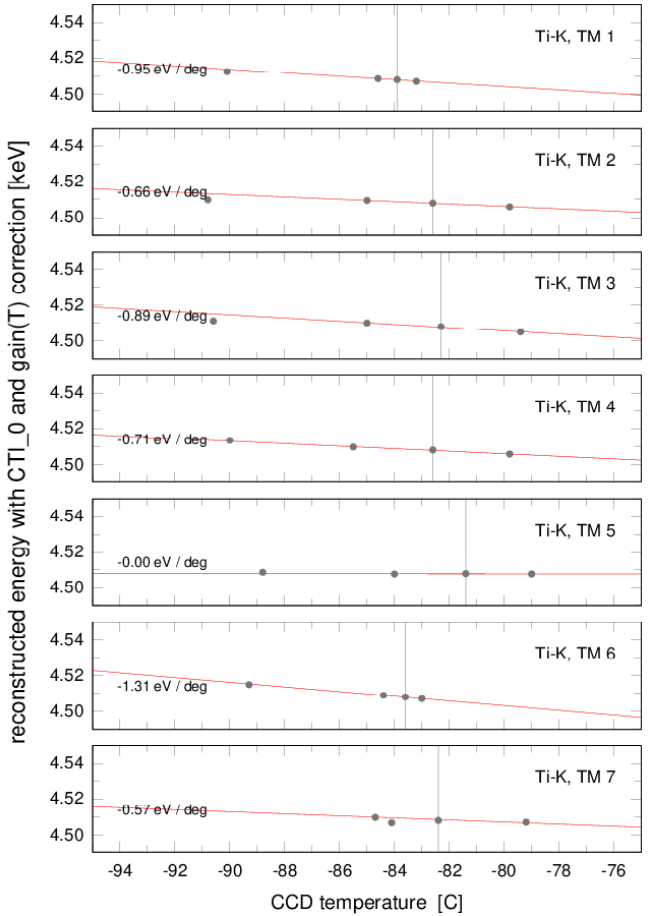

without temperature dependent energy correction

with temperature dependent energy correction

Ti-K

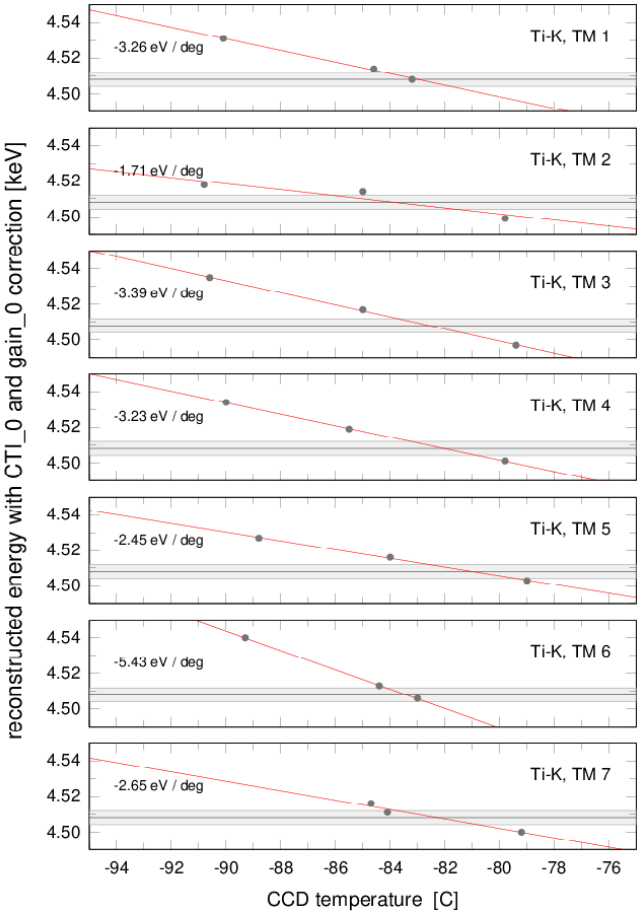

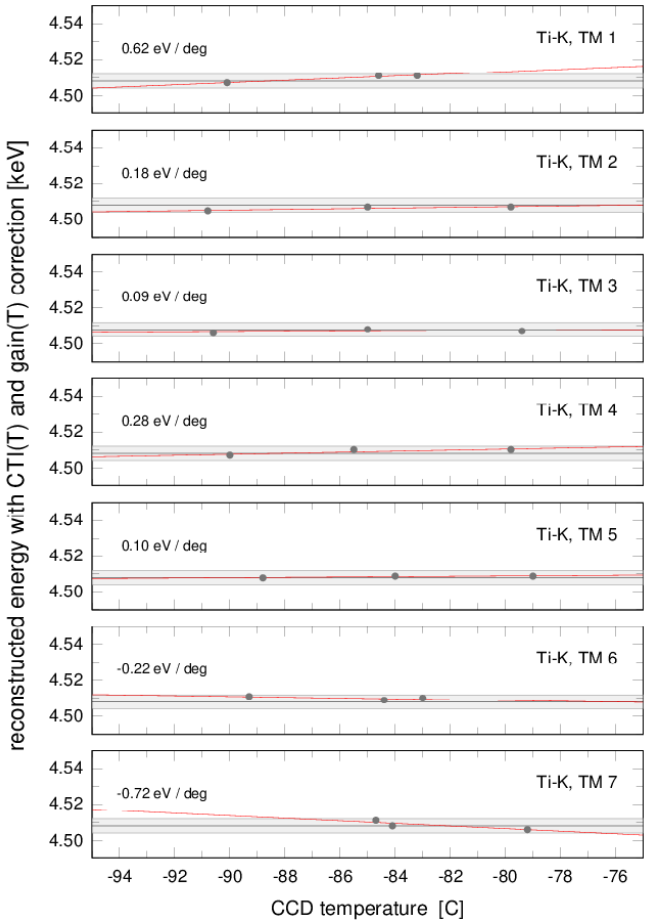

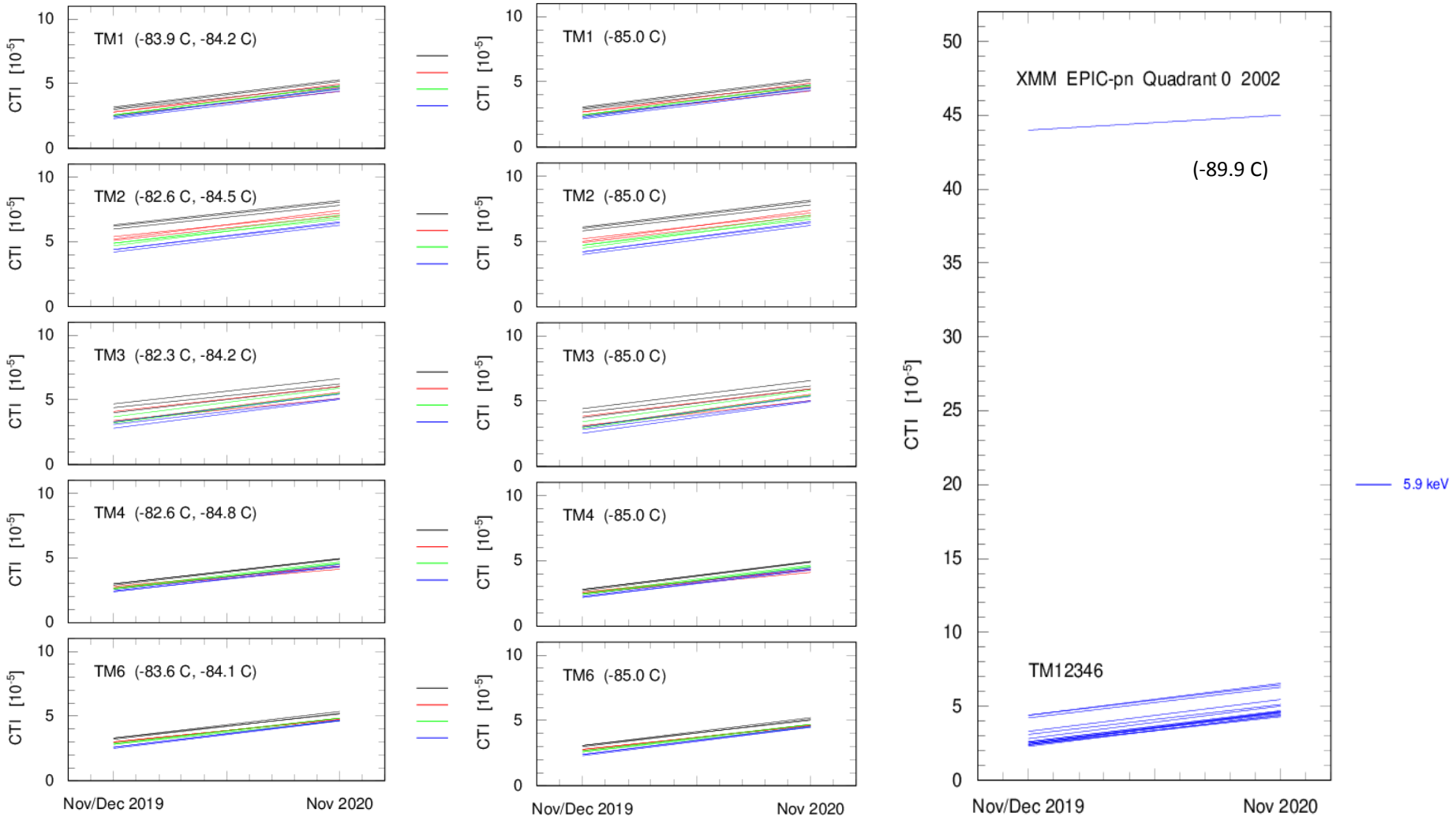
TM1 (-83.9 C, -84.2 C)
TM2 (-82.6 C, -84.5 C)
TM3 (-82.3 C, -84.2 C)
TM4 (-82.6 C, -84.8 C)
TM6 (-83.6 C, -84.1 C)
TM1 (-85.0 C)
TM2 (-85.0 C)
TM3 (-85.0 C)
TM4 (-85.0 C)
TM6 (-85.0 C)
CTI [10^-5]
Nov/Dec 2019
Nov 2020
XMM EPIC-pn Quadrant 0 2002
(-89.9 C)
TM12346
5.9 keV

Expected CTI increase

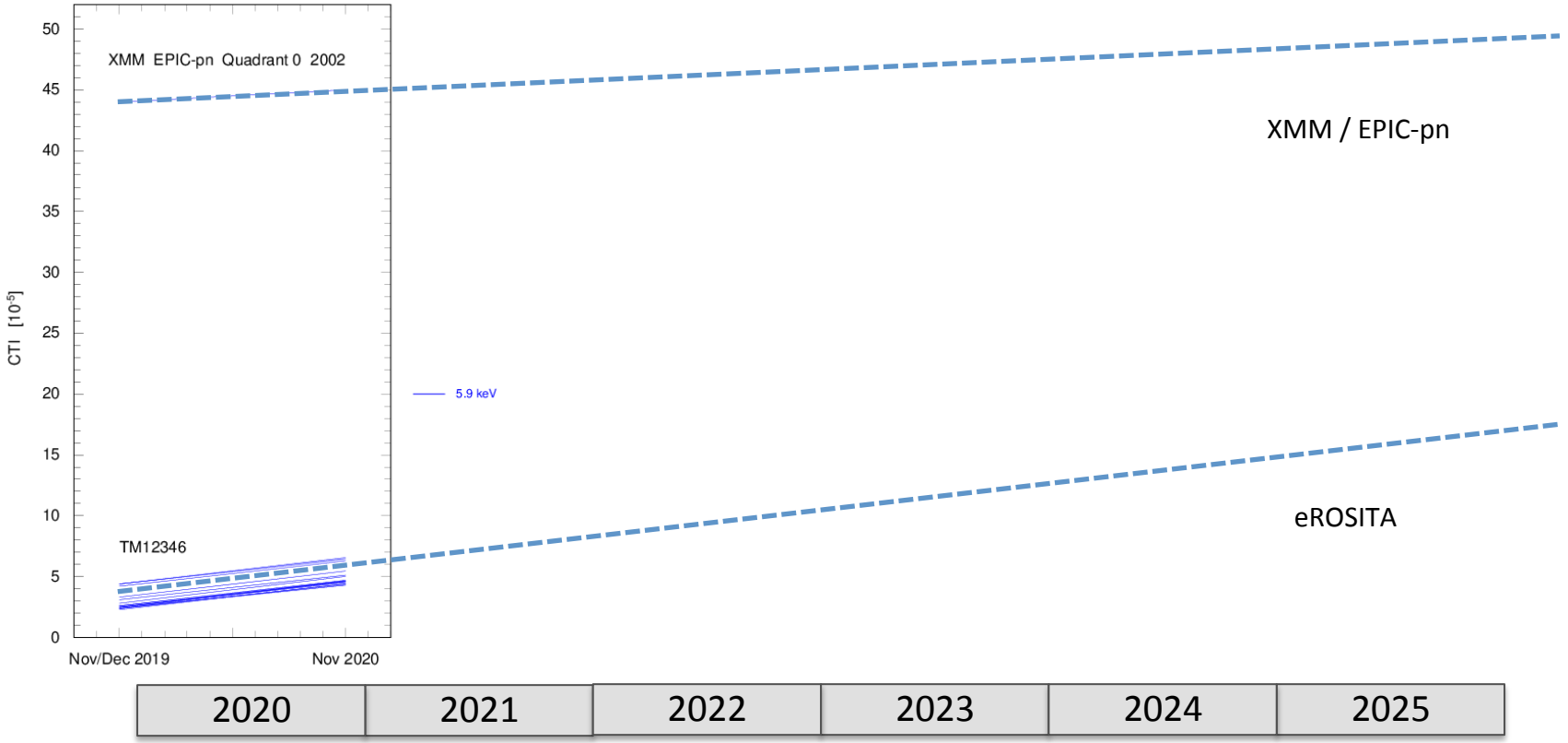

FWHM evolution (with long-term correction)

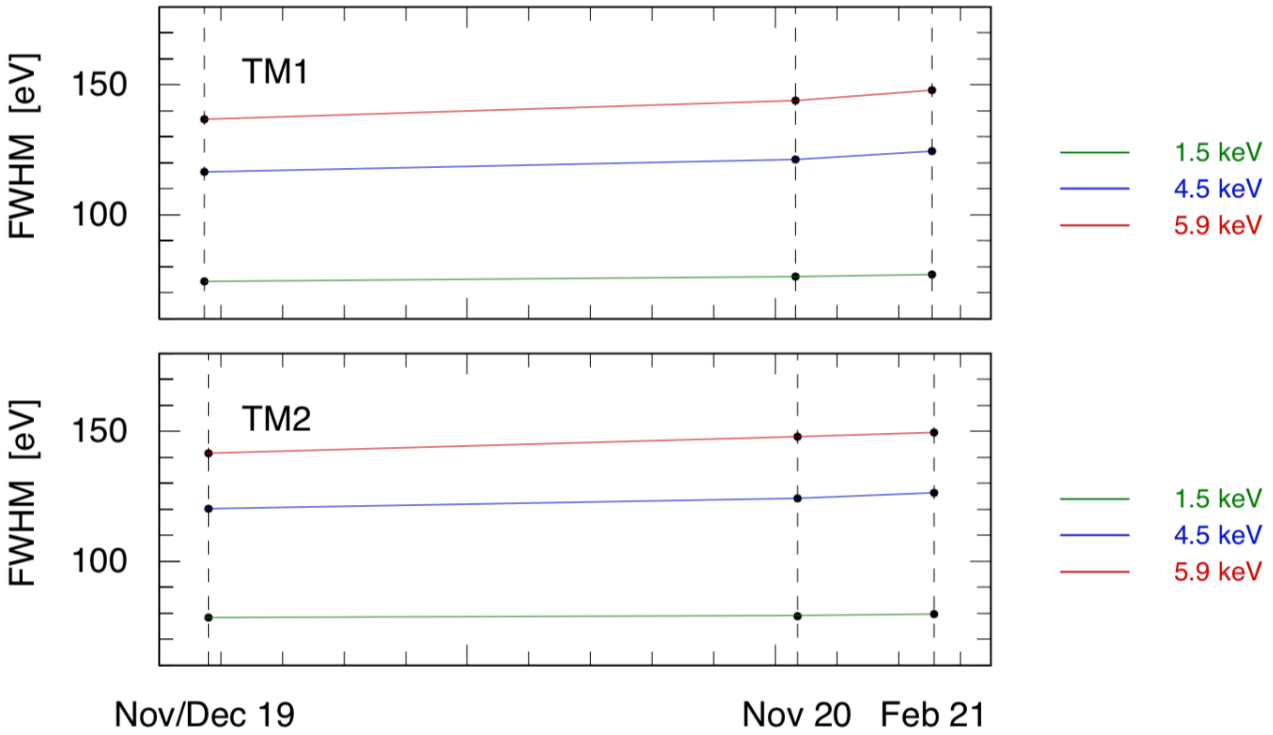

Calibration observations during the CalPV phase

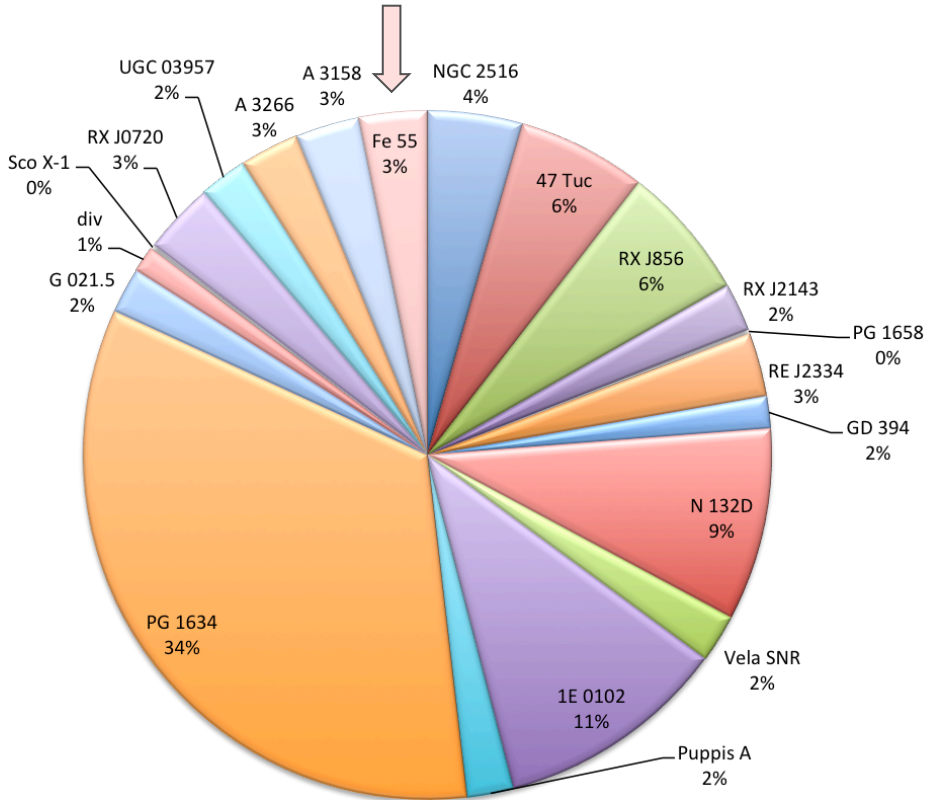

The segments scale with the average exposure time per TM

From Munich to Moscow

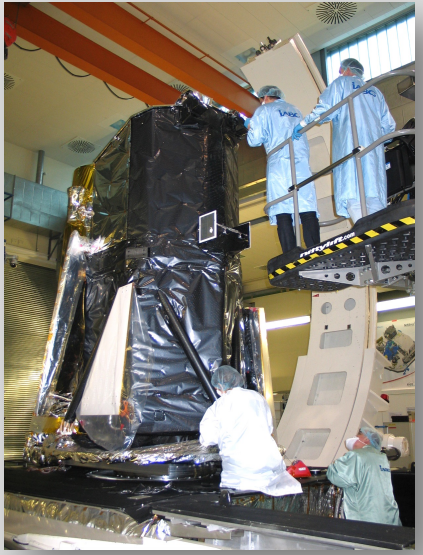

Transport in Moscow from SVO airport to NPOL

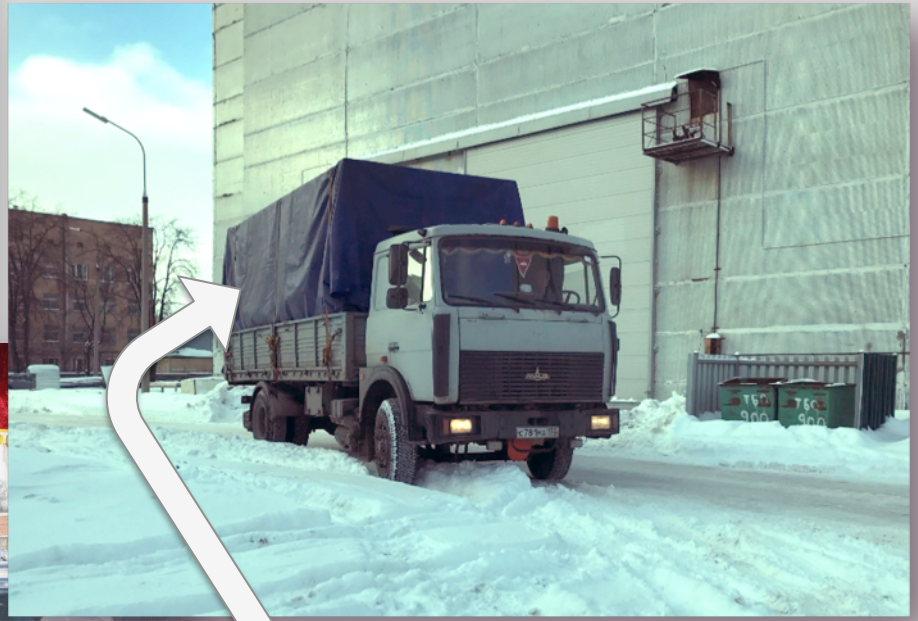

> 10 years of development
> and > 90 Million €

From Moscow to Baikonur


Roskosmos


БЛОК Ц
БЛОК Ц
БЛОК Ц


ПРОТОН

Baikonur, Kazakhstan, 2019 July 13

Comparison with expectations

?

- detector noise
- telemetry bandwidth
- particle background
- filter integrity
- contamination
- radiation damage
- observing efficiency
- the unexpected

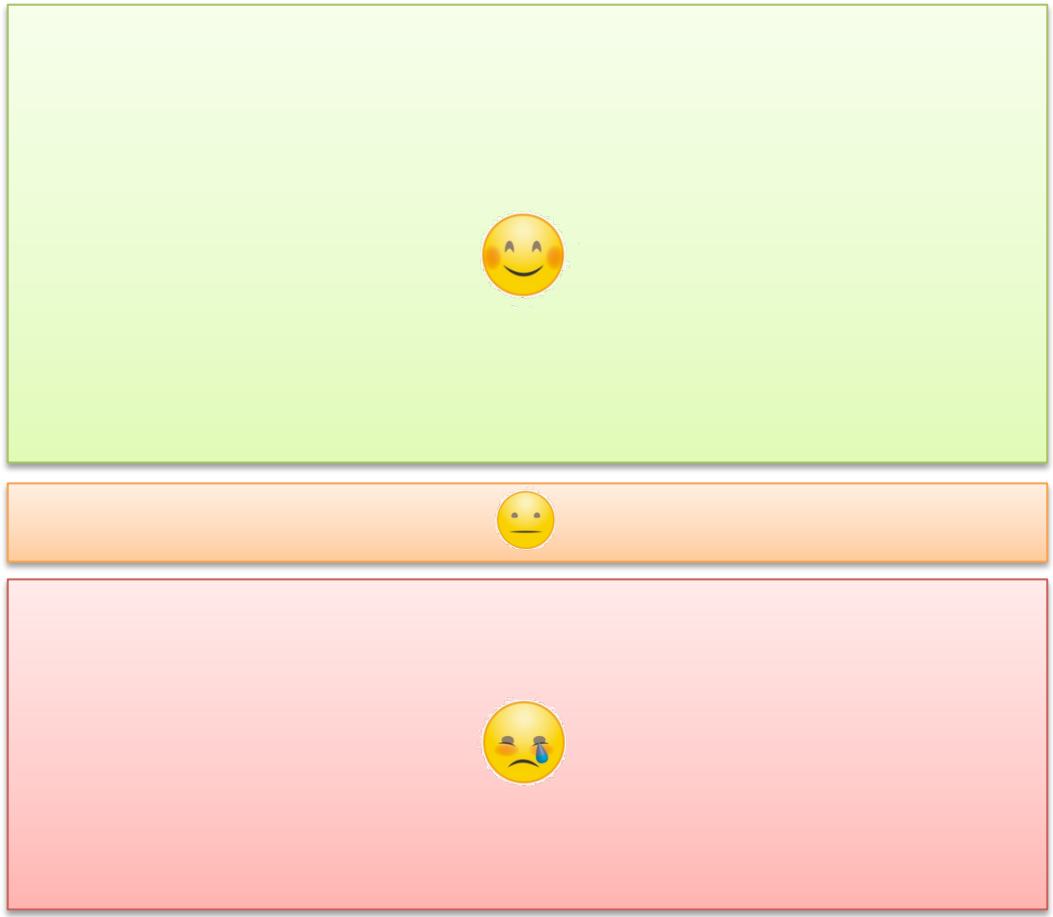

Comparison with expectations

?

detector noise

✓ detector noise: lower than expected

Comparison with expectations

?

telemetry bandwidth

- ✓ detector noise: lower than expected
- ✓ telemetry bandwidth: sufficient
  - ✓ efficient onboard data compression
  - ✓ more telemetry available than expected

Comparison with expectations

?

particle background

- ✓ detector noise: lower than expected
- ✓ telemetry bandwidth: sufficient
  - ✓ efficient onboard data compression
  - ✓ more telemetry available than expected
- ✓ particle background: less variable than expected

- − particle background: higher than expected

Background

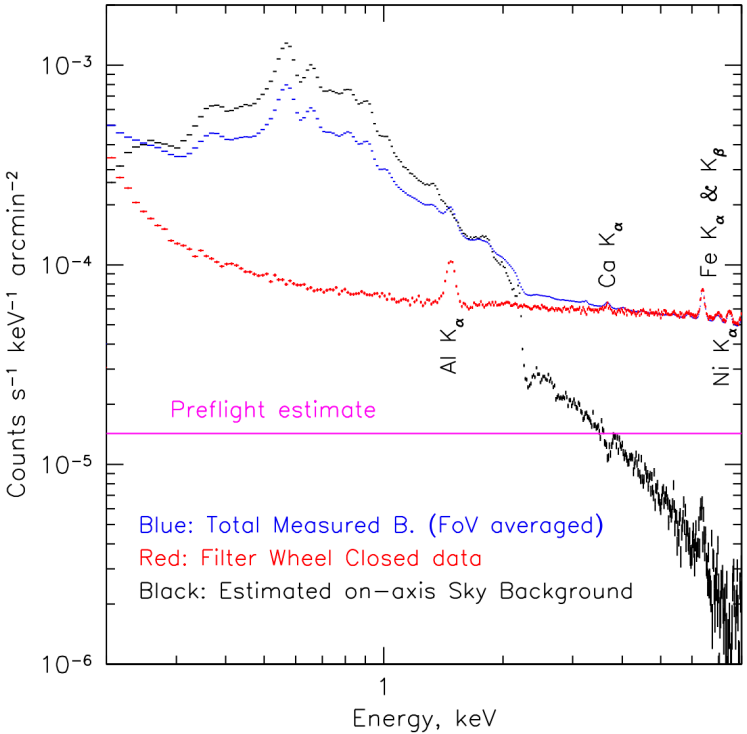
Counts s^{-1} keV^{-1} arcmin^{-2}
10^{-3}
10^{-4}
10^{-5}
10^{-6}
1
Energy, keV
Al K_α
Ca K_α
Fe K_α & K_β
Ni K_α
Preflight estimate
Blue: Total Measured B. (FoV averaged)
Red: Filter Wheel Closed data
Black: Estimated on−axis Sky Background

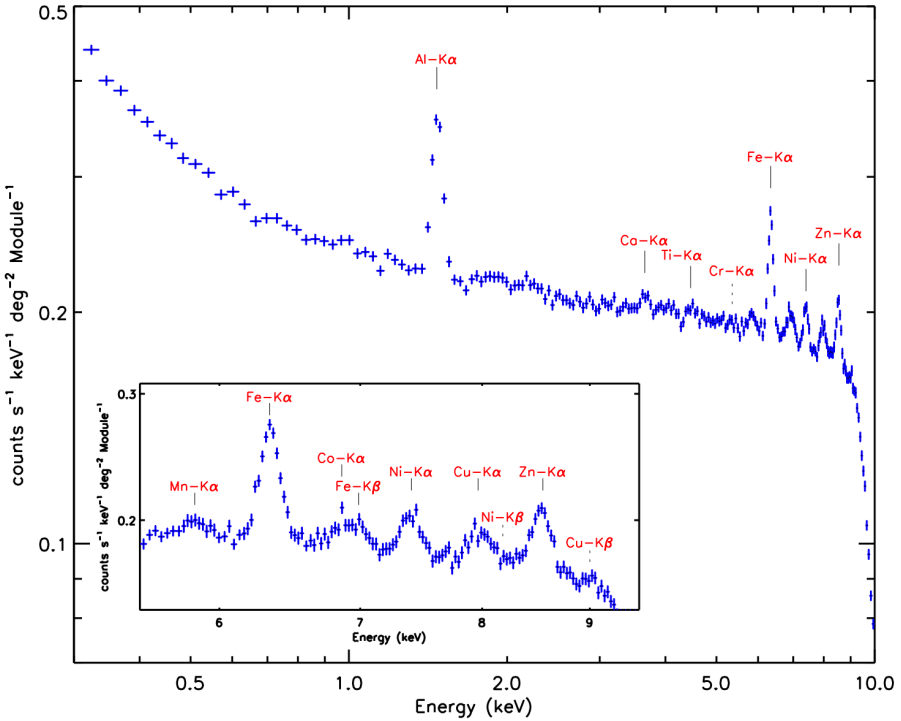
counts s^{-1} keV^{-1} deg^{-2} Module^{-1}
0.5
0.2
0.1
0.5
1.0
2.0
5.0
10.0
Energy (keV)
Al−Kα
Fe−Kα
Ca−Kα
Ti−Kα
Cr−Kα
Ni−Kα
Zn−Kα
Mn−Kα
Fe−Kβ
Co−Kα
Cu−Kα
Ni−Kβ
Cu−Kβ
0.3
0.2
6
7
8
9

Comparison with expectations

?

- ✓ detector noise: lower than expected
- ✓ telemetry bandwidth: sufficient
  - ✓ efficient onboard data compression
  - ✓ more telemetry available than expected
- ✓ particle background: less variable than expected
- ✓ filters ok

filter integrity

- − particle background: higher than expected

Comparison with expectations

?

- ✓ detector noise: lower than expected
- ✓ telemetry bandwidth: sufficient
  - ✓ efficient onboard data compression
  - ✓ more telemetry available than expected
- ✓ particle background: less variable than expected
- ✓ filters ok
- ✓ contamination: no indication seen yet (!)

contamination

- − particle background: higher than expected

Contamination Monitoring

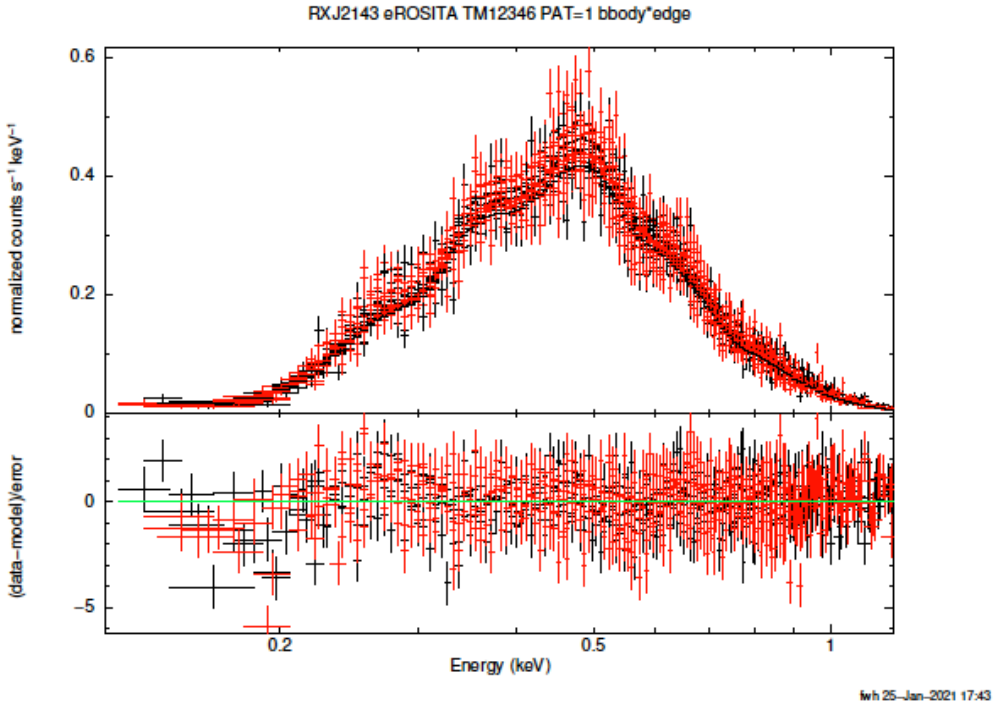

Analysis of eROSITA spectra from isolated neutron stars for contamination monitoring

F. Haberl, M. Freyberg, K. Dennerl, H. Brunner

January 27, 2021

RXJ2143:

observed on

① 2019-12-02/03

② 2020-11-25/26

Simultaneous fit to the 10 spectra (5 TMs at 2 occasions) with common n_H and C-K edge depth → **no evidence of contamination** (!)

Comparison with expectations

?

- ✓ detector noise: lower than expected
- ✓ telemetry bandwidth: sufficient
  - ✓ efficient onboard data compression
  - ✓ more telemetry available than expected
- ✓ particle background: less variable than expected
- ✓ filters ok
- ✓ contamination: no indication seen yet (!)

- ○ radiation damage: CTI increase slightly higher than expected

radiation damage

- − particle background: higher than expected

Comparison with expectations

?

- ✓ detector noise: lower than expected
- ✓ telemetry bandwidth: sufficient
  - ✓ efficient onboard data compression
  - ✓ more telemetry available than expected
- ✓ particle background: less variable than expected
- ✓ filters ok
- ✓ contamination: no indication seen yet (!)

- ○ radiation damage: CTI increase slightly higher than expected

„radiation“ damage

- − particle background: higher than expected
- − micrometeoroid damages

Comparison with expectations

?

- ✓ detector noise: lower than expected
- ✓ telemetry bandwidth: sufficient
  - ✓ efficient onboard data compression
  - ✓ more telemetry available than expected
- ✓ particle background: less variable than expected
- ✓ filters ok
- ✓ contamination: no indication seen yet (!)
- ✓ satellite platform: very stable and reliable
- ✓ observing efficiency: very high

- ○ radiation damage: CTI increase slightly higher than expected

- − particle background: higher than expected
- − micrometeoroid damages

observing efficiency

Observing Efficiency

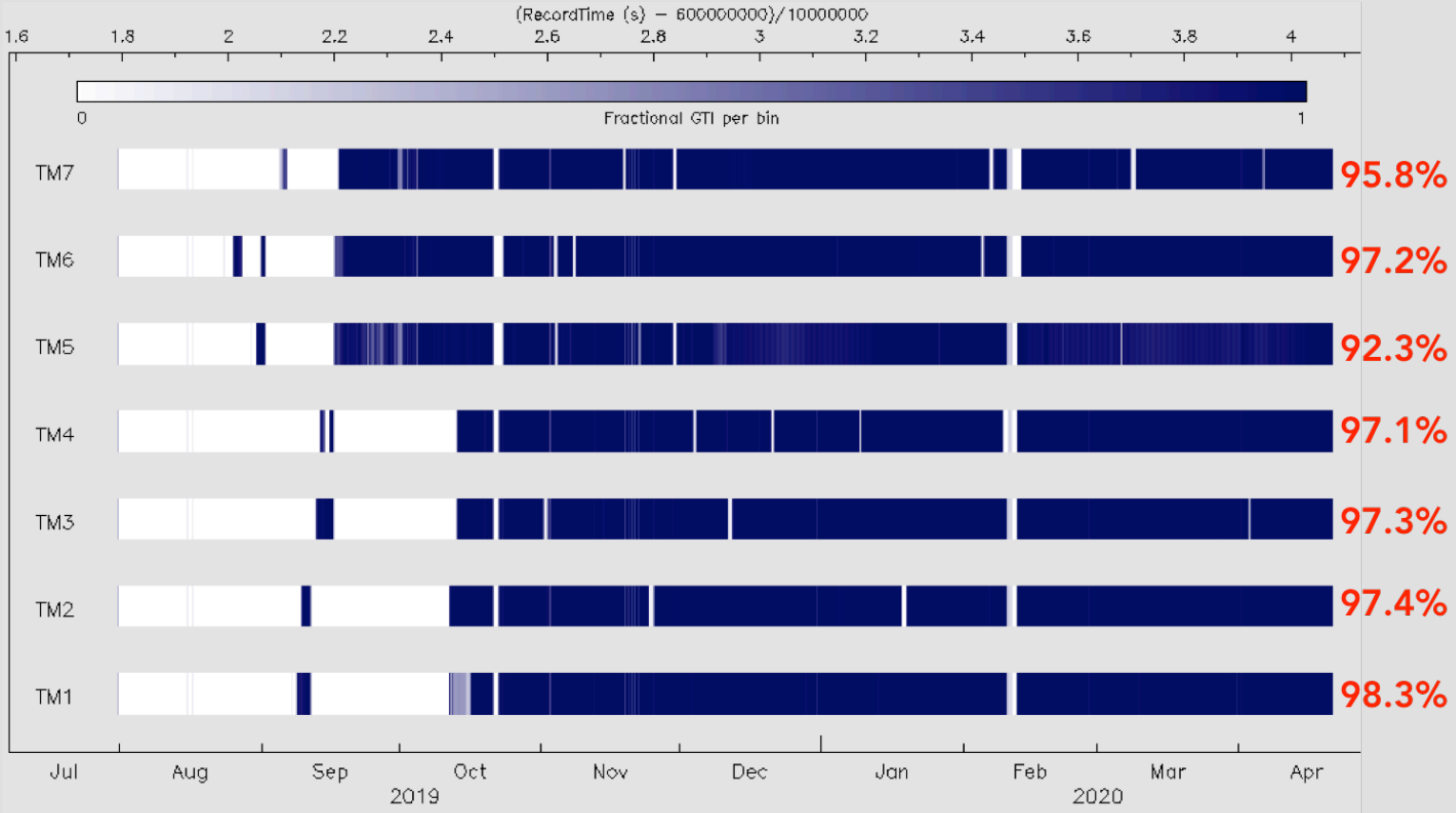

Courtesy I. Stewart (MPE)

TOTAL GTI fraction since eRASS start ~96.5%

Operations Team at MPE

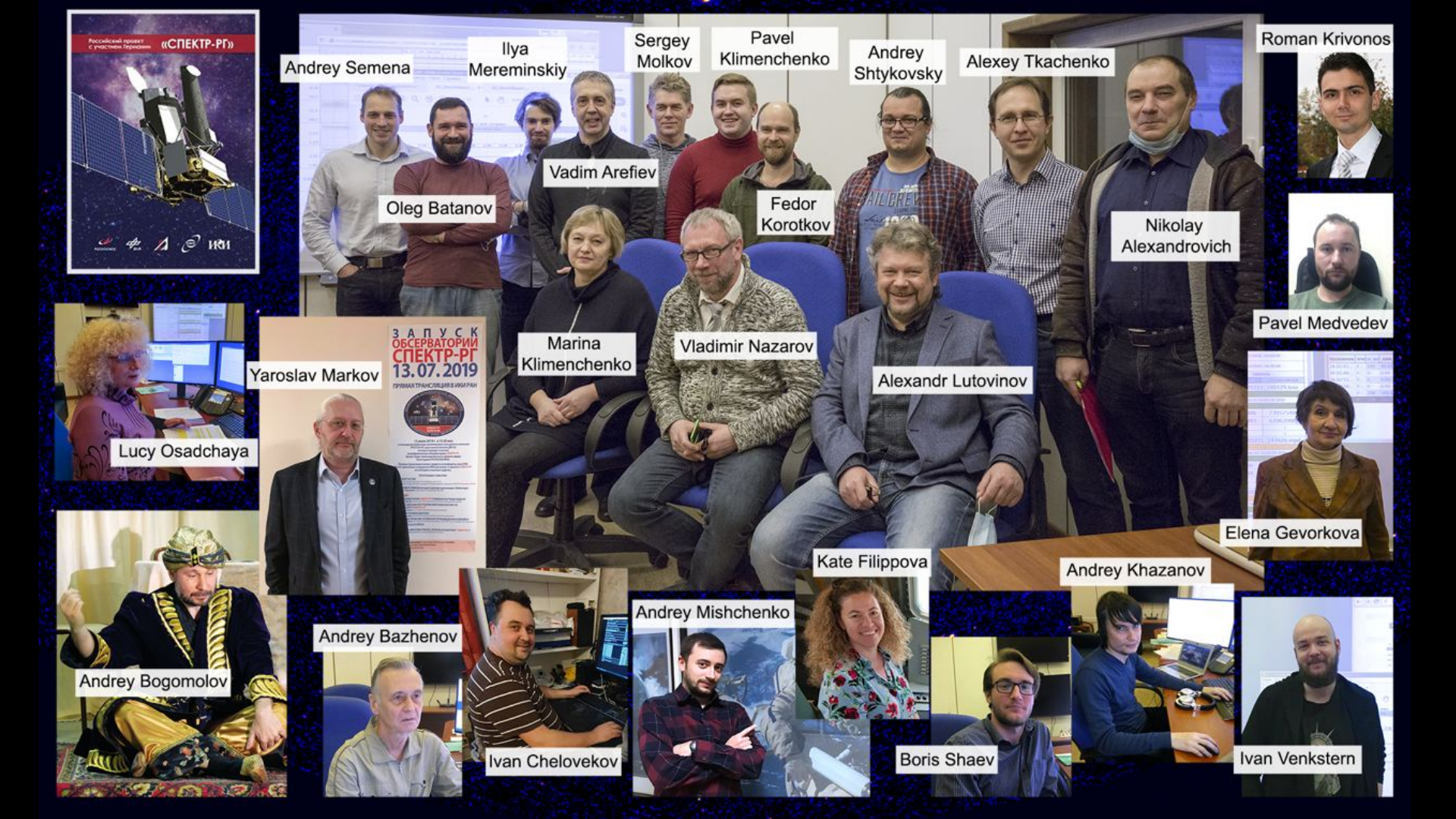
Российский проект с участием Германии
«СПЕКТР-РГ»
Andrey Semena
Ilya Mereminskiy
Sergey Molkov
Pavel Klimenchenko
Andrey Shtykovsky
Alexey Tkachenko
Roman Krivonos
Vadim Arefiev
Oleg Batanov
Fedor Korotkov
Nikolay Alexandrovich
Pavel Medvedev
Lucy Osadchaya
Yaroslav Markov
ЗАПУСК ОБСЕРВАТОРИИ СПЕКТР-РГ 13.07.2019
ПРЯМАЯ ТРАНСЛЯЦИЯ В ИКИ РАН
Marina Klimenchenko
Vladimir Nazarov
Alexandr Lutovinov
Elena Gevorkova
Andrey Bogomolov
Andrey Bazhenov
Ivan Chelovekov
Andrey Mishchenko
Kate Filippova
Andrey Khazanov
Boris Shaev
Ivan Venkstern

Comparison with expectations

?

- ✓ detector noise: lower than expected
- ✓ telemetry bandwidth: sufficient
  - ✓ efficient onboard data compression
  - ✓ more telemetry available than expected
- ✓ particle background: less variable than expected
- ✓ filters ok
- ✓ contamination: no indication seen yet (!)
- ✓ satellite platform: very stable and reliable
- ✓ observing efficiency: very high

- o radiation damage: CTI increase slightly higher than expected

- − particle background: higher than expected
- − micrometeoroid damages
- − CCD temperatures: higher and more variable than expected

the unexpected

Comparison with expectations

?

- ✓ detector noise: lower than expected
- ✓ telemetry bandwidth: sufficient
  - ✓ efficient onboard data compression
  - ✓ more telemetry available than expected
- ✓ particle background: less variable than expected
- ✓ filters ok
- ✓ contamination: no indication seen yet (!)
- ✓ satellite platform: very stable and reliable
- ✓ observing efficiency: very high

- o radiation damage: CTI increase slightly higher than expected

- − particle background: higher than expected
- − micrometeoroid damages
- − CCD temperatures: higher and more variable than expected
- − severe optical light leak problem in two cameras

the unexpected

SRG/eROSITA-TM5

optical light leak

10 min time bins

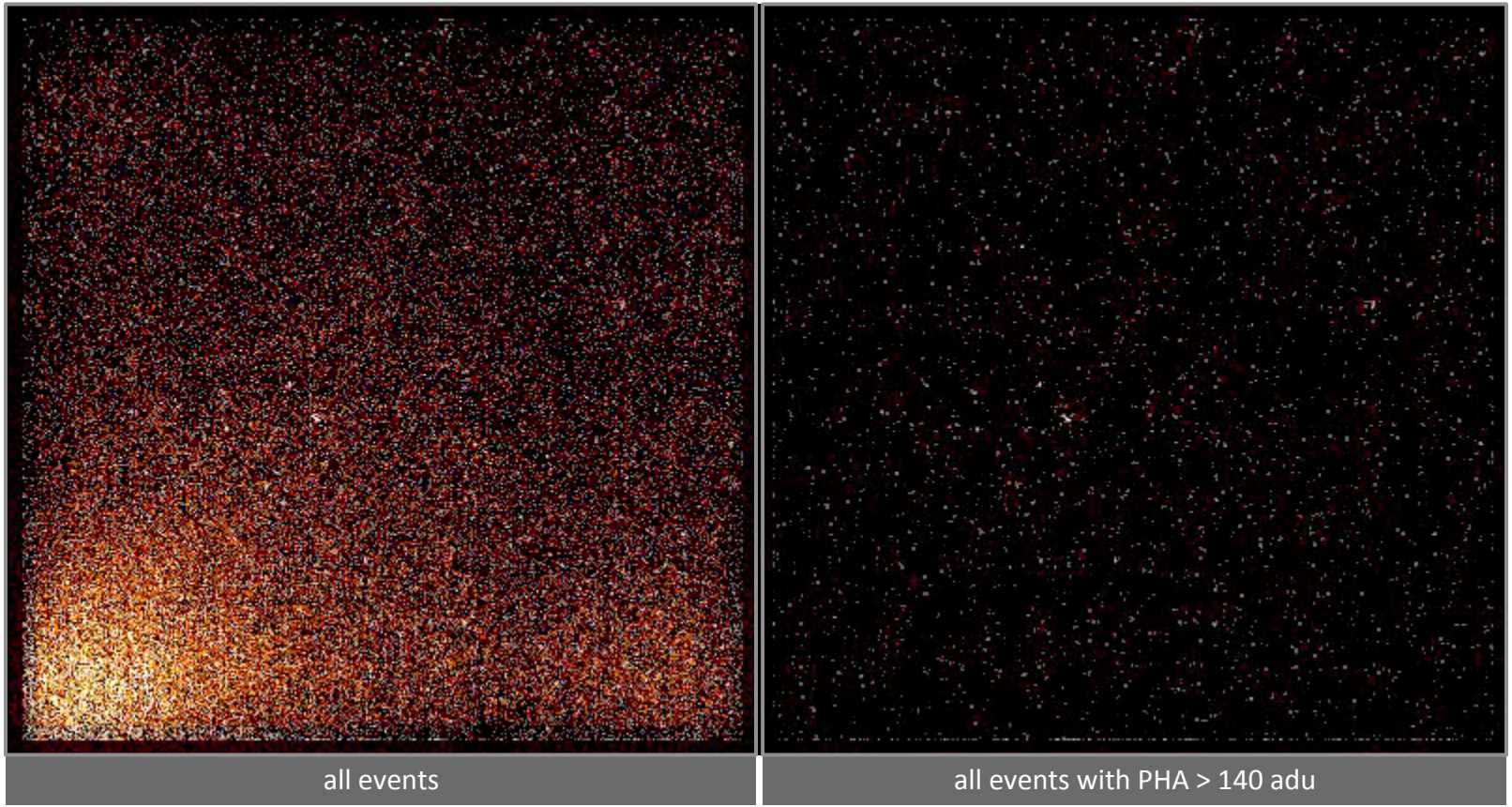

all events

all events with PHA > 140 adu

SRG/eROSITA-TM7

optical light leak

10 min time bins

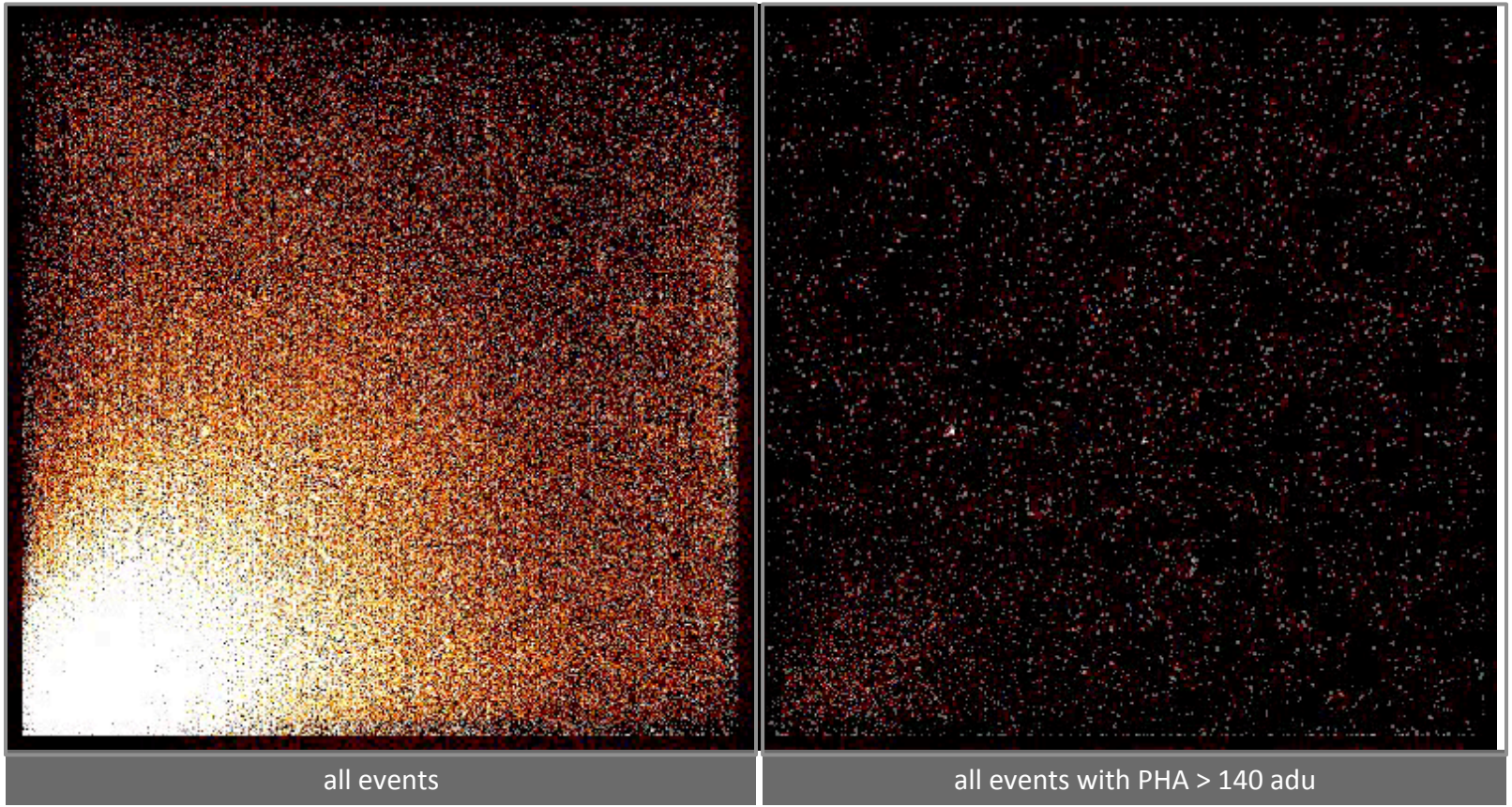

all events

all events with PHA > 140 adu

Energy Calibration: optical light leak in TM5 and TM7

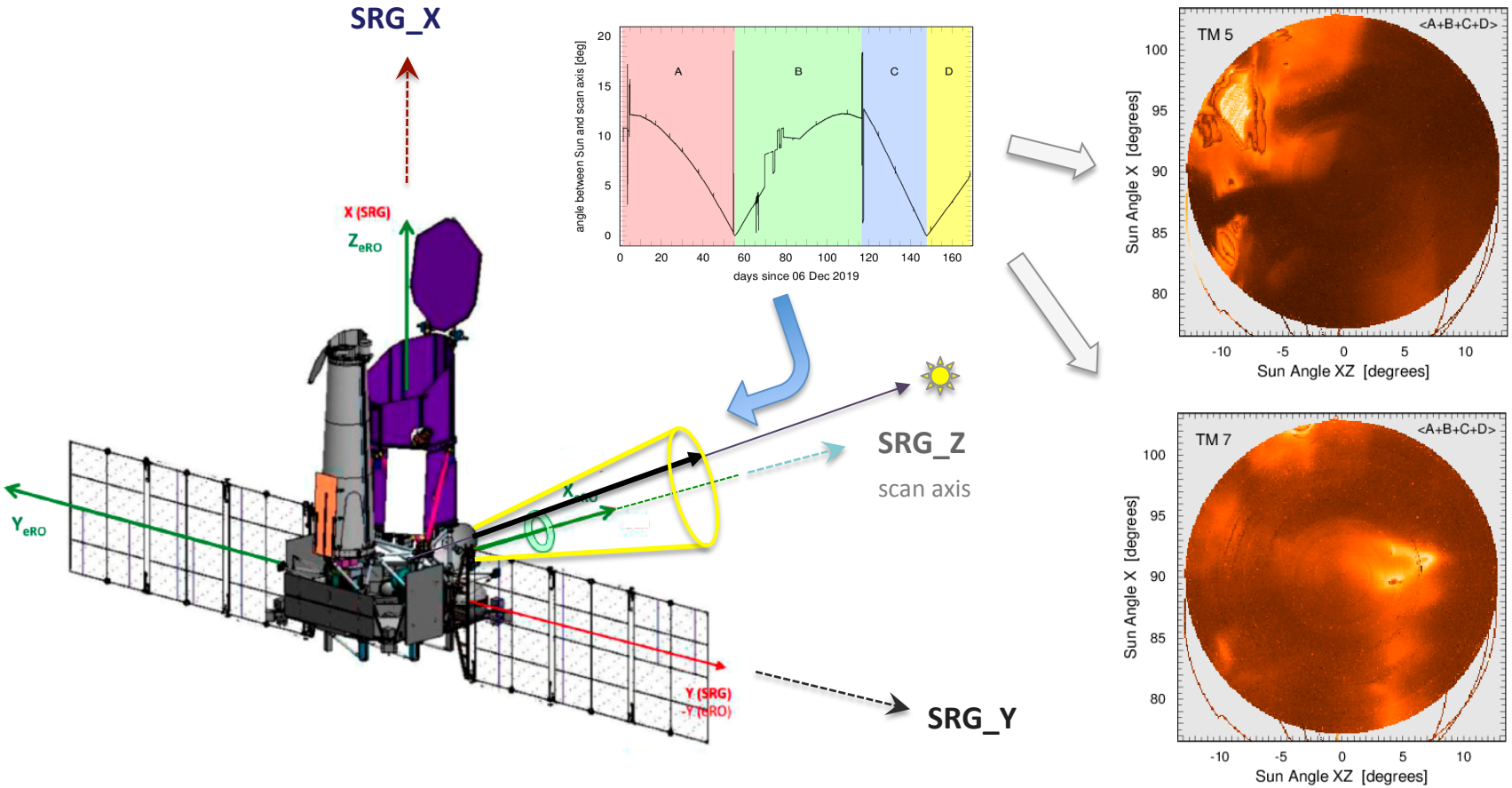

Energy Calibration: optical light leak in TM5 and TM7

residual offset map caused by optical light

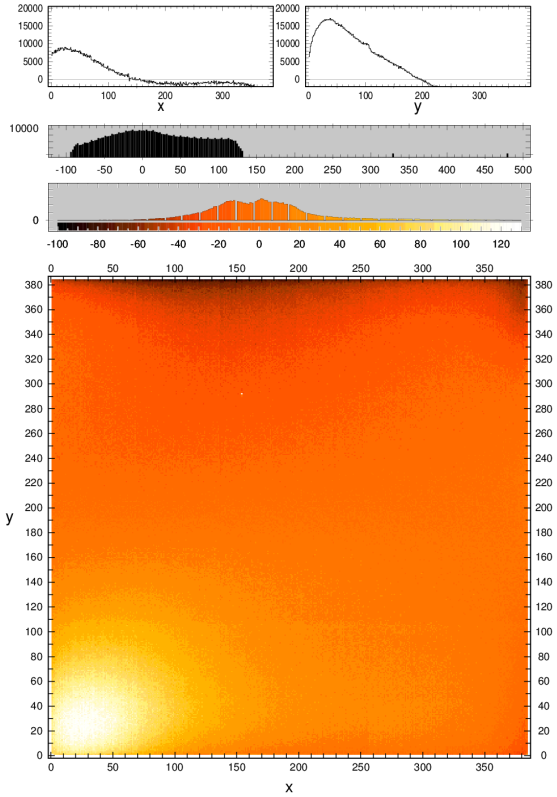

after common mode subtraction

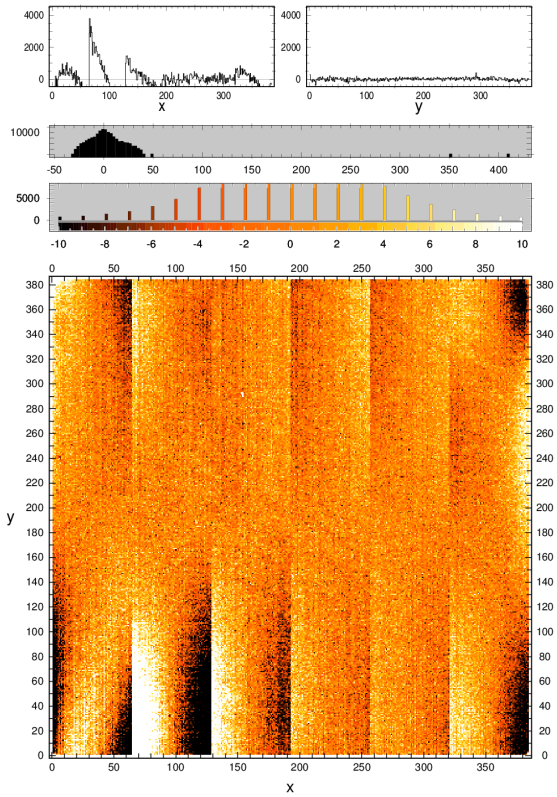

observed event rate (TM7)

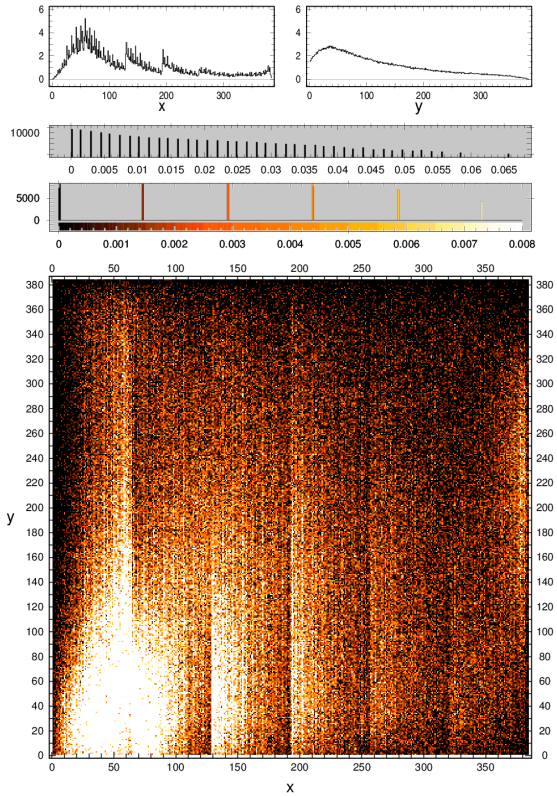

Energy Calibration: optical light leak in TM5 and TM7

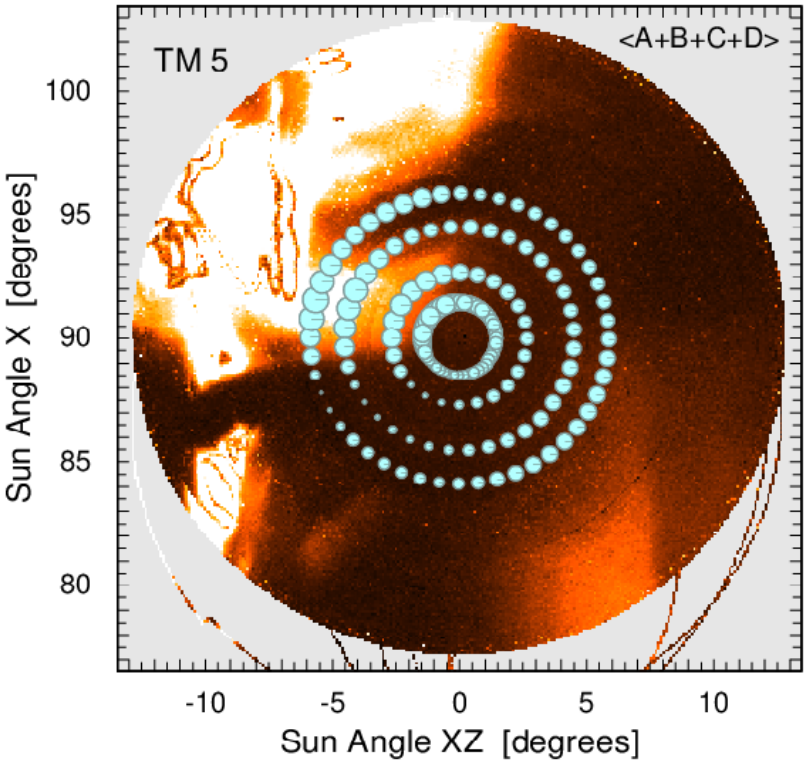

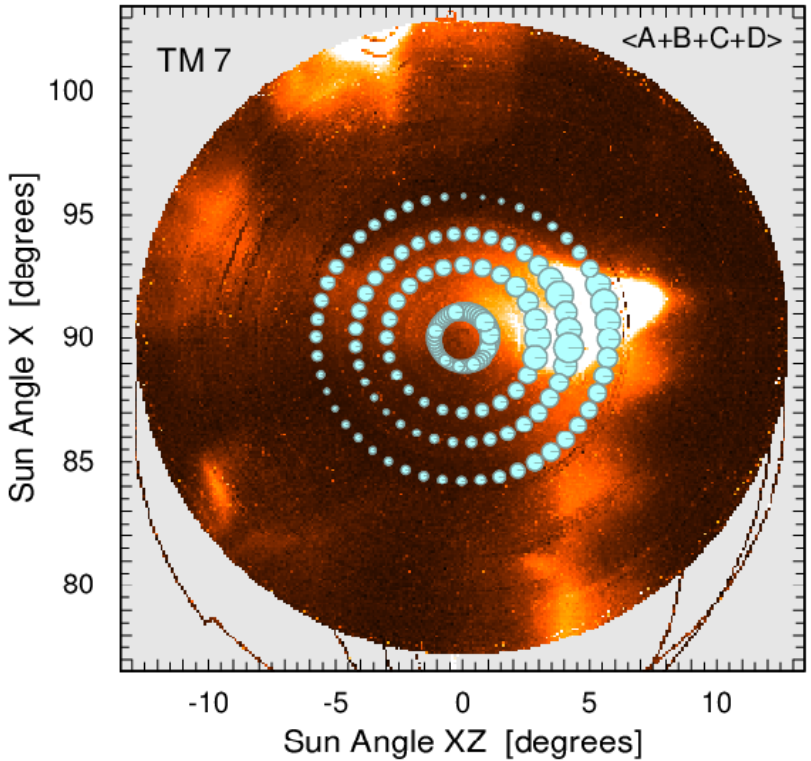

Comparison with expectations

?

- ✓ detector noise: lower than expected
- ✓ telemetry bandwidth: sufficient
  - ✓ efficient onboard data compression
  - ✓ more telemetry available than expected
- ✓ particle background: less variable than expected
- ✓ filters ok
- ✓ contamination: no indication seen yet (!)
- ✓ satellite platform: very stable and reliable
- ✓ observing efficiency: very high

- o radiation damage: CTI increase slightly higher than expected

- − particle background: higher than expected
- − micrometeoroid damages
- − CCD temperatures: higher and more variable than expected
- − severe optical light leak problem in two cameras
- − frequent camera resets required, may result in time shifts
- − some CCD frames not usable due to artefacts, data cleaning required

the unexpected

Comparison with expectations

?

- detector noise
- telemetry bandwidth
- particle background
- filter integrity
- contamination
- radiation damage
- observing efficiency
- the unexpected

- ✓ detector noise: lower than expected
- ✓ telemetry bandwidth: sufficient
  - ✓ efficient onboard data compression
  - ✓ more telemetry available than expected
- ✓ particle background: less variable than expected
- ✓ filters ok
- ✓ contamination: no indication seen yet (!)
- ✓ satellite platform: very stable and reliable
- ✓ observing efficiency: very high

- ○ radiation damage: CTI increase slightly higher than expected

- − particle background: higher than expected
- − micrometeoroid damages
- − CCD temperatures: higher and more variable than expected
- − severe optical light leak problem in two cameras
- − frequent camera resets required, may result in time shifts
- − some CCD frames not usable due to artefacts, data cleaning required

eROSITA Calibration and First Results

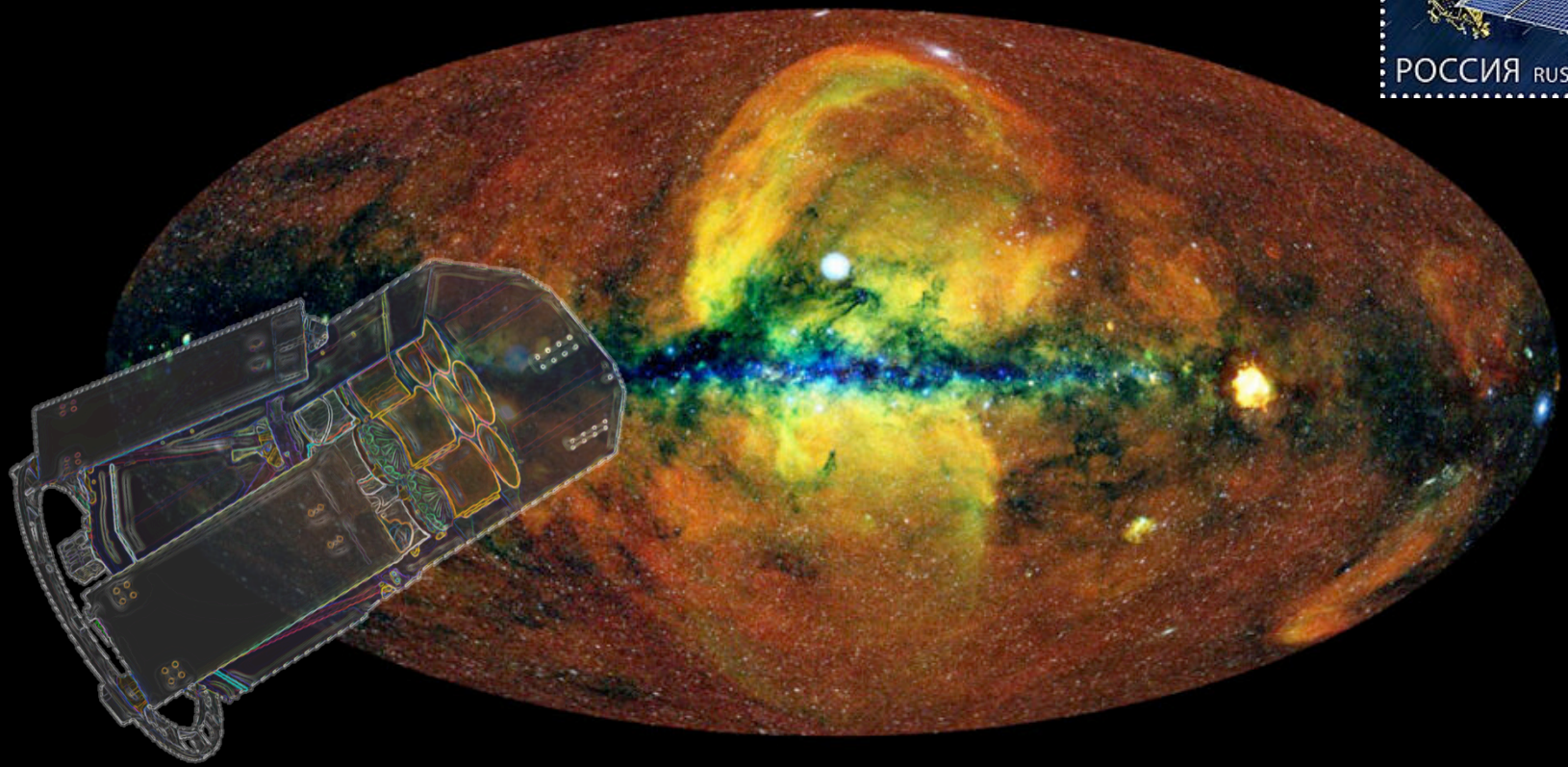

IACHEC, 2021 April 23

Konrad Dennerl, MPE